Positron Emission Tomography and Autoradiography: Principles and Applications for the Brain and Heart, edited by M. Phelps, J. Mazziotta, and H. Schelbert. Raven Press, New York © 1986.

1

Cerebral Circulation, Energy Metabolism, and Protein Synthesis: General Characteristics and Principles of Measurement

Louis Sokoloff

Laboratory of Cerebral Metabolism, National Institute of Mental Health, Public Health Service, Department of Health and Human Services, Bethesda, Maryland 20205

Measurement of Overall Cerebral Blood Flow and Metabolism, 3
Delivery of Nutrients to Brain, 4
  Cerebral Circulation, 4
  Blood-Brain Barrier, 6
Normal Rates of Cerebral Energy Metabolism, 8
  Energy Metabolism of Brain as a Whole, 8
Substrates of Cerebral Energy Metabolism, 9
  Glucose, 9
  Ketone Bodies, 14
  Miscellaneous Substrates, 16
Measurement of Local Cerebral Blood Flow, 18
  Theory of Tissue Indicator Equilibration Technique, 18
  [^{131}I]Trifluoriodomethane Technique, 19
  [^{14}C]Iodoantipyrine Technique, 21
Principles for Measurement of Rates of Biochemical Reactions with Radioisotopes *In Vivo*, 23
Deoxyglucose Method, 25
  Theory, 25
  Procedure for Measurement of Local Cerebral Glucose Utilization, 31
  Theoretical and Practical Considerations, 33
  Computerized Color-Coded Image Processing, 41
  Rates of Local Cerebral Glucose Utilization, 42
  Relation Between Local Functional Activity and Energy Metabolism, 42
  Applications of the Deoxyglucose Method, 47
  Microscopic Resolution, 62
  Potential Usefulness of [^{14}C]DG Method, 63
Development of Autoradiographic Method for Measurement of Local Cerebral Protein Synthesis, 63
  Theory, 64
  Applications of [^{14}C]Leucine Method, 65
References, 67

The orderly control, coordination, and regulation of a myriad of processes throughout the body are continuously dependent on the uninterrupted functional activity of the central nervous system (CNS). The vast array of physical and chemical processes that sustain and comprise cerebral functional activity are largely energy-dependent. The required energy is provided by cerebral energy metabolism, and the brain is metabolically one of the most active organs in the body. In adult humans, for example, in whom the brain comprises only 2% of body weight, the brain alone accounts for approximately 20% of the total body basal oxygen consumption and maintains a steady rate of energy expenditure of at least 20 watts (147). The brain's relatively voracious nutritional demands reflect primarily its need for oxidizable substrates to fuel its energy metabolism.

The endogenous stores of available substrates for energy metabolism in the brain are almost negligible compared to their rates of utilization, and the brain is therefore dependent on the continuous replenishment of its substrate supplies by the cerebral circulation. Complete interruption of the cerebral circulation results in the loss of consciousness within less than 10 sec (116) and the appearance of irreversible pathological changes in brain tissue within a matter of minutes. In cardiac arrest, for example, it is the damage to the brain that is the critical determinant of recovery; it is mainly to provide protection against the brain's insatiable substrate demands that hypothermia or cardiac bypass is employed in surgical procedures that necessitate temporary interruption of the cerebral circulation.

The function of the circulation is to provide the substrates and remove the products of tissue metabolism. Its capacity to accomplish the former is limited by the concentrations of the substrates in the arterial blood. If the concentration of a substrate in the arterial blood is too low, then, regardless of the rate of blood flow, the substrate is not adequately supplied to the tissue. For example, hypoxia or hypoglycemia leads to disturbances in cerebral function nearly as rapidly as interruption of the cerebral circulation, even though cerebral blood flow may be markedly increased. Both blood flow and arterial concentration are therefore critical factors in the nutrition of the brain.

In contrast to almost all other organs except the eye and testis (112), the brain exhibits an additional property that profoundly influences its nutritional supply. The cerebral vasculature has the property of selectively excluding, retarding, or facilitating the transport of soluble substances between the blood and cerebral tissues. This property is due to the blood-brain barrier. Although under normal circumstances its role is probably protective and regulatory, it limits the number of substances in the blood that are suitable substrates for cerebral energy metabolism. Numerous substances in the blood—which might otherwise serve as substrates of cerebral energy metabolism and are in fact metabolized further when produced endogenously within the cerebral tissues in the course of intermediary metabolism—cannot traverse the blood-brain barrier at sufficient rates to support the brain's energy demands. In unphysiological states (e.g., hypoglycemia) the blood-brain barrier may serve to deprive the brain of possible alternative substrates of energy metabolism, even though these substances are plentiful in the blood and the blood flow is adequate.

The nutrition of the brain, even when limited merely to its energy metabolism, is therefore not a simple qualitative problem that requires only the identification of its essential and nonessential nutrients. It is a complex matter that involves not only the peculiar nutritional requirements of the brain but also the balance between supply and demand, which in turn is determined

by the brain's energy demands, the cerebral circulatory supply, the concentration of the nutrients in the arterial blood, and the properties of the blood-brain barrier. Each of these factors is subject to a variety of controls and regulation under normal conditions, and each is affected in different ways in various pathological and pharmacological states. Understanding the nutrition of the brain with respect to its energy metabolism requires the consideration of all.

MEASUREMENT OF OVERALL CEREBRAL BLOOD FLOW AND METABOLISM

In a steady state the tissue concentration of any substance utilized or produced by the brain is presumed to remain constant. When a substance is exchanged between brain and blood, the difference between its rates of delivery to the brain in the arterial blood and of removal in the venous blood must be equal to the net rate of its utilization or production by the brain. This relation can be expressed as follows:

$$CMR = CBF(A - V)$$

where $(A - V)$ is the difference in concentration of the substance in arterial and cerebral venous blood, *CBF* is the rate of cerebral blood flow in volume of blood per unit time, and *CMR* (cerebral metabolic rate) is the steady-state rate of utilization or production of the substance by the brain.

Therefore if both the rate of cerebral blood flow and the arteriovenous difference are known, the net rate of utilization or production of the substance by the brain can be calculated. This has been the basis of most quantitative studies of cerebral metabolism *in vivo* (64,66,76,142,144).

The most reliable method for determining cerebral blood flow is the inert gas method of Kety and Schmidt (69). It was originally designed for use in studies of conscious, unanesthetized humans, and it has been most widely employed for this purpose, although it also has been adapted for use in animals (34,95). The method is based on the Fick Principle, or the law of conservation of matter, and it utilizes low concentrations of a freely diffusible, chemically inert gas as a tracer substance. The original gas used was nitrous oxide, but subsequent modifications have substituted other gases, e.g., ^{85}Kr, ^{79}Kr, ^{133}Xe, or hydrogen (8,34,37,67,78,79,95,143), which can be measured more conveniently in blood. During inhalation of 15% N_2O in air, for example, arterial and cerebral venous blood samples are withdrawn at intervals and analyzed for N_2O content. The cerebral blood flow (in ml/100 g brain tissue/min) can be calculated from the equation

$$CBF = 100\lambda V_T \Big/ \int_0^T (A - V)dt$$

where

A and V = arterial and cerebral venous blood concentrations of N_2O, respectively

V_T = concentration of N_2O in venous blood at time T

λ = partition coefficient for N_2O between brain tissue and blood

T = duration of inhalation (min)

t = variable, time (min)

$\int_0^T (A - V)dt$ = integrated arteriovenous difference in N_2O concentration over T min of inhalation

The brain-blood partition coefficient for N_2O is approximately 1.0. At least 10 min of inhalation is required to approach equilibrium, but it became customary to extend T to 15 or 20 min or longer to achieve more complete equilibrium and accuracy. At the

end of this interval, the N_2O concentration in brain tissue is then approximately equal to the cerebral venous blood concentration.

Because the method requires sampling of both arterial and cerebral venous blood, it lends itself readily to the simultaneous measurement of arteriovenous differences of substances involved in cerebral metabolism. This method and its modifications have provided most of our knowledge of the rates of substrate utilization or product formation by the brain *in vivo*.

A thorough discussion of all the methods for measuring cerebral blood flow is beyond the scope of this chapter (see Chapter 7), but the subject has been comprehensively reviewed (8,67,76,142,143).

DELIVERY OF NUTRIENTS TO BRAIN

Cerebral Circulation

The brain utilizes oxygen and glucose at very rapid rates and is absolutely dependent on uninterrupted oxidative carbohy-

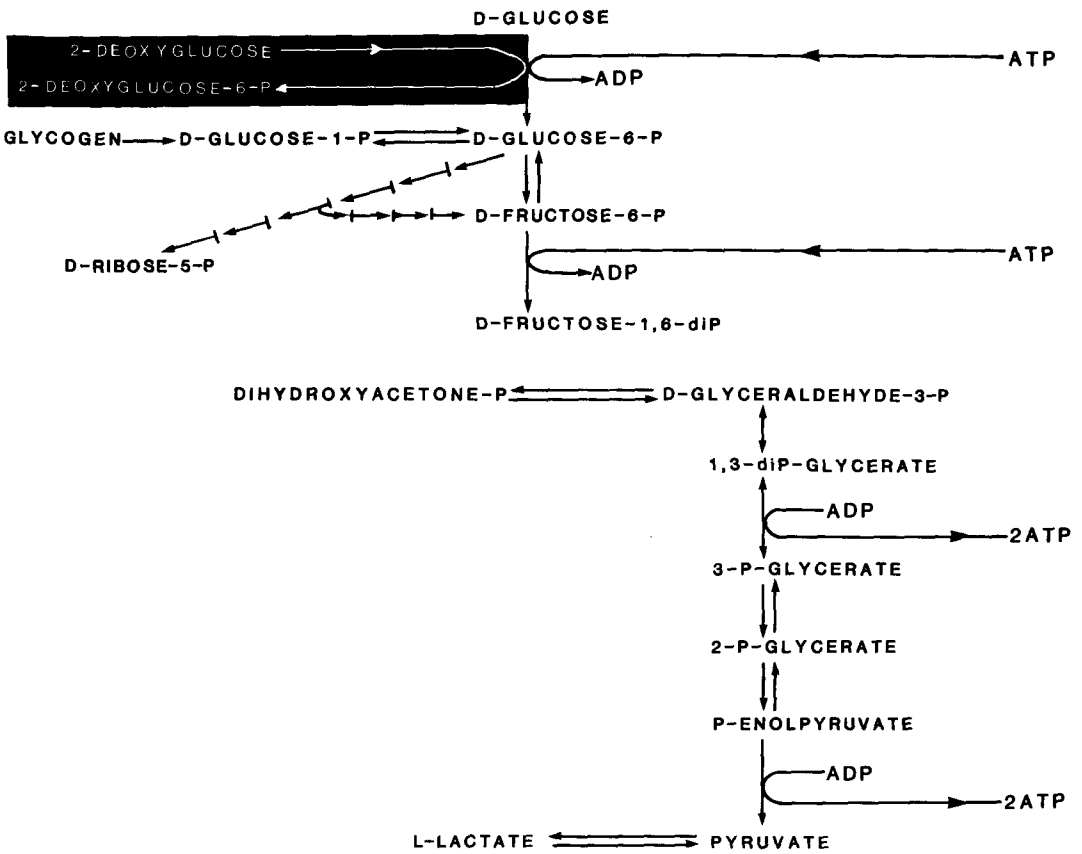

FIG. 1-1. The glycolytic pathway of glucose utilization. Glycolysis is defined as the metabolism of glucose to pyruvate and lactate as shown in figure. If end-product of this reaction is lactate, the reaction is referred to as anaerobic glycolysis. If the reaction proceeds to pyruvate which is then oxidized to carbon dioxide and water via the tricarboxylic acid cycle (see Fig. 1-2), then the reaction is referred to as aerobic glycolysis. The portion of the schema in the *black block* illustrates the site in the glycolytic pathway at which the analog of glucose, 2-deoxy-D-glucose (2-deoxyglucose), is metabolized like glucose (see Fig. 1-6A). The terms P, diP, ATP, and ADP refer to phosphate, diphosphate, adenosine triposphate, and adenosine diphosphate, respectively.

drate metabolism for maintenance of its functional and structural integrity. Under anaerobic conditions glycolysis is limited to the conversion of glucose to lactate (Fig. 1-1) and provides two molecules of ATP for each molecule of glucose consumed. Under fully aerobic conditions glucose is metabolized to pyruvate, which is then metabolized via the tricarboxylic cycle (Fig. 1-2) to carbon dioxide and water with a net production of 36 molecules of ATP per molecule of glucose consumed. The gain in ATP production is the result of oxidative phosphorylation that is associated with oxygen consumption. The availability of oxygen inhibits the rate of glycolysis and reduces lactate production to zero or near zero levels, an effect generally known as the

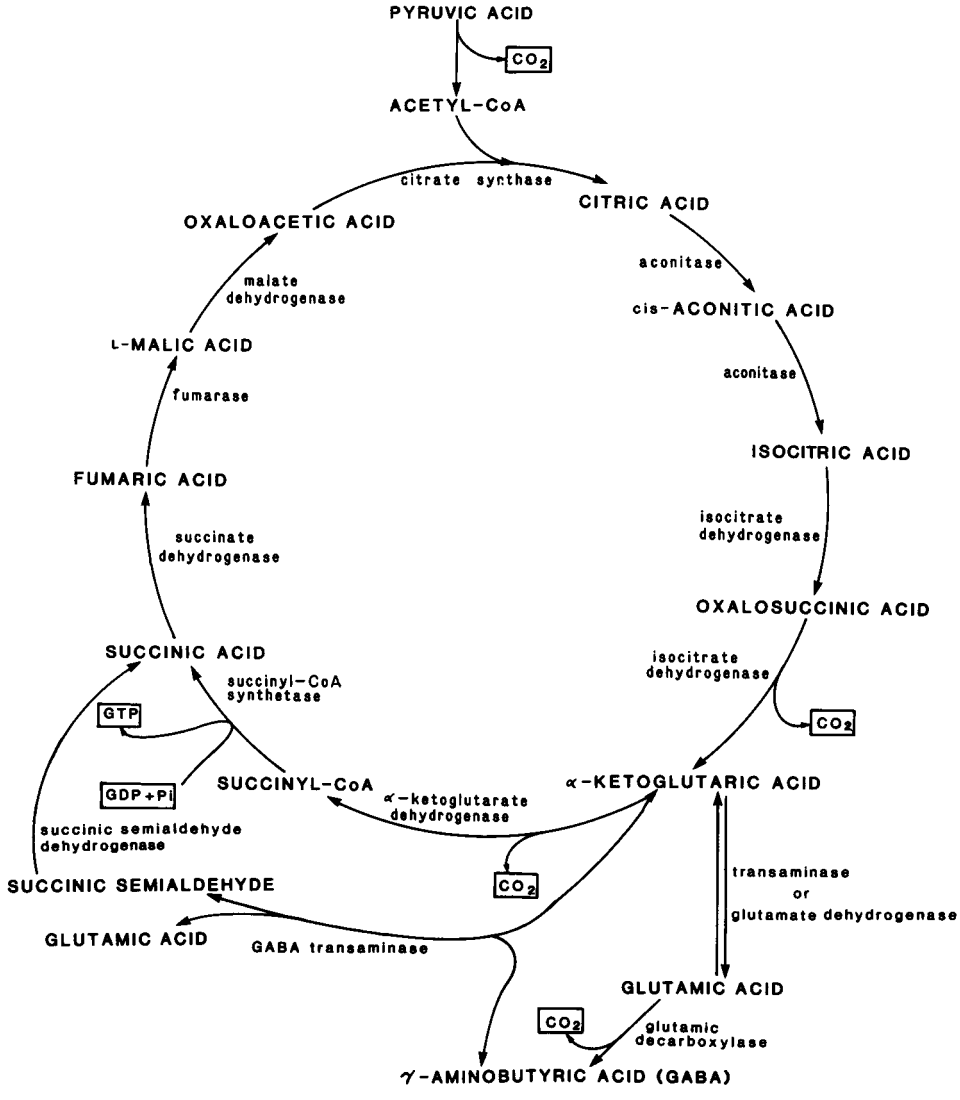

FIG. 1-2. Metabolic pathway of the tricarboxylic acid cycle, including the α-ketoglutarate → glutamate → γ-aminobutyrate → succinate shunt, which is unique to the brain. The terms Pi, GDP, and GTP refer to inorganic phosphate, guanosine diphosphate, and guanosine triphosphate, respectively.

Pasteur effect. There is a large Pasteur effect in brain (88), and glycolysis can be increased as much as 10-fold under anaerobic conditions. Even at its maximal rate, however, anaerobic glycolysis is unable to provide sufficient ATP to meet the brain's energy demands. Since the stores of oxygen and glucose in brain are extremely small compared with their rates of utilization, the brain requires their continuous replenishment by the circulation. If cerebral blood flow is completely interrupted, consciousness is lost within less than 10 sec, or the amount of time required to consume the oxygen contained within the brain and its blood content (64). Irreversible pathological changes rapidly follow. Loss of consciousness as a result of anoxemia caused by anoxia or asphyxia takes only slightly longer because of the additional oxygen present in the lungs and still-circulating blood. There is evidence that the critical level of oxygen tension in the cerebral tissues, below which consciousness and the normal electroencephalogram (EEG) pattern are invariably lost, lies between 15 and 20 mm Hg (142). This appears to be so whether the tissue anoxia is achieved by lowering the cerebral blood flow or the arterial oxygen content.

The cerebral blood flow must be able to satisfy the brain's avaricious appetite for oxygen and glucose. The average rate of blood flow in the brain of normal conscious adult man is approximately 57 ml/100 g tissue/min (Table 1-1). For the whole brain this amounts to almost 800 ml/min, or approximately 15% of the total basal cardiac output. This level must be maintained within relatively narrow limits, for the brain cannot tolerate any major drop in its perfusion rate. A fall in cerebral blood flow to approximately half of its normal rate is sufficient to cause loss of consciousness in normal, healthy young men (27,76,142). With such constraints it is to be expected that vascular insufficiency is a common cause of cerebral nutritional deficiency and dysfunction. Fortunately, the physiological mechanisms normally regulating the cerebral circulation are particularly well adapted to the special requirements of the brain.

Blood-Brain Barrier

Mere delivery of potential metabolic substrates to the brain by the circulation does not ensure that these compounds are available to the intracellular enzyme systems that could metabolize them. They must first traverse the vascular endothelium, the perivascular and interstitial spaces, and finally the cellular membranes to reach the intracellular loci of the biochemical machinery. In contrast to most other organs, the exchange of solutes between tissue and capillary blood in brain constitutes a major problem that is largely responsible for the brain's parochial tastes in metabolic substrates. There exist blood-brain, blood-cerebrospinal fluid (CSF), and

TABLE 1-1. *Cerebral blood flow and metabolic rate in normal young adult human males*

Function	Rate	
	Per 100 g brain tissue	Per whole brain[a]
Cerebral blood flow (ml/min)	57	798
Cerebral O_2 consumption (μmol/min)	156	2,188
Cerebral glucose utilization (μmol/min)	30.6	428

[a]Brain weight assumed to be 1,400 g. From Sokoloff (147).

CSF-brain barriers that selectively limit and regulate the transfer rate of solutes between brain and blood. The role of these barriers is probably to exclude potentially noxious agents and to maintain an optimal chemical environment for CNS functions; in effect, they may be more responsible for the uniqueness of the brain's energy metabolism *in vivo* than is its enzyme composition.

There are, in general, a variety of processes by which substances can traverse the capillary endothelium to exchange between blood and tissue. One such process is *pinocytosis,* in which a portion of the endothelial cell membrane extends around and engulfs a portion of the external medium, fuses and separates as an intracellular vesicle containing the sample of medium within it, and then crosses to the other side of the cell and releases its contents into the medium on the opposite side by the reverse process. Another process is simple *diffusion,* by which the solute diffuses directly through the entire capillary endothelial layer from regions of higher concentration to those of lower concentration. The effectiveness of this process varies with the lipophilicity of the solute and its ability to dissolve in the lipoidal cell membranes of the endothelial cells; the passage of charged, polar, and lipophobic substances is retarded or excluded. Most gases (e.g., the respiratory gases oxygen and carbon dioxide) are transported between blood and tissues by simple diffusion.

In most tissues substances can penetrate the capillary endothelium through the intercellular spaces between the endothelial cells. In brain this possibility is essentially nonexistent because the endothelial cells are so tightly apposed that there exists essentially a solid sheet of membrane around the vascular compartment. These *tight junctions* are readily visualized by electron microscopy. Inasmuch as macromolecules (e.g., proteins) cannot pass from blood to tissue via such tight junctions, exogenous macromolecules can normally play only a negligible role in biochemical processes within the brain tissue itself.

With all other routes for transfer between blood and brain effectively blocked, hydrophilic compounds, which include most of the potential substrates for cerebral energy metabolism, must have other means to traverse the blood-brain barrier. Most of these compounds are transported via *carrier-mediated mechanisms,* in which a cellular carrier molecule binds the compound on one side of the barrier and translocates and releases it on the other side. The carrier mechanism may be *passive* (in which case the transport is down a concentration gradient) or *active* (i.e., against a concentration gradient, which requires the expenditure of energy). Carrier mechanisms are always saturable and to a large extent stereospecific, if not to the individual chemical species at least to their structural classes. Carrier-mediated transport follows Michaelis-Menten kinetics. The rate of unidirectional transport depends, therefore, on the concentration of the transported molecule and the Michaelis-Menten kinetic constants (Chapter 7), i.e., the K_m (substrate concentration at which the carrier is half saturated) and V_{max} (the maximum velocity of reaction) of the carrier for the chemical species. If the carrier is not fully specific, then competitive inhibition may occur if more than one species of compound with affinity for the carrier are present. The carrier-mediated transport system is also characterized by a maximal transport rate, which occurs when the carrier is saturated. Even this maximal rate may be rate limiting, however, and severely restrict the usefulness of a compound to serve as a substrate for biochemical processes (e.g., cerebral energy metabolism) that proceed at very rapid rates.

A number of blood-brain carrier systems have been well defined, particularly by Oldendorf and his co-workers (98–100). At least three carrier systems for amino

acids—one each for acidic, basic, and neutral amino acids—have been described (98,100; Chapter 10). The hexoses, including glucose, the major substrate for cerebral energy metabolism, are transported by a single carrier that operates effectively with D-glucose, D-mannose, and D-galactose (98). It is essentially inoperable with L-glucose and D-fructose, the latter of which could serve as a substrate for cerebral metabolism but does not because it cannot be adequately transported across the blood-brain barrier. There is also a carrier system for short-chain monocarboxylic acids that functions with formate, acetate, propionate, butyrate, pyruvate, and L-lactacte. D-Lactate is not transported by this system and appears to enter brain much more slowly, probably by simple diffusion on the basis of its limited lipid solubility. The ketone bodies, D-β-hydroxybutyrate and acetoacetate, have also been reported to be transported across the blood-brain barrier by a carrier-mediated system (35,91), but no evidence was presented to indicate if it is the same carrier used for the other monocarboxylic acids. Fatty acids with longer chain lengths (e.g., decanoic and octanoic acid) cross the blood-brain barrier effectively by simple diffusion because of their greater lipid solubility (99).

The blood-brain barrier obviously plays a critical and decisive role in determining which of the many energy-rich oxidizable compounds present in the blood can serve as suitable substrates for cerebral energy metabolism. It is necessary but insufficient for the brain to have the requisite enzyme systems to oxidize them; the compounds must be able to traverse the blood-brain barrier and reach the enzyme sites at rates sufficient to maintain the metabolic flux. It is beyond the scope of this chapter to discuss more comprehensively the functions of the blood-brain barrier, but the subject recurs in subsequent sections in regard to specific compounds and situations. For detailed and comprehensive reviews of the blood-brain-CSF barriers, there are a number of recent, excellent reviews available (16,56,72,112).

NORMAL RATES OF CEREBRAL ENERGY METABOLISM

Energy Metabolism of Brain as a Whole

Cerebral Oxygen Consumption

The brain's demands for energy are among the greatest of all the body tissues. This is reflected in its relatively enormous rate of oxygen consumption, which provides the energy required for its intense physiochemical activity. The most reliable data on cerebral metabolic rate have been obtained in humans. Cerebral oxygen consumption in normal, conscious, young men is approximately 156 μmol/100 g brain/min (Table 1-1); the rate is similar in young women. The rate of oxygen consumption by an entire brain of average weight (1,400 g) is then approximately 2.2 mmol/min.

The magnitude of this rate can be more fully appreciated when it is compared with the metabolic rate of the body as a whole. The average man weighs 70 kg and consumes approximately 11.2 mmol oxygen/min in the basal state. Therefore, the brain alone, which represents only 2% of total body weight, accounts for 20% of the resting total body oxygen consumption. In children during the first decade of life, the brain comprises a larger fraction of body weight and utilizes oxygen at almost twice the adult level; it may then account for at least 50% of the total body basal oxygen consumption (62).

Oxygen is normally utilized in the brain almost entirely for the oxidation of carbohydrate (66,144,147). On the basis of the caloric value of oxygen in the oxidation of carbohydrate, the energy equivalent of the cerebral metabolic rate can be estimated to be approximately 20 watts, or 0.25 kcal/min. If it is assumed that this energy is uti-

lized mainly for the synthesis of high-energy phosphate bonds, that the efficiency of the energy conservation is approximately 20%, and that the free energy of hydrolysis of the terminal phosphate of ATP is 7 kcal/mol, this energy expenditure then can be estimated to support the steady turnover of close to 7 mmol (approximately 4×10^{21} molecules) of ATP/min in the entire brain.

There has been considerable speculation about the nature of the functions responsible for the brain's energy demands. The brain does not do mechanical work like cardiac and skeletal muscle. It does not do osmotic work, as the kidney does in concentrating urine. It does not have the complex, energy-consuming metabolic functions of liver, and, despite the synthesis of hormones, neuropeptides, neurotransmitters (Chapter 2), and a variety of lipids, it is not noted for its biosynthetic activities. Clearly the functions of nervous tissues are mainly excitation, inhibition, and conduction (Chapter 2), and these are reflected in the unceasing electrical activity of the brain. The electrical energy is ultimately derived from chemical processes, and it is likely that most of the brain's energy consumption is utilized for active transport of ions to sustain and restore the membrane potentials discharged during the processes of excitation, inhibition, and conduction.

Cerebral Glucose Consumption

The oxygen consumption of the brain reflects primarily its energy metabolism, and in the normal state the main substrate for cerebral energy metabolism is glucose taken up from the blood (see below). The rate of cerebral glucose utilization is, therefore, also high like that of oxygen consumption (Table 1-1). Glucose traverses the blood-brain barrier by facilitated transport via the hexose-specific carrier (98). Glucose concentration in the blood is normally at the level (i.e., about 4–10 mM) needed to achieve approximately half-saturation of the carrier and, therefore, also half the maximal transport velocity. The transport capacity is sufficiently high that the normal influx of glucose is considerably in excess of the need, and the rate of glucose consumption represents only a fraction of the flow of glucose into and out of the brain via the blood-brain barrier (112). The rate of cerebral glucose utilization is never limited by the transport of glucose through the blood-brain barrier except when that transport is itself limited by restrictions in the delivery of glucose to the brain, either by hypoglycemia or cerebral ischemia, or the rate of glucose utilization is inordinately increased, as in status epilepticus, to levels beyond the capacity of the cerebral circulation and transport mechanisms to adapt.

SUBSTRATES OF CEREBRAL ENERGY METABOLISM

Glucose

Stoichiometry of Glucose Utilization and Oxygen Consumption

In contrast to most other tissues, which exhibit considerable flexibility with regard to the nature of the foodstuffs extracted and consumed from the blood, the brain is normally restricted almost exclusively to glucose as the substrate for its energy metabolism. Under normal circumstances no other potential energy-yielding substance has been found to be extracted by the brain from the blood in more than relatively trivial amounts compared to glucose. The stoichiometry of glucose utilization and oxygen consumption is summarized in Table 1-2. The normal, conscious human brain consumes oxygen at a rate of 156 μmol/100 g tissue/min. Carbon dioxide production is the same, leading to a respiratory quotient (ratio of CO_2 production to oxygen consumption) of 1.0, further evidence that carbohydrate is the ultimate substrate for oxidative metabolism. The oxygen con-

TABLE 1-2. *Relationship between cerebral oxygen consumption and glucose utilization in normal young adult man*

Function	Value
Oxygen consumption (μmol/100 g brain tissue/min)	156
Glucose utilization (μmol/100 g brain tissue/min)	31
Oxygen/glucose ratio (μmol/μmol)	5.5
Glucose equivalent of oxygen consumption (μmol glucose/100 g brain tissue/min)	26[a]
CO_2 production (μmol/100 g brain tissue/min)	156
Cerebral respiratory quotient	0.97

[a]Calculated on the basis of 6 mol oxygen required for complete oxidation of 1 mol glucose. Values are the median of the values reported in the literature.
From Sokoloff (144,147).

sumption and carbon dioxide production are equivalent to a rate of glucose utilization of 26 μmol/100 g/min, assuming 6 μmol of oxygen consumed and carbon dioxide produced for each micromole of glucose completely oxidized to carbon dioxide and water. The glucose utilization actually measured is 31 μmol/100 g/min, however, which indicates that glucose consumption is not only sufficient to account for the total oxygen consumption but is in excess by 5 μmol/100 g/min. For the complete oxidation of glucose, the theoretical oxygen/glucose utilization ratio is 6.0 μmol/μmol; the excess glucose utilization is responsible for a measured ratio of only 5.5 μmol of oxygen per micromole of glucose. The fate of the excess glucose is unknown, but it is probably distributed in part in lactate, pyruvate, and other intermediates of carbohydrate metabolism that are released from the brain into the blood, each in an insufficient amount to be detectable in significant arteriovenous differences. Some of the glucose is also utilized not for the production of energy but for the synthesis of other chemical constituents of the brain such as glycolipids, glycoproteins, phospholipids, acetylcholine, etc.

The combination of a cerebral respiratory quotient of near unity, an almost stoichiometric relationship between oxygen uptake and glucose consumption, and the absence of any significant arteriovenous difference for any other energy-rich substrate is strong evidence that the brain normally derives its energy from the oxidation of glucose. In this respect, cerebral metabolism is unique because no other tissue, with the possible exception of the testis (45), has been found to rely only on carbohydrate for energy. This does not imply that the pathways of glucose metabolism in the brain lead, like combustion, directly and exclusively to oxidation. Various chemical and energy transformations occur between the uptake of the primary substrates (glucose and oxygen) and the liberation of the end-products (carbon dioxide and water). Various compounds derived from glucose are intermediates in the process. Glucose carbon is incorporated, for example, into amino acids, protein, lipids, glycogen, and so on. These are turned over and act as intermediates in the overall pathway from glucose to carbon dioxide and water. There is clear evidence from studies with [^{14}C]glucose that the glucose is not entirely oxidized directly; at any given moment some of the carbon dioxide being produced is derived from sources other than the glucose that has just entered the brain (33,119). That oxygen and glucose consumption and carbon dioxide production are essentially in stoichiometric balance and no other energy-laden substrate is

taken from the blood means, however, that the net energy made available to the brain must ultimately be derived from the oxidation of glucose. It should be noted that this is the situation in the normal state; as is discussed later, other substrates may be used in special circumstances or in abnormal states.

Obligatory Utilization of Glucose

The brain normally derives almost all of its energy from the aerobic oxidation of glucose, but this does not distinguish between preferential and obligatory utilization of glucose. Most tissues are largely facultative in their choice of substrates and can use them interchangeably, more or less in proportion to their availability (e.g., see substrate dependence of myocardium, Chapters 4 and 12). This does not appear to be so in brain. The present evidence indicates that, except in some unusual and very special circumstances, only the aerobic utilization of glucose is capable of providing the brain with enough energy to maintain normal function and structure. The brain appears to have almost no flexibility in its choice of substrates *in vivo*. The conclusion is derived from the following evidence.

Effects of glucose deprivation.

It is well known clinically that a fall in blood glucose concentration, if of sufficient degree, is rapidly followed by aberrations of cerebral function. Hypoglycemia, produced by excessive insulin or occurring spontaneously in hepatic insufficiency, is associated with changes in mental state ranging from mild, subjective sensory disturbances to coma, the severity depending on both the degree and the duration of the hypoglycemia. The behavioral effects are paralleled by abnormalities in EEG patterns and cerebral metabolic rate. The EEG pattern exhibits increased prominence of slow, high-voltage delta rhythms, and the rate of cerebral oxygen consumption falls. In studies on the effects of insulin hypoglycemia in humans (70), it was observed that when the arterial glucose concentration fell from a normal level of 3.9 to 5.6 mM (70–100 mg/100 ml) to an average of 1.1 mM (19 mg/100 ml), the subjects became confused and their cerebral oxygen consumption fell to 116 μmol/100 g/min (2.6 ml/100 g/min), a value 79% of the normal level. When the arterial glucose level fell to 0.44 mM (8 mg/100 ml), a deep coma ensued and the cerebral oxygen consumption decreased even further to 85 μmol/100 g/min (1.9 ml/100 g/min). These changes were not caused by insufficient cerebral blood flow, which actually increased slightly during the coma. In the depths of the coma, when the blood glucose content was very low, there was almost no measurable cerebral uptake of glucose from the blood. Cerebral oxygen consumption, although reduced, was still far from negligible, and there was no longer any stoichiometric relationship between glucose and oxygen uptake by the brain, evidence that the oxygen was utilized for the oxidation of other substances. The cerebral respiratory quotient remained approximately 1.0, however, indicating that these other substrates were still carbohydrate, presumably derived from the brain's endogenous carbohydrate stores.

The effects of insulin are clearly the result of hypoglycemia and not some other direct effect of insulin in the brain. In all cases, the behavioral, functional, and cerebral metabolic abnormalities associated with insulin hypoglycemia are rapidly and completely reversed by the administration of glucose. The severity of the effects is correlated with the degree of hypoglycemia and not the insulin dosage, and the effects of the insulin can be completely prevented by simultaneously administering glucose with the insulin.

Similar effects are observed in hypoglycemia produced by other means, e.g., hepatectomy. The inhibition of glucose utili-

zation at the phosphohexoseisomerase step with 2-deoxyglucose also produces the cerebral effects of hypoglycemia despite an associated elevation in blood glucose content (161). It appears then that when the brain is deprived of its glucose supply in an otherwise normal adult individual, no other substance present in the blood can satisfactorily substitute for it as the substrate for the brain's energy metabolism.

Substitute substrates in hypoglycemia.

The hypoglycemic state provides convenient test conditions to determine whether a substance is capable of substituting for glucose as a substrate for cerebral energy metabolism. If it can, its administration during hypoglycemic shock should restore consciousness and normal cerebral electrical activity without raising the blood glucose level. Numerous potential substrates have been tested in humans and animals. Very few can restore normal cerebral functions in hypoglycemia, and of these all but one appear to operate through a variety of mechanisms to raise the blood glucose level rather than by serving as a substrate directly.

Mannose appears to be the only substance that can be utilized by the brain directly and rapidly enough to restore or maintain normal function in the absence of glucose (135). It traverses the blood-brain barrier and is converted to mannose-6-phosphate. Hexokinase catalyzes this reaction as effectively as it does the phosphorylation of glucose. The mannose-6-phosphate is then converted to fructose-6-phosphate by phosphomannoseisomerase, which is active in brain tissue (135). Through these reactions mannose can enter directly into the glycolytic pathway and replace glucose. Maltose has also been found to be effective occasionally in restoring normal behavior and EEG activity in hypoglycemia, but only by raising the blood glucose level through its conversion to glucose by maltase activity in blood and other tissues (135,144).

Epinephrine is effective in producing arousal from insulin coma, but this is achieved through its well-known stimulation of glycogenolysis and the elevation of blood glucose concentration. Glutamate, arginine, glycine, *p*-aminobenzoate, and succinate also are effective occasionally, but they probably act through adrenergic effects that raise the epinephrine level and consequently the glucose concentrations of the blood (144).

It is clear then that no substance normally present in the blood can replace glucose as the substrate for the brain's energy metabolism. Thus far the one substance found to do so, mannose, is not normally present in blood in significant amounts and is, therefore, of no physiological significance. It should be noted, however, that failure to restore normal cerebral function in hypoglycemia is not synonymous with an inability of the brain to utilize the substance. Many of the substances that have been tested and found ineffective are compounds normally formed and utilized within the brain and are normal intermediates in its intermediary metabolism. Lactate, pyruvate, fructose, 1,6-diphosphate, acetate, D-β-hydroxybutyrate, and acetoacetate are examples. These can be utilized by brain slices, homogenates, or cell-free fractions, and the enzymes for their metabolism are present in the brain. Enzymes for the metabolism of glycerol (136,137) or ethanol (113), for example, may not be present in sufficient amounts. For other substrates, e.g., D-β-hydroxybutyrate and acetoacetate (54,110,166; Fig. 1-3), the enzymes are adequate, but the substrate is not normally available to the brain because of inadequate blood level or restricted transport through the blood-brain barrier.

Nevertheless, the functioning of the nervous system in the intact animal depends on substrates supplied by the blood, and no

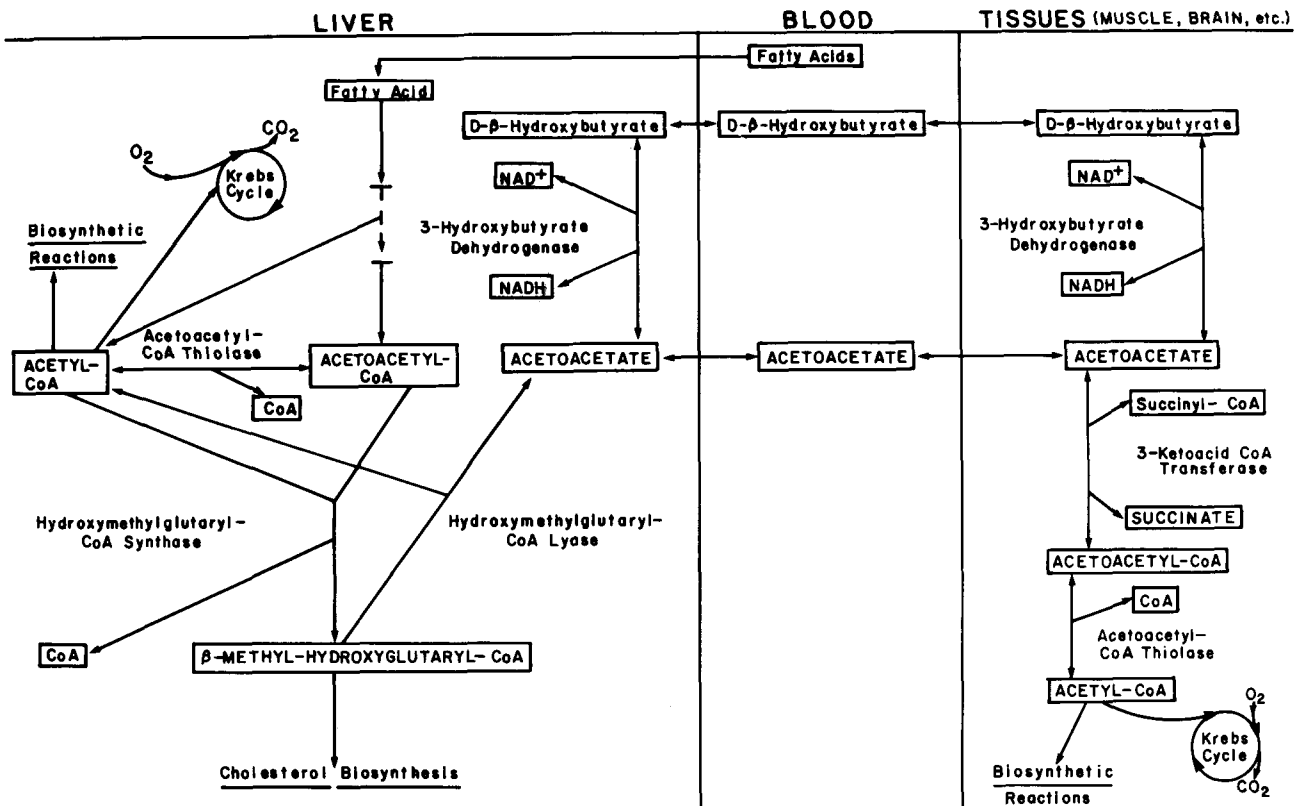

FIG. 1-3. Metabolic pathways of synthesis of the ketone bodies, D-β-hydroxbutyrate, and acetoacetate, in the liver and their utilization in the brain and muscle. The terms NAD^+, NADH, and CoA refer to nicotinamide adenine dinucleotide, the reduced form of NAD^+, and coenzyme A, respectively.

satisfactory normal, endogenous substitute for glucose has been found. Glucose must therefore be considered essential for normal physiological behavior of the CNS.

Ketone Bodies

Although glucose is always essential and in normal circumstances almost the sole substrate for the brain's energy metabolism, there are some naturally occurring conditions in which the brain can substitute other substances, at least in part, for glucose. The ketone bodies, D-β-hydroxybutyrate and acetoacetate, are such substances, and the brain utilizes them in a variety of ketotic states in proportion to their concentrations in blood. These ketone bodies, which are interconvertible into one another, are by-products of the metabolism of fatty acids. Their levels in blood are normally very low, but their rate of production in the body is enhanced when fatty acid degradation is increased. Their primary source is the liver, which can produce but not utilize them because it lacks the enzyme, succinyl-CoA:3-oxo-acid CoA-transferase, to convert free acetoacetate to acetoacetyl-CoA, a necessary step in the utilization of ketone bodies. As the liver increases its rate of production of ketone bodies in association with increased fatty acid metabolism, it releases them into the blood for utilization by other tissues. The pathways of ketone body production and utilization are diagrammatically summarized in Fig. 1-3.

Starvation

Evidence that the brain can extract and utilize ketone bodies from the blood was first obtained by Owen et al. (102) in human subjects being treated for obesity by complete and prolonged starvation. The total body carbohydrate stores of the patients at the onset of the fast were estimated to be 150 to 300 g, and metabolic balance studies indicated that their maximum rate of gluconeogenesis from protein and glycerol during the fast could not have exceeded 33 g/day. Inasmuch as normal cerebral glucose utilization is approximately 110 g/day, the body's total actual and potential glucose reserves were clearly insufficient to satisfy the brain's normal glucose requirements for more than a few days. Nevertheless, after 6 to 7 weeks of starvation, these patients exhibited none of the usual signs of cerebral dysfunction indicative of cerebral glucose insufficiency. Their level of consciousness, EEG, and performance on psychometric testing remained within normal limits, evidence of adequate rates of cerebral energy metabolism despite the insufficiency of glucose to support it. Clearly the brain must have turned to the utilization of other substrates. The enigma of the nature of the substrate was resolved by examination of the cerebral arteriovenous differences. Although the glucose level in blood was only mildly reduced, the cerebral glucose arteriovenous difference had declined to approximately half of its normal level; of this, half was accounted for by lactate and pyruvate release and therefore did not support oxidative metabolism. Net lactate and pyruvate production by brain is under normal conditions barely, if at all, detectable (66,144). The arteriovenous oxygen difference was normal, and glucose utilization, after correction for lactate and pyruvate recovery, accounted for only 30% of it. Most of the remainder of the oxygen consumption was apparently supported by the ketone bodies, D-β-hydroxybutyrate and acetoacetate, which accounted for 52 and 8%, respectively. A small fraction of the oxygen consumption could be accounted for by the uptake of α-amino nitrogen-containing material, presumably amino acids, although the arteriovenous difference for α-amino nitrogen was not statistically significant. No evidence of fatty acid utilization was observed. An ancillary finding of interest was the remarkably low cere-

bral respiratory quotient (RQ) of 0.63. None of the substrates being oxidized could lead to such a low RQ, which suggests that there may be considerable carbon dioxide fixation in the brain during starvation.

The changes in cerebral metabolism during starvation demonstrate that the mature brain is capable of adapting to altered nutrient supply. Normally it relies on glucose almost exclusively as the substrate for its energy metabolism, but availability of glucose becomes limited during starvation. On the other hand, starvation causes mobilization of fatty acids from the fat stores of adipose tissue, and the accelerated metabolism of fatty acids by liver leads in turn to enhanced formation of ketone bodies and elevation of their levels in blood. The brain adapts to the altered conditions by switching in part from consumption of the endangered glucose supply to utilization of the ketone bodies made available by the alterations in body metabolism.

Infancy

Like the human infant, the newborn rat is transiently hypoglycemic after birth, and its blood ketone levels are initially very low—as low as those of the normally fed adult rat (71). With the onset of suckling, the blood ketone levels rise as much as 10-fold, and a true ketosis ensues (71). This ketosis is of nutritional origin; it reflects the ketogenic nature of maternal rat milk, which consists of 50% fat on a dry weight basis (22). The ketosis lasts until 20 to 22 days of age, when the rat is weaned onto standard high-carbohydrate food; the ketosis then gradually disappears (71). During the ketosis of the suckling period ketone bodies constitute a significant source of the brain's substrates (15), and positive arteriovenous differences proportional to the concentration of the ketone bodies in the arterial blood are observed (43,71). Similar evidence for significant cerebral ketone utilization during normal infancy has been obtained in puppies (157) and human infants (103). The enzymes of ketone utilization in brain are more active during early postnatal than adult life; therefore, the infant brain is more efficient than the adult brain in extracting and utilizing ketone bodies from the blood at any given arterial concentration (71).

Miscellaneous Ketotic States

The brain can utilize D-β-hydroxybutyrate and acetoacetate whenever they are available but does not normally do so in adults because of the low concentration of these substances in the arterial blood. Ketosis of various origins can therefore lead to significant utilization of ketones by brain during any period of life. For example, fat feeding or the infusion of D-β-hydroxybutyrate or acetoacetate, which raises the blood levels of one or both ketone bodies, also leads to uptake of the ketones by brain in approximate proportion to their levels in the arterial blood. The same appears to occur in diabetic ketoacidosis. Studies by Kety and his associates (66,68) revealed no significant cerebral arteriovenous difference for total ketones in diabetic acidosis or coma, but more recent studies by Göttstein et al. (38) provide evidence of some cerebral uptake of ketone bodies in diabetic acidosis. It is possible that the hyperglycemia and reduced cerebral metabolic rate present in diabetic acidosis tend to obscure the demonstration of cerebral ketone body utilization in that condition.

Relationship of Cerebral Ketone Utilization to Dependence on Glucose

The finding that the brain can and does utilize ketone bodies under certain circumstances is not necessarily in conflict with earlier observations that neither D-β-hydroxybutrate nor acetoacetate can restore normal cerebral function and metabolism in hypoglycemia (144,147). In all the stud-

ies demonstrating cerebral ketone utilization, glucose consumption may have been reduced but was still present to an appreciable degree (15,102). There is no evidence that ketone bodies can completely replace glucose. Indeed there is evidence to the contrary; in the perfused rat brain complete replacement of glucose with D-β-hydroxybutyrate results in just as rapid deterioration of cerebral functional and metabolic activities as is observed with complete removal of all substrate (H. A. Sloviter, *personal communication*, 1973).

Miscellaneous Substrates

Although the nutritional demands of the brain are generally fully supplied by glucose with occasional supplementation by ketone bodies, there are some other substances that are taken up by the brain from the blood and oxidized in small and variable amounts. Their quantitative contribution to the brain's energy metabolism is negligible, but they may serve some special functions other than supplying energy.

Monocarboxylic Acids

Lactic and pyruvic acid, as well as the short-chain fatty acids acetic, propionic, and butyric acid, share a common facilitated, carrier-mediated transport system through the blood-brain barrier (99). The carrier is stereospecific for the L-isomer of lactate and is saturated at a concentration only three to four times that of the normal plasma lactate level (94,99). Inasmuch as they share a common carrier, the transport of any one of these potential substrates is competitively inhibited by the others, and both the relative and total concentrations of all influence their entry into brain. The mutual competitive inhibition of the short-chain acids, the saturability of the carrier at fairly low blood concentrations, and the relatively low maximal velocity of the transport system severely limit the uptake of these substances by brain. Since the carrier system in all likelihood is bidirectional, the exit of these substances from brain is probably also limited. Although the uptake by brain of all of them can be demonstrated experimentally, particularly by techniques that employ radioisotopes, their uptakes in mature brain are never sufficient to contribute significantly to cerebral energy metabolism. Small cerebral uptakes of lactate can be caused by infusions of lactate that raise the arterial concentration (93), but cerebral arteriovenous differences for lactate and pyruvate in man are not statistically significantly different from zero (66), except in conditions of cerebral ischemia or hypoxia, when they are negative, indicating their net release from brain (88).

Long-chain fatty acids become more lipophilic with increasing chain length and can cross the blood-brain barrier by passive diffusion in more or less direct proportion to their lipid solubility (99,112). There is ample experimental evidence, mainly with labeled substrates, that the brain is capable of oxidizing fatty acids (e.g., butyrate, octanoate, and palmitate) to carbon dioxide and water (3,7,80,158,162). There has been no demonstration, however, of significant contributions of fatty acids to cerebral energy metabolism. Even in prolonged starvation in obese human subjects, in whom blood fatty acid levels are elevated and the brain is supplementing its glucose utilization with ketone body consumption, there is no evidence of appreciable utilization of fatty acids by brain (102).

Glycerol

Brain slices *in vitro* oxidize glycerol to carbon dioxide, but it requires a glycerol concentration of 23 mM in the medium to achieve a rate of carbon dioxide production equal to that with 2 mM glucose (136,137). Glycerol administered *in vivo* can reverse the effects of insulin-induced hypoglycemia on the EEG, but it requires at least 10 times

as much glycerol as glucose to produce this effect, and sufficient amounts of glycerol can be administered only by intracarotid injection (136,137). The brain can therefore utilize glycerol, but so slowly and ineffectively that its contribution to cerebral energy metabolism cannot be of significance under any circumstance except the most extreme experimental conditions.

Amino Acids

There is active amino acid metabolism in brain. In addition to the utilization of amino acids for protein synthesis and for synthesis of the various amine neurotransmitters, the brain can oxidize amino acids to carbon dioxide and water. First of all, the brain utilizes carbon skeletons derived from glucose metabolism to synthesize the dicarboxylic α-amino acids glutamate and aspartate, via branching metabolic pathways from the citric acid cycle. It can synthesize alanine from pyruvate by transamination, glutamine from glutamate by amidation, and γ-aminobutyrate from glutamate by decarboxylation. All of these amino acids are in dynamic interchange with intermediates of the pathways of carbohydrate metabolism, particularly the citric acid cycle, via a variety of enzymatic reactions, and they can therefore reenter the carbohydrate pools and be oxidized to carbon dioxide and water. It has been found with brain slices that the α-ketoglutarate $\rightarrow$ glutamate $\rightarrow$ γ-aminobutyrate $\rightarrow$ succinic semialdehyde $\rightarrow$ succinate shunt may carry a significant share of the flux between α-ketoglutarate and succinate in the operation of the citric acid cycle (87; Fig. 1-2). Presumably amino acid molecules of the same species as those endogenously synthesized, which may be taken up by the brain from the blood, enter the same pools and are similarly oxidized.

Brain tissue is also capable of oxidizing essential amino acids, i.e., those that it cannot synthesize endogenously. Brain slices oxidize branched-chain amino acids (e.g., leucine) to carbon dioxide at rates comparable to those in kidney, liver, or diaphragm (97). Isoleucine and valine are similarly oxidized (160). In fact, in brain slices *in vitro* more than 90% of the leucine taken up is oxidized and less than 10% is used for protein synthesis (13,97).

Cerebral uptake of amino acids from the blood and their utilization for energy *in vivo,* however, are limited because of their relatively low concentrations in the arterial blood and the restrictions imposed by the blood-brain barrier. There is clearly uptake into brain of all radioactive amino acids administered intravascularly (5,98,100). Oldendorf and Szabo (100) demonstrated that the amino acids are transported into brain by three separate, saturable, stereospecific, carrier-mediated transport systems, one each for neutral, basic, and acidic amino acids (Chapter 10). Within each group there is competition among the various members so that the transport of any one amino acid is competitively inhibited by others of the class. Thus both the absolute and relative concentrations of the amino acids regulate their transport into brain. These transport systems are saturated at relatively low concentrations and have low maximal transport capacities when compared to the amounts needed for a significant contribution to energy metabolism.

Those amino acids essential to the brain (e.g., L-phenylalanine, L-tyrosine, L-leucine, L-valine, L-methionine, and L-threonine) are transported more effectively than the nonessential amino acids that can be synthesized by brain, e.g., L-asparate or L-glutamate (5,98; Table 10-1, Fig. 10-18). Measurements of cerebral arteriovenous differences of the individual amino acids in normal human subjects in the postabsorptive state have indicated measurable uptake of 15 of 16 amino acids tested; the exception was taurine (26). The uptake of the branched-chain amino acids tended in gen-

eral to be higher than those of the other amino acids (26). The largest single arteriovenous difference was for valine and equaled 19.3 μmol/liter of blood. The total for all the amino acids was 125 μmol/liter. When this value is compared with an average arteriovenous difference for glucose of approximately 560 μmol/liter (144,147) and allowance is made for the fact that much if not most of the amino acid uptake is for synthesis of proteins, neurotransmitters, etc., rather than oxidation, it is clear that exogenously supplied amino acids contribute relatively little to the gross energy metabolism of the brain. Even in the starved patients studied by Owen et al. (102), in whom cerebral glucose consumption was reduced to half, the total arteriovenous difference for α-amino nitrogenous compounds was statistically insignificant and at most could account for less than 10% of the total oxygen consumption.

MEASUREMENT OF LOCAL CEREBRAL BLOOD FLOW

The rates of blood flow and metabolism presented in Tables 1-1 and 1-2 and discussed above represent the average values in the brain as a whole. The brain is a heterogeneous organ, however, and is composed of almost innumerable structures and tissues that often function independently or even inversely with respect to one another and consist of widely divergent structural elements. Correspondingly, their local rates of blood flow and energy metabolism vary widely but under physiological conditions are closely correlated with one another (150).

The measurement of local rates of cerebral metabolism will be discussed below. Most of the methods for the measurement of local rates of cerebral blood flow have been based on the principles of inert gas exchange between blood and tissues developed by Kety (65). All these methods utilize a freely diffusible, chemically inert radioactive tracer that exchanges freely between blood and cerebral tissues. They are generally referred to as tissue indicator equilibration techniques and are essentially the same, differing only with respect to the species of radioactive tracer utilized, whether the procedure is carried out during saturation of the tissues with the tracer or clearance of the tracer from the tissues, and the nature of the computational routine employed.

Theory of Tissue Indicator Equilibration Technique

Kety's (65) principles of inert gas exchange were first applied to the measurement of local cerebral blood flow by Kety and his associates (29,67,73). The method is ultimately based on the Fick Principle, which states that the rate of change of the amount of a chemically inert tracer substance in the tissue under study is equal to the difference between the amounts brought to the tissue in the arterial blood and removed from it in the venous blood. This relationship can be expressed as follows:

$$dQ_i/dt = F(Ca - Cv) \qquad (1\text{-}1)$$

where Q_i is the quantity of tracer in tissue, i, F is the rate of blood flow through the tissue, and Ca and Cv are the tracer concentrations in the arterial blood and representative venous blood draining the tissue, respectively.

Dividing by tissue mass W:

$$dCi/dt = F/W(Ca - Cv) \qquad (1\text{-}2)$$

where Ci equals the tissue concentration of tracer.

For tissues that are homogeneous with respect to tissue perfusion rate and solubility of tracer, Kety (65) derived the following relationship between the tissue arteriovenous and arterial-tissue concentration differences:

$$(Ca - Cv) = m(Ca - Ci/\lambda) \qquad (1\text{-}3)$$

where λ equals the tissue/blood partition coefficient (Chapter 7) for the tracer and m is a constant between 0 and 1 that represents the net effect of diffusion limitations, capillary impermeability, arteriovenous shunts, and all other factors that might tend to limit the equilibration of the tissue with the blood perfusing it. In the absence of diffusion limitations, $m = 1$, and Eq. 1-3 simplifies to

$$Cv = (Ci/\lambda) \tag{1-4}$$

Substituting Eq. 1-3 into Eq. 1-2:

$$dCi/dt = \frac{mF}{\lambda W}(\lambda Ca - Ci) \tag{1-5}$$

Let $K = mF/\lambda W$, the so-called clearance constant.

Integrating Eq. 1-5 between time 0 and time T:

$$Ci(T) = Ci(0)e^{-KT} + \lambda K e^{-KT} \int_0^T Ca(t)e^{Kt}\,dt \tag{1-6}$$

Equation 1-6 is the general equation for all conditions for time courses of the arterial curve. In studies carried out during desaturation following a period of saturation, Eq. 1-6 can be used with the second term on the right side of the equation correcting for recirculation. Zero time is then the time of the onset of desaturation. This is the form generally used in ^{133}Xe clearance studies of regional cerebral blood flow in humans (77). If Ca drops to zero at zero time after a period of saturation, as is approximately so after an intracarotid injection of radioactive inert gas, then Eq. 1-6 reduces to

$$Ci(T) = Ci(0)e^{-KT} \tag{1-7}$$

The method has generally been applied during saturation when used with autoradiography in animals. In that case $Ci(0)$ equals zero, and Eq. 1-6 reduces to

$$Ci(T) = \lambda K e^{-KT} \int_0^T Ca(t)e^{Kt}\,dt \tag{1-8}$$

or, alternatively,

$$Ci(T) = \lambda K \int_0^T Ca(t)e^{-K(T-t)}\,dt \tag{1-9}$$

Equations 1-8 and 1-9 are the basis of the autoradiographic technique for measuring local cerebral blood flow. They state that if the time course of the arterial concentration of the tracer between time 0 and time T is measured, the tissue/blood partition coefficient is known, and the local tissue concentration of tracer at time T is measured, then the local clearance constant K can be computed. If there are no arteriovenous shunts and no diffusion limitations (i.e., $m = 1$), then the local blood flow can be calculated from the clearance constant by the relationship

$$K = mF/\lambda W$$

If the complete time course of the local tissue tracer concentration can also be measured, as it can with emission tomography, then the integrated form of Eq. 1-8 can be used. Thus

$$\int_0^T Ci(t)\,dt = \lambda\left[\int_0^T Ca(t)dt - e^{-KT}\int_0^T Ca(t)e^{Kt}\,dt\right] \tag{1-10}$$

[^{131}I]Trifluoroiodomethane Technique

Procedure

The first method for the measurement of local cerebral blood flow by the tissue indicator equilibration technique was the [^{131}I]trifluoroiodomethane ([^{131}I]CF_3I) technique (29,73). The tracer was the radioactive, relatively chemically stable gas, which could diffuse freely through the blood-brain barrier. The species was the cat. The tracer was administered by continuous intravenous infusion of a solution of the tracer in blood or physiological saline for 1 min during which timed arterial samples were

drawn. Arterial blood concentration of tracer was measured in a well-type crystal scintillation counter. At approximately 1 min after the onset of the infusion, the cat was decapitated, and the head was frozen as quickly as possible in liquid nitrogen. Local tissue concentrations of tracer were determined by a unique, new quantitative autoradiographic technique. Holes were drilled longitudinally through the extracerebral tissues of the frozen head and filled with 5% gelatin standards containing varying concentrations of $K^{131}I$, which were calibrated by crystal scintillation counting. The head was kept frozen with liquid nitrogen and cut in 0.5-cm coronal sections. These sections were then autoradiographed with X-ray film at −75°C. It was essential to keep the head and sections frozen at these low temperatures to avoid loss of the $[^{131}I]CF_3I$, which is volatile at temperatures above −15° but a solid at −75°C.

Local tissue/blood partition coefficients were determined in a separate group of cats. The animals were allowed to breathe a constant concentration of $[^{131}I]CF_3I$ in the inspired air for at least an hour until the arterial blood concentration had equilibrated with the inspired air and had remained constant for a sufficient period of time for the local cerebral tissues to come into equilibrium with the arterial blood. Blood samples were then drawn, and the cat was decapitated. Blood and local cerebral tissue concentrations of ^{131}I were then assayed by scintillation counting and quantitative autoradiography as described above, and the local tissue/blood partition coefficients λ were determined as the ratios of tissue to blood concentrations at equilibrium. The partition coefficients varied widely among the various structures of the brain, with values in white structures generally between 1.0 and 1.5 and values in gray structures between 0.7 and 1.0 (29).

From the values of the local partition coefficients, local tissue concentrations of tracer, and the time course of the arterial concentration corrected for the lag and the dead space washout of the arterial catheter (29), local clearance constants K were calculated by Eq. 1-8 or 1-9. Local rates of blood flow were calculated from the clearance constants by the relationship $K = mF/\lambda W$, with the assumptions that there were no arteriovenous shunts in brain, there were no diffusion limitations with the gaseous tracer, and $m = 1$.

Local Rates of Cerebral Blood Flow

The results obtained with the $[^{131}I]CF_3I$ technique demonstrated a wide distribution of rates of blood flow in the component structures of the conscious brain (Table 1-3). Blood flow in gray matter was generally three to four times that of values in white matter, but in gray matter there was a wide range, with the inferior colliculus exhibiting the highest rate of blood flow in the brain of the cat.

Under the conditions of the procedure (i.e., infusion of tracer for 1 min), the distribution of the tracer in the various structures of the brain reflects primarily their local perfusion rates. The autoradiographs, which are images of the distribution of the isotope, are therefore pictorial representations of the relative rates of blood flow in the component structures of the brain (Fig. 1-4).

Light thiopental anesthesia depressed blood flow in almost all gray matter structures, particularly in the primary sensory cortical regions, which in the conscious state had high perfusion rates (Table 1-3). The net effect of the anesthesia was to reduce blood flow differentially for the various structures and to produce a more uniform distribution of blood flow throughout the brain.

Effects of Functional Activity on Local Cerebral Blood Flow

The $[^{131}I]CF_3I$ technique demonstrated that there is a close relationship between the level of functional activity in discrete

TABLE 1-3. *Local cerebral blood flow in the cat*

Structure	Blood flow: mean ± SE (ml/g/min)	
	Conscious (10 cats)	Light thiopental anesthesia (11 cats)
Superficial cerebral structures		
Cortex		
Sensory-motor	1.38 ± 0.12	0.65 ± 0.07[a]
Auditory	1.30 ± 0.05	0.72 ± 0.07[a]
Visual	1.25 ± 0.06	0.77 ± 0.09[a]
Miscellaneous-association	0.88 ± 0.04	0.67 ± 0.06[a]
Olfactory	0.77 ± 0.06	0.62 ± 0.07
White matter	0.23 ± 0.02	0.26 ± 0.04
Deep cerebral structures		
Medial geniculate ganglion	1.22 ± 0.04	0.81 ± 0.09[a]
Lateral geniculate ganglion	1.21 ± 0.08	0.79 ± 0.07[a]
Caudate nucleus	1.10 ± 0.08	0.91 ± 0.11
Thalamus	1.03 ± 0.05	0.71 ± 0.09[a]
Hypothalamus	0.84 ± 0.05	0.55 ± 0.06[a]
Basal ganglia and amygdala	0.75 ± 0.03	0.58 ± 0.05[a]
Hippocampus	0.61 ± 0.03	0.59 ± 0.04
Optic tract	0.27 ± 0.02	0.22 ± 0.08
Midbrain and pons		
Inferior colliculus	1.80 ± 0.11	1.41 ± 0.14[a]
Superior olive	1.17 ± 0.13	1.56 ± 0.27
Superior colliculus	1.15 ± 0.07	0.82 ± 0.10[a]
Pontine gray	0.88 ± 0.04	0.61 ± 0.03[a]
Reticular formation	0.59 ± 0.05	0.49 ± 0.06
Pontine white	0.24 ± 0.02	0.31 ± 0.04
Cerebellum, medulla, and spinal cord		
Cerebellum		
Nuclei	0.79 ± 0.05	0.56 ± 0.08[a]
Cortex	0.69 ± 0.04	0.57 ± 0.05[a]
White matter	0.24 ± 0.01	0.29 ± 0.06
Medulla		
Vestibular nuclei	0.91 ± 0.04	0.84 ± 0.10
Cochlear nuclei	0.87 ± 0.07	0.99 ± 0.14
Pyramids	0.26 ± 0.02	0.28 ± 0.03
Spinal cord		
Gray matter	0.63 ± 0.04	0.53 ± 0.07
White matter	0.14 ± 0.02	0.15 ± 0.06

[a]Statistically significantly different from conscious control values ($p < 0.05$).
From Sokoloff (145).

structures of the brain and their rates of blood flow. Retinal stimulation by photoflash in the cat produced increases in local blood flow in the superior colliculi, lateral geniculate nuclei, and visual cortex (e.g., lateral gyrus) which were clearly visible in the autoradiographic images (Fig. 1-4) (145). These experiments produced, in fact, the first examples of imaging of local functional activity in the brain in animals. In a corresponding manner the development of positron emission tomography (PET) (104) provided the means to produce the first functional images of the human brain (106).

[^{14}C]Iodoantipyrine Technique

The basic principles of the tissue-tracer indicator equilibration technique were first applied to the measurement of local cerebral blood flow for use with the chemically inert, radioactive gas [^{131}I]trifluoroiodomethane, but they apply equally well to any

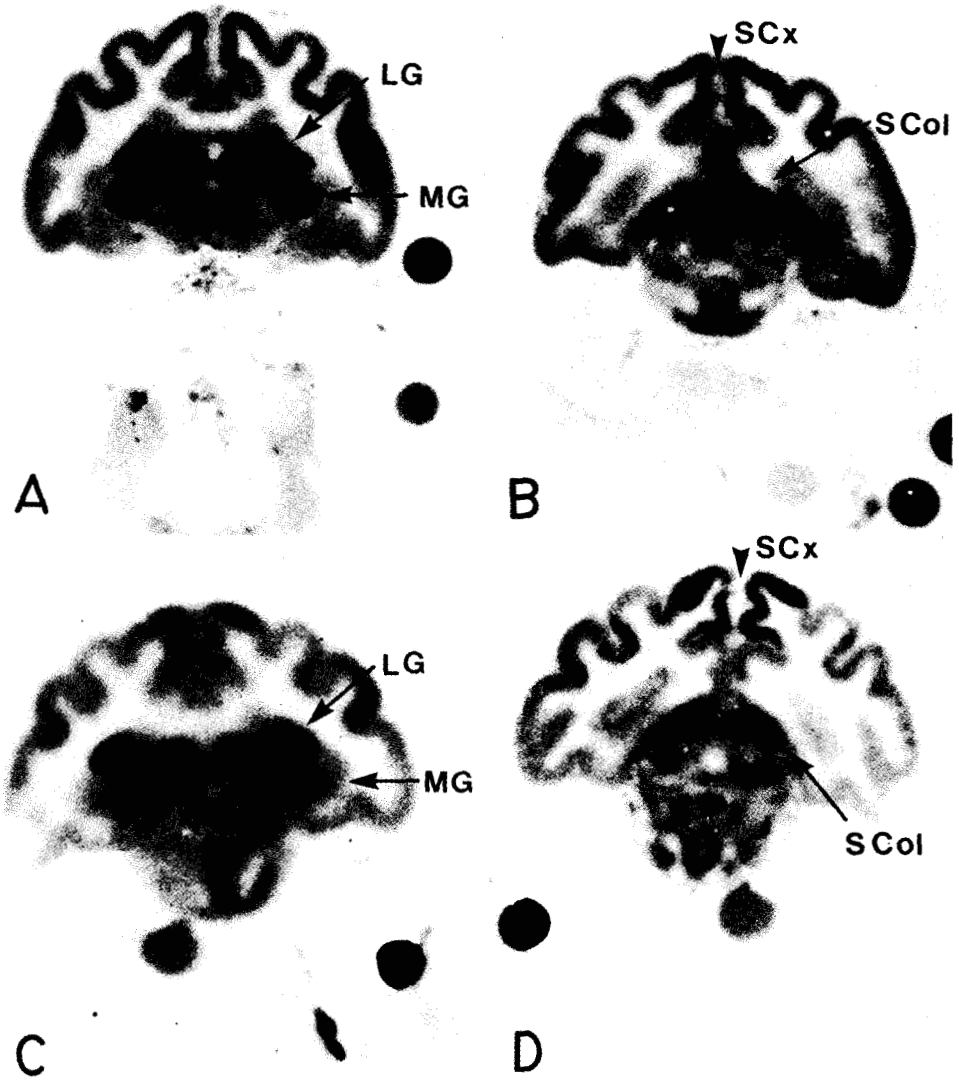

FIG. 1-4. Typical autoradiographs of sections of brains from conscious cats showing effects of different concentrations of radioactive gas, [^{131}I]trifluoroiodomethane, in the various cerebral structures. In general, the differences in optical density reflect differences in blood flow, the greater the density (i.e., darkness), the higher the blood flow (see text). Circular areas of uniform density represent calibrated ^{131}I-containing gelatin solutions used for quantitative densitometric analysis. **A:** Control experiment in blindfolded conscious cat. Note striate cortex (SCx) and lateral (LG) and medial geniculate (MG) nuclei. **B:** Autoradiograph from different brain section of the same cat. Note striate cortex and superior colliculi (SCol). **C:** Effects of 5 min of photic stimulation of the retina. Note marked increases in optical density of striate cortex and lateral geniculate nuclei relative to that of other structures such as medial geniculate nuclei. **D:** Autoradiograph from different brain section of same stimulated cat. Note the more prominent areas in the striate cortex and the superior colliculi. Courtesy of Sokoloff (145).

freely diffusible, chemically stable tracer. There were, in fact, a number of technical disadvantages associated with the use of [^{131}I]CF_3I. The radioactive gas was not commercially available, and because of the 8-day half-life of ^{131}I it had to be regularly synthesized and purified by relatively complex chemical procedures. The assay of a volatile tracer in blood and tissue, particularly by the autoradiographic technique, proved to be cumbersome. Also, the tissue/blood partition coefficient varied widely among the local cerebral tissues, and these varied further with the hematocrit (29). Finally, the autoradiographic resolution that was achieved with the radiations of ^{131}I from 0.5-cm frozen tissue sections was rather limited (Chapter 5). A commercially available nonvolatile ^{14}C-labeled tracer to substitute for [^{131}I]CF_3I was therefore sought. Reivich et al. (114) adapted the method for use with [^{14}C]antipyrine, which appeared to satisfy these requirements. It greatly enhanced the convenience of the technique and improved the quality of the autoradiographic images. The autoradiographic procedure was modified for use with ^{14}C and applied to dried brain sections, 20 μm in thickness, at room temperature. Because of the long half-life of ^{14}C, permanent ^{14}C-labeled plastic standards could be prepared and calibrated for quantitative calibration of the autoradiographic images. The autoradiographic procedure is described in detail below in the description of the procedure for the autoradiographic measurement of local cerebral glucose utilization with 2-[^{14}C]deoxyglucose and in Chapter 5.

Further experience with [^{14}C]antipyrine indicated, however, that it was not a completely suitable tracer for measurement of local cerebral blood flow. Its use led to values for local cerebral blood flow considerably below those obtained with radioactive gases (24,25). The problems with [^{14}C]antipyrine were demonstrated to arise from limitations in its diffusion through the blood-brain barrier, leading to values for m considerably less than 1.0 and therefore values for K that reflected not only blood flow but diffusion limitations as well (24).

The limitations of [^{14}C]antipyrine were overcome by the substitution of 4-iodo-[*N*-methyl-^{14}C]antipyrine as the tracer (121). Iodoantipyrine has a higher oil/water partition coefficient and is therefore more freely diffusible through the blood-brain barrier. An additional advantage of [^{14}C]iodoantipyrine is that its tissue/blood partition coefficient is uniform (0.8) in all the tissues of the central nervous system and does not vary with the hematocrit. The autoradiographic images represent, therefore, relative rates of blood flow uncontaminated by differences in solubility of the tracer in the tissues. In all respects, the procedure used with [^{14}C]iodoantipyrine is identical to that employed with [^{14}C]antipyrine. The values for local cerebral blood flow are essentially the same as those obtained with [^{131}I]trifluoroidomethane, and the [^{14}C]iodoantipyrine technique has now become the standard method for the measurement of local cerebral blood flow by autoradiography.

PRINCIPLES FOR MEASUREMENT OF RATES OF BIOCHEMICAL REACTIONS WITH RADIOISOTOPES *IN VIVO*

Radioisotopes are frequently used to facilitate the assay of biochemical reactions. Usually they are used to study chemical reactions *in vitro,* and the procedure is to label one of the reactants and to measure the rate of accumulation of a labeled product. From assay or knowledge of the specific activity of the reactant molecule, the rate of the overall reaction rate can be calculated from the rate of radioactive product formation. The application of this approach generally necessitates, however, specialized biochemical procedures to

identify and isolate the labeled product so as to limit the measurement of the radioactivity to a specific chemical product of the reaction.

Quantitative autoradiography makes it possible to measure the concentrations of isotopes in tissues of animals labeled *in vivo*. In a few cases, the administration of a judiciously selected labeled chemical compound and a properly designed procedure have made it possible to use this capability to measure the rate of a chemical process in animals *in vivo*. The development of emission tomography, and particularly of PET by Phelps et al. (104), provides a means to extend this capability to humans and to assay the rates of biochemical processes in human tissues *in vivo* (106; Chapter 6). Autoradiography and emission tomography do not, however, obviate the need to adhere to established principles of chemical and enzyme kinetics and tracer theory. Generally, all such methods, whether to be used in humans with PET or in animals with autoradiography, must first be developed by research in animals, because it is only in animals that the measurements needed to validate the basic assumptions of the method can be tested and evaluated.

A chemical reaction is the conversion of one species of molecule to another. The rate of this reaction can be measured by determining the rate of disappearance of one or more of the reactants or the rate of formation of one or more of the products. The addition of a radioactive label to one of the reactants in molecular concentrations too negligible to alter the kinetics of the reaction facilitates the measurement of either the reactants or the products, but it does not solve all the problems. The rate of chemical transformation of the labeled species can easily be measured, but this is not the rate of the reaction of interest. To derive the rate of the total reaction from measurement of the reaction rate of the labeled species, it is necessary to know the integrated specific activity (i.e., the ratio of labeled to total molecules) of the precursor pool. Occasionally the labeled species exhibits a kinetic difference from the natural compound, the so-called isotope effect; this isotope effect can be evaluated and appropriate correction made for it. The general equation for the determination of the rate of a biochemical reaction with radioactive tracers is presented in Fig. 1-5.

In assays of biochemical reactions *in vivo* it is generally impossible to measure the integrated specific activity of the precursor pool directly. This would require the measurement of the complete time courses of the concentrations of the labeled and unlabeled precursor molecules in the tissue at the enzyme site. It is therefore necessary to determine the precursor pool specific activity indirectly from measurements in the blood supplied to the tissue. The specific activity in the arterial blood or plasma can be readily measured directly, and the precursor-specific activity calculated from it by correcting for the lag in the equilibration of the precursor pool in the tissue with that of the plasma. To apply this correction it is necessary to know the kinetics of the equilibration process between the precursor pools in the tissue and plasma.

The rate of a chemical reaction can be determined by measurement of precursor disappearance or product accumulation; generally the errors are smaller with the latter measurement because the percent in-

$$\text{Rate of Reaction} = \frac{\text{Labeled Product Formed or Substrate Consumed in Interval of Time, 0 to T}}{\left[\begin{array}{c}\text{Isotope Effect} \\ \text{Correction Factor}\end{array}\right] \qquad \left[\begin{array}{c}\text{Integrated Specific Activity} \\ \text{of Precursor}\end{array}\right]}$$

FIG. 1-5. General equation for the determination of rates of biochemical reactions with radioisotopes (see text).

crease in amount of product is much greater than the percent loss in amount of precursor. Autoradiography and emission tomography, which measure only the total concentration of the radioactive molecules, cannot distinguish among the various chemical species that may be labeled, including the precursor and the possible labeled products. Strategies must therefore be developed that ensure that the radioactivity is contained exclusively in the precursor and/or in one or more of the products specific to the chemical reaction to be assayed. The labeled precursor should be so selected that its chemical transformations are limited only to the pathway under study.

These general principles have been more or less successfully applied in two currently operational methods for the measurement of energy metabolism in the nervous system of animals and humans. One method is the steady-state O_2 consumption technique (Chapters 7 and 11), which is based on the measurement of substrate disappearance (28). Cerebral blood flow is measured by PET with $C^{15}O_2$ and, when multiplied by arterial O_2 content, provides the steady-state delivery of O_2 to the tissues. Local cerebral O_2 extraction from the blood is measured by PET with $[^{15}O]O_2$. The product of local oxygen extraction, blood flow, and arterial O_2 content provides the values for local O_2 consumption. The other method is the radioactive deoxyglucose technique for the measurement of local cerebral glucose utilization. It has been used extensively in animals with quantitative autoradiography (152,154), but it has been adapted to humans by the use of [^{18}F]fluorodeoxyglucose and PET (105,115). The deoxyglucose technique is based on the measurement of product accumulation. Because it encompasses almost all the principles to be considered in the measurement of biochemical processes *in vivo,* it will serve as an informative example of their application. A comparable method, but one designed to measure local rates of cerebral protein synthesis, is currently under development (139,140), and it serves to illustrate an additional approach to the assay of biochemical processes *in vivo.*

DEOXYGLUCOSE METHOD

Theory

The method is derived from a model based on the biochemical properties of 2-deoxyglucose (Fig. 1-6A) (154). 2-Deoxyglucose (DG) is transported bidirectionally between blood and brain by the same carrier that transports glucose across the blood-brain barrier (4,9,98). In the cerebral tissues it is phosphorylated by hexokinase to 2-deoxyglucose-6-phosphate (DG-6-P) (156). Deoxyglucose and glucose are therefore competitive substrates for both blood-brain transport and hexokinase-catalyzed phosphorylation. However, unlike glucose-6-P, which is further metabolized eventually to CO_2 and water, and to a lesser degree via the hexosemonophosphate shunt, DG-6-P cannot be converted to fructose-6-phosphate and is not a substrate for glucose-6-P dehydrogenase (156). There is very little glucose-6-phosphatase activity in brain (44) and even less deoxyglucose-6-phosphatase activity (154). DG-6-P can be converted into deoxyglucose-1-P and then into uridine diphosphate (UDP)-deoxyglucose and eventually into glycogen, glycolipids, and glycoproteins, but these reactions are slow, and in mammalian tissues only a very small fraction of the DG-6-P formed proceeds to these products (92). In any case, these compounds are secondary, relatively stable products of DG-6-P, and all together represent the products of deoxyglucose phosphorylation. DG-6-P and its derivatives, once formed, are therefore essentially trapped in the cerebral tissues, at least long enough for the duration of the measurement.

If the interval of time following intrave-

nous administration of [^{14}C]deoxyglucose ([^{14}C]DG) is kept short enough (i.e., less than 1 hr) to allow the assumption of negligible loss of [^{14}C]deoxyglucose-6-phosphate ([^{14}C]DG-6-P) and/or its secondary products from the tissues, then the quantity of labeled products accumulated in any cerebral tissue at any given time following the introduction of [^{14}C]DG into the circulation is equal to the integral of the rate of

A

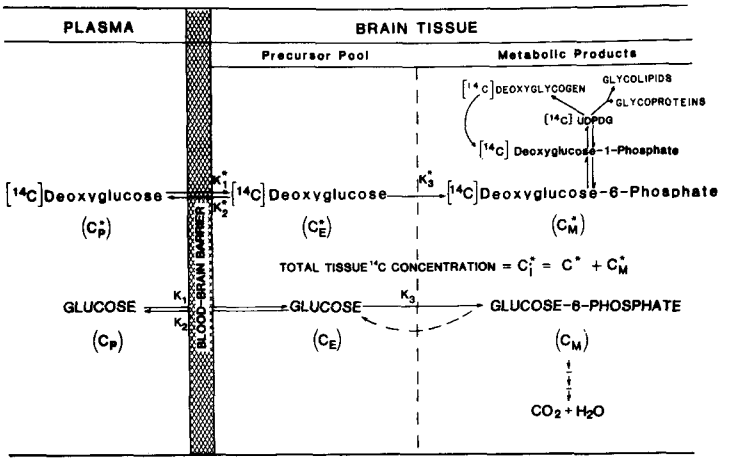

B

Functional Anatomy of the Operational Equation of the [^{14}C] Deoxyglucose Method

General Equation for Measurement of Reaction Rates with Tracers:

$$\text{Rate of Reaction} = \frac{\text{Labeled Product Formed in Interval of Time, 0 to T}}{\left[\begin{array}{c}\text{Isotope Effect}\\ \text{Correction Factor}\end{array}\right]\left[\begin{array}{c}\text{Integrated Specific Activity}\\ \text{of Precursor}\end{array}\right]}$$

Operational Equation of [^{14}C]Deoxyglucose Method:

$$R_i = \frac{\overbrace{\underbrace{C_i^*(T)}_{\substack{\text{Total } ^{14}\text{C in Tissue}\\ \text{at Time, T}}} - \underbrace{k_1^{\bullet}\, e^{-(k_2^*+k_3^*)T}\int_0^T C_p^*\, e^{(k_2^*+k_3^*)t}\,dt}_{^{14}\text{C in Precursor Remaining in Tissue at Time, T}}}^{\text{Labeled Product Formed in Interval of Time, 0 to T}}}{\underbrace{\left[\frac{\lambda \cdot V_m^* \cdot K_m}{\Phi \cdot V_m \cdot K_m^*}\right]}_{\substack{\text{"Isotope Effect"}\\ \text{Correction}\\ \text{Factor}}}\underbrace{\left[\int_0^T \left(\frac{C_p^*}{C_p}\right)dt}_{\substack{\text{Integrated Plasma}\\ \text{Specific Activity}}} - \underbrace{e^{-(k_2^*+k_3^*)T}\int_0^T \left(\frac{C_p^*}{C_p}\right)e^{(k_2^*+k_3^*)t}\,dt\right]}_{\substack{\text{Correction for Lag in Tissue}\\ \text{Equilibration with Plasma}}}}$$

Integrated Precursor Specific Activity in Tissue

[^{14}C]DG phosphorylation by hexokinase in that tissue during that interval of time. This integral is in turn related to the amount of glucose that has been phosphorylated over the same interval, depending on the time courses of the relative concentrations of [^{14}C]DG and glucose in the precursor pools and the Michaelis-Menten kinetic constants for hexokinase with respect to both [^{14}C]DG and glucose. With cerebral glucose consumption in a steady state, the amount of glucose phosphorylated during the interval of time equals the steady-state flux of glucose through the hexokinase-catalyzed step times the duration of the interval, and the net rate of flux of glucose through this step equals the rate of glucose utilization.

These relationships can be mathematically defined and an operational equation derived if the following assumptions are made: (a) a steady state for glucose (i.e., constant plasma glucose concentration and constant rate of glucose consumption) throughout the period of the procedure; (b) homogeneous tissue compartment within which the concentrations of [^{14}C]DG and glucose are uniform and exchange directly with the plasma; and (c) tracer concentrations of [^{14}C]DG and [^{14}C]DG-6-P (i.e., molecular concentrations of free [^{14}C]DG and [^{14}C]DG-6-P are negligibly small compared to those of glucose and glucose-6-P, respectively). The operational equation that defines R_i, the rate of glucose consumption per unit mass of tissue, i, in terms of measurable variables is presented in Fig. 1-6B.

The rate constants are determined in a separate group of animals by a nonlinear, iterative process that provides the least-squares best fit of an equation that defines the time course of total tissue ^{14}C concentration in terms of the time, the history of the plasma concentration, and the rate constants to the experimentally determined time courses of tissue and plasma concentrations of ^{14}C (154). The rate constants have thus far been completely determined only in normal conscious albino rats (Table 1-4). Partial analyses indicate that the values are quite similar in the conscious monkey (61), dog (20), cat (M. Miyaoka, J. Magnes, C. Kennedy, and L. Sokoloff, *unpublished data*), and human (49,105).

The λ, Φ, and the enzyme kinetic constants are grouped together to constitute a single, lumped constant (Fig. 1-6B). It can be shown mathematically that this lumped constant is equal to the asymptotic value of the product of the ratio of the cerebral extraction ratios of [^{14}C]DG and glucose and the ratio of the arterial blood to plasma spe-

FIG. 1-6. **A:** Diagrammatic representation of the theoretical model of the deoxyglucose method. C_i^* represents the total ^{14}C concentration in a single homogeneous tissue of the brain. C_P^* and C_P represent the concentrations of [^{14}C]DG and glucose in the arterial plasma, respectively; C_E^* and C_E represent their respective concentrations in the tissue pools that serve as substrates for hexokinase. C_M^* represents the combined concentration of [^{14}C]DG-6-P and its products in the tissue. The constants k_1^*, k_2^*, and k_3^* represent the rate constants for carrier-mediated transport of [^{14}C]DG from plasma to tissue, for carrier-mediated transport back from tissue to plasma, and for phosphorylation by hexokinase, respectively. The constants k_1, k_2, and k_3 are the equivalent rate constants for glucose. [^{14}C]DG and glucose share and compete for the carrier that transports both between plasma and tissue and for hexokinase, which phosphorylates them to their respective hexose-6-phosphates. The *dashed arrow* represents the possibility of glucose-6-P hydrolysis by glucose-6-Pase activity, if any. **B:** Operational equation of radioactive deoxyglucose method and its functional anatomy. T represents the time at the termination of the experimental period; λ equals the ratio of the distribution space of deoxyglucose in the tissue to that of glucose; Φ equals the fraction of glucose which, once phosphorylated, continues down the glycolytic pathway; and K_m^* and V_m^* and K_m and V_m represent the familiar Michaelis-Menten kinetic constants of hexokinase for deoxyglucose and glucose, respectively. The other symbols are the same as those defined in Fig. 1-6A. Note the similarity in the structures of the operational equation and of the general equation in Fig. 1-5. Courtesy of Sokoloff (149).

TABLE 1-4. *Values of rate constants for deoxyglucose in the normal conscious albino rat (N = 15)*[a]

Structure	Rate constants (min^{-1})			Distribution volume (ml/g)	Half-life of precursor pool (min)
	k_1^*	k_2^*	k_3^*	$k_1^*/(k_2^* + k_3^*)$	$Log_e 2/(k_2^* + k_3^*)$
Gray matter					
Visual cortex	0.189 ± 0.048	0.279 ± 0.176	0.063 ± 0.040	0.553	2.03
Auditory cortex	0.226 ± 0.068	0.241 ± 0.198	0.067 ± 0.057	0.734	2.25
Parietal cortex	0.194 ± 0.051	0.257 ± 0.175	0.062 ± 0.045	0.608	2.17
Sensory-motor cortex	0.193 ± 0.037	0.208 ± 0.112	0.049 ± 0.035	0.751	2.70
Thalamus	0.188 ± 0.045	0.218 ± 0.144	0.053 ± 0.043	0.694	2.56
Medial geniculate body	0.219 ± 0.055	0.259 ± 0.164	0.055 ± 0.040	0.697	2.21
Lateral geniculate body	0.172 ± 0.038	0.220 ± 0.134	0.055 ± 0.040	0.625	2.52
Hypothalamus	0.158 ± 0.032	0.226 ± 0.119	0.043 ± 0.032	0.587	2.58
Hippocampus	0.169 ± 0.043	0.260 ± 0.166	0.056 ± 0.040	0.535	2.19
Amygdala	0.149 ± 0.028	0.235 ± 0.109	0.032 ± 0.026	0.558	2.60
Caudate-putamen	0.176 ± 0.041	0.200 ± 0.140	0.061 ± 0.050	0.674	2.66
Superior colliculus	0.198 ± 0.054	0.240 ± 0.166	0.046 ± 0.042	0.692	2.42
Pontine gray matter	0.170 ± 0.040	0.246 ± 0.142	0.037 ± 0.033	0.601	2.45
Cerebellar cortex	0.225 ± 0.066	0.392 ± 0.229	0.059 ± 0.031	0.499	1.54
Cerebellar nucleus	0.207 ± 0.042	0.194 ± 0.111	0.038 ± 0.035	0.892	2.99
Mean +SEM	0.189 ± 0.012	0.245 ± 0.040	0.052 ± 0.010	0.647 ± 0.073	2.39 ± 0.40
White matter					
Corpus callosum	0.085 ± 0.015	0.135 ± 0.075	0.019 ± 0.033	0.552	4.50
Genu of corpus callosum	0.076 ± 0.013	0.131 ± 0.075	0.019 ± 0.034	0.507	4.62
Internal capsule	0.077 ± 0.015	0.134 ± 0.085	0.023 ± 0.039	0.490	4.41
Mean ±SEM	0.079 ± 0.008	0.133 ± 0.046	0.020 ± 0.020	0.516 ± 0.171	4.51 ± 0.90

[a]All errors are as the standard error of the mean (SEM).
From Sokoloff et al. (154).

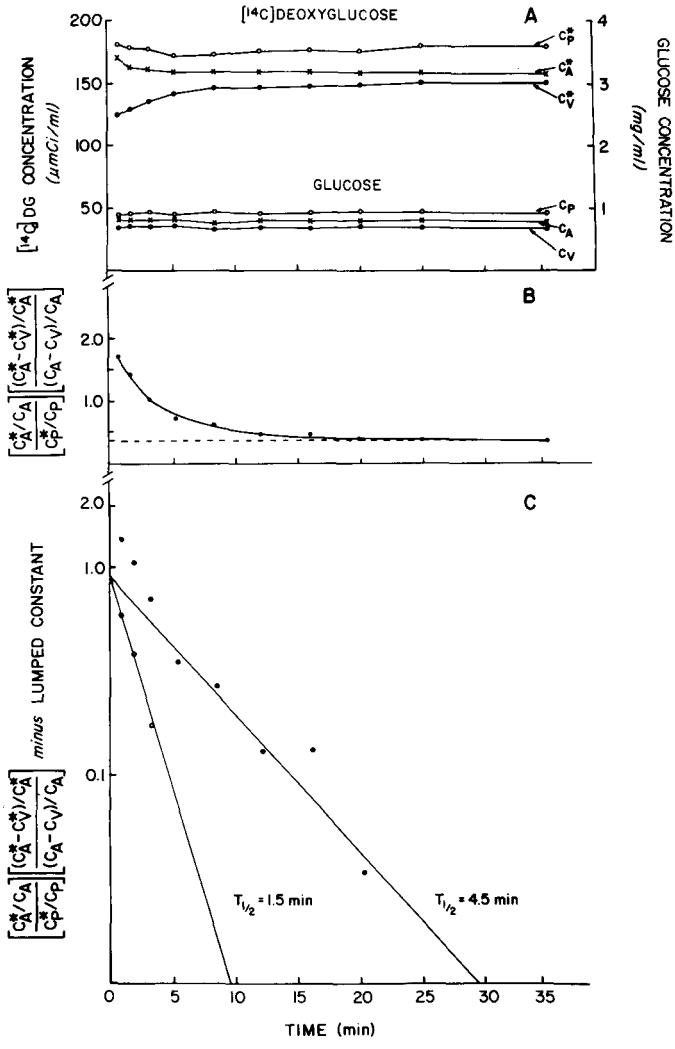

FIG. 1-7. Data obtained and their use in determination of the lumped constant and the combination of rate constants, $(k_2^* + k_3^*)$, in a representative experiment in a monkey. **A:** Time courses of arterial blood C_A and plasma C_P concentrations of [^{14}C]DG and glucose and cerebral venous blood C_V concentrations of [^{14}C]DG and glucose during programmed intravenous infusion of [^{14}C]DG designed to achieve and maintain a constant arterial plasma [^{14}C]DG concentration. **B:** Arithmetic plot of the function derived from the variables in (A) and combined as indicated in the formula on the ordinate against time. This function declines exponentially, with a rate constant equal to $(k_2^* + k_3^*)$, until it reaches an asymptotic value equal to the lumped constant 0.35 in this experiment *(dashed line).* **C:** Semilogarithmic plot of the curve in (B) less the lumped constant, i.e., its asymptotic value. ●, Actual values. This curve is analyzed into two components by a standard curve-peeling technique to yield the two *straight lines* representing the separate components. ○, Points for the fast component, obtained by subtracting the values for the slow component from the solid circles. The rate constants for these two components represent the values of $(k_2^* + k_3^*)$ for two compartments; the fast and slow compartments are assumed to represent gray and white matter, respectively. In this experiment the values for $(k_2^* + k_3^*)$ were found to equal 0.462 ($t_{1/2}$ = 1.5 min) and 0.154 ($t_{1/2}$ = 4.5 min) in gray and white matter, respectively. Courtesy of Kennedy et al. (61).

cific activities when the arterial plasma [^{14}C]DG concentration is maintained constant (154). The lumped constant is also determined in a separate group of animals from arterial and cerebral venous blood samples drawn during a programmed intravenous infusion that produces and maintains a constant arterial plasma [^{14}C]DG concentration (154). An example of such a determination in a conscious monkey is illustrated in Fig. 1-7. Thus far the lumped constant has been determined only in the albino rat, monkey, cat, dog, sheep, and human (Table 1-5). Under normal conditions the lumped constant appears to be characteristic of the species and does not appear to change significantly in a wide range of physiological conditions (Table 1-5) (154). It has been found to change in pathophysiological conditions, markedly in severe hypoglycemia (159), slightly in hyperglycemia (125), and whenever the rate of glucose utilization becomes limited by glucose supply as in status epilepticus.

Despite its complex appearance, the operational equation in Fig. 1-6B is really nothing more than a general statement of the standard relationship by which rates of enzyme-catalyzed reactions are determined from measurements made with radioactive tracers (Fig. 1-5; Chapter 7). The numerator of the equation represents the amount of radioactive product formed in a given interval of time; it is equal to C_1^*, the combined concentrations of [^{14}C]DG and [^{14}C]DG-6-P in the tissue at time T, measured by the quantitative autoradiographic technique, less a term that represents the free unmetabolized [^{14}C]DG still remaining in the tissue. The denominator represents the integrated specific activity of the precursor pool times a factor, the lumped constant, which is analogous to a correction factor for an isotope effect. The term with the exponential factor in the denominator takes into account the lag in the equilibration of the tissue precursor pool with the plasma.

TABLE 1-5. *Values of the lumped constant in several species*

Animal	No. of animals	Mean ± SD	SEM
Albino rat			
Conscious	15	0.464 ± 0.099[a]	± 0.026
Anesthetized	9	0.512 ± 0.118[a]	± 0.039
Conscious (5% CO_2)	2	0.463 ± 0.122[a]	± 0.086
Combined	26	0.481 ± 0.119	± 0.023
Rhesus monkey			
Conscious	7	0.344 ± 0.095	± 0.036
Cat			
Anesthetized	6	0.411 ± 0.013	± 0.005
Dog (beagle puppy)			
Conscious	7	0.558 ± 0.082	± 0.031
Sheep			
Fetus	5	0.416 ± 0.031	± 0.014
Newborn	4	0.382 ± 0.024	± 0.012
Mean	9	0.400 ± 0.033	± 0.011
Human			
Conscious	6	0.568 ± 0.105	± 0.043

[a]No statistically significant difference between normal conscious and anesthetized rats ($0.3 < p < 0.4$) and conscious rats breathing 5% CO_2 ($p > 0.9$).

The values were obtained as follows: rat, Sokoloff et al. (154); monkey, Kennedy et al. (61); cat, M. Miyaoka, J. Magnes, C. Kennedy, M. Shinohara, and L. Sokoloff *(unpublished data);* dog, Duffy et al. (20); sheep, R. Abrams et al. (1); humans, M. Reivich *(unpublished data).*

Procedure for Measurement of Local Cerebral Glucose Utilization

Theoretical Considerations in the Design of the Procedure

The operational equation of the method specifies the variables to be measured in order to determine R_i, the local rate of glucose consumption in the brain. The following variables are measured in each experiment: (a) the entire history of the arterial plasma [^{14}C]DG concentration C_P^*, from zero time to the time of killing T; (b) the steady-state arterial plasma glucose level C_P, over the same interval; and (c) the local concentration of ^{14}C in the tissue at the time of killing C_i^* (T). The rate constants k_1^*, k_2^*, and k_3^* and the lumped constant $\lambda\ V_m^* K_m / \Phi V_m K_m^*$ are not measured in each experiment; the values for these constants that are used are those determined separately in other groups of animals as described above and presented in Tables 1-4 and 1-5.

The operational equation is generally applicable with all types of arterial plasma [^{14}C]DG concentration curves. Its configuration, however, suggests that a declining curve approaching zero by the time of killing is the choice to minimize certain potential errors. The quantitative autoradiographic technique measures only total ^{14}C concentration in the tissue and does not distinguish between [^{14}C]DG-6-P and [^{14}C]DG. It is, however, [^{14}C]DG-6-P concentration that must be known to determine glucose consumption. [^{14}C]DG-6-P concentration is calculated in the numerator of the operational equation, which equals the total tissue ^{14}C content $C_i^*(T)$ minus the [^{14}C]DG concentration present in the tissue, estimated by the term containing the exponential factor and rate constants. In the denominator of the operational equation there is also a term containing an exponential factor and rate constants. Both these exponential terms have the useful property of approaching zero with increasing time if C_P^* is also allowed to approach zero. The rate constants k_1^*, k_2^*, and k_3^* are not measured in the same animals in which local glucose consumption is being measured, and the standard normal rate constants in Table 1-1 may not be equally applicable in all physiological, pharmacological, and pathological states. One possible solution is to redetermine the rate constants for each condition to be studied. An alternative solution, and the one chosen, is to administer the [^{14}C]DG as a single intravenous pulse at zero time and to allow sufficient time for the clearance of [^{14}C]DG from the plasma and the terms containing the rate constants to fall to levels too low to influence the final result. To wait until these terms reach zero is impractical because of the long time required and the risk of effects of the small but finite rate of loss of [^{14}C]DG-6-P from the tissues. A reasonable time interval is 45 min; by this time the plasma level has fallen to very low levels, and, on the basis of the values of ($k_2^* + k_3^*$) in Table 1-4, the exponential factors have declined through at least 10 half-lives, at least under physiological conditions (Fig. 1-8).

Experimental Protocol

The animals are prepared for the experiment by the insertion of polyethylene catheters in an artery and vein. Any convenient artery or vein can be used. In the rat the femoral or the tail arteries and veins have been found satisfactory. In the monkey and cat the femoral vessels are probably most convenient. The catheters are inserted under anesthesia, and anesthetic agents without long-lasting aftereffects should be used. Light halothane anesthesia with or without supplementation with nitrous oxide has been found to be quite satisfactory. At least 2 hr are allowed for recovery from the surgery and anesthesia before initiation of the experiment.

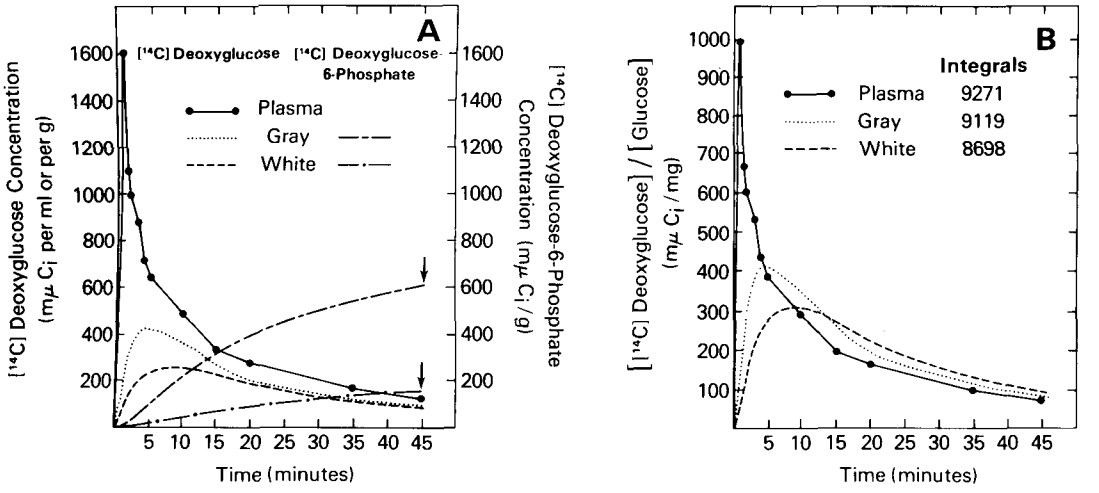

FIG. 1-8. Graphical representation of the significant variables in the operational equation used to calculate local cerebral glucose utilization. **A:** Time courses of [^{14}C]DG concentrations in arterial plasma and in average gray and white matter and [^{14}C]DG-6-P concentrations in average gray and white matter following an intravenous pulse of 50 μCi of [^{14}C]DG. The plasma curve is derived from measurements of plasma [^{14}C]DG concentrations. The tissue [^{14}C]DG concentrations were calculated from the plasma curve and the mean values of k_1^*, k_2^*, and k_3^* for gray and white matter in Table 1-1 according to the second term in the numerator of the operational equation. The [^{14}C]DG-6-P concentrations in the tissues were calculated from the mean values of k_3^* and the integral of the [^{14}C]DG concentrations in the tissues. The *arrows* point to the concentrations of [^{14}C]DG and [^{14}C]DG-6-P in the tissues at the time of killing; the autoradiographic technique measures the total ^{14}C content (i.e., the sum of these concentrations) at that time, which is equal to $C_1^*(T)$, the first term in the numerator of the operational equation. Note that at the time of killing, the total ^{14}C content represents mainly [^{14}C]DG-6-P concentration, especially in gray matter. **B:** Time courses of ratios of [^{14}C]DG to glucose concentrations (i.e., specific activities) in plasma and average gray and white matter. The curve for plasma was determined by division of the plasma curve in (A) by the plasma glucose concentrations. The curves for the tissues were calculated by the derivative of the function in the right set of brackets in the denominator of the operational equation. The integrals in (B) are the integrals of the specific activities with respect to time and represent the areas under the curves over the 45-min period. The integrals under the tissue curves are equivalent to all of the denominator of the operational equation, except for the lumped constant. Note that by the time of killing, the integrals of the tissue curves approach equality with each other and with that of the plasma curve.

The design of the experimental procedure for the measurement of local cerebral glucose utilization was based on the theoretical considerations discussed above. At zero time a pulse of 125 μCi (no more than 2.5 μmol) of [^{14}C]DG/kg body weight is administered to the animal via the venous catheter. Arterial sampling is initiated with the onset of the pulse, and timed 50- to 100-μl samples of arterial blood are collected consecutively as rapidly as possible during the early period so as not to miss the peak of the arterial curve. Arterial sampling is continued at less frequent intervals later in the experimental period but at sufficient frequency to define fully the arterial curve. The arterial blood samples are immediately centrifuged to separate the plasma, which is stored on ice until assayed for [^{14}C]DG concentration by liquid scintillation counting and glucose concentration by standard enzymatic methods. At approximately 45 min the animal is decapitated and the brain is removed and frozen in Freon XII or iso-

pentane maintained between −50 and −70°C with liquid nitrogen. When fully frozen, the brain is stored at −70°C until sectioned and autoradiographed. The experimental period may be limited to 30 min. This is theoretically permissible and may sometimes be necessary for reasons of experimental expediency, but greater errors due to possible inaccuracies in the rate constants may result.

Autoradiographic Measurement of Tissue ^{14}C Concentration

The ^{14}C concentrations in localized regions of the brain are measured by a modification of the quantitative autoradiographic technique previously described (114; Chapter 5). The frozen brain is coated with chilled embedding medium (Lipshaw Manufacturing Co., Detroit, MI) and fixed to object holders appropriate to the microtome to be used. Brain sections, precisely 20 μm in thickness, are cut in a cryostat maintained at −21 to −22°C. The brain sections are picked up on glass cover slips, dried on a hot plate at 60°C for at least 5 min, and placed sequentially in an X-ray cassette. A set of [^{14}C]methyl methacrylate standards (Amersham Corp., Arlington Heights, IL), which include a blank and a series of progressively increasing ^{14}C concentrations, are also placed in the cassette. These standards must previously have been calibrated for their autoradiographic equivalence to the ^{14}C concentrations in brain sections 20 μm in thickness prepared as described above. The method of calibration has been previously described (114).

Autoradiographs are prepared from these sections directly in the X-ray cassette with Kodak single-coated, blue-sensitive medical X-ray film, Type SB-5 (Eastman Kodak Co., Rochester, NY). The exposure time is generally 5 to 6 days with the doses used as described above, and the exposed films are developed according to the instructions supplied with the film. The SB-5 X-ray film is rapid but coarse-grained. For finer-grained autoradiographs, and therefore better defined images with higher resolution, it is possible to use mammographic films, such as DuPont LoDose or Kodak MR-1 films, or fine-grain panchromatic film, such as Kodak Plus-X, but the exposure times are two to three times longer.

The autoradiographs provide a pictorial representation of the relative ^{14}C concentrations in the various cerebral structures and the plastic standards (Fig. 1-9). A calibration curve of the relationship between optical density and tissue ^{14}C concentration for each film is obtained by densitometric measurements of the portions of the film representing the various standards. The local tissue concentrations are then determined from the calibration curve and the optical densities of the film in the regions representing the cerebral structures of interest. Local cerebral glucose utilization is calculated from the local tissue concentrations of ^{14}C and the plasma [^{14}C]DG and glucose concentrations according to the operational equation (Fig. 1-6B).

Theoretical and Practical Considerations

The design of the deoxyglucose method is based on an operational equation, derived by the mathematical analysis of a model of the biochemical behavior of [^{14}C]DG and glucose in brain (Fig. 1-6). Although the model and its mathematical analysis are as rigorous and comprehensive as reasonably possible, it must be recognized that models almost always represent idealized situations and cannot possibly take into account all the known, let alone the unknown, properties of a complex biological system. Several years have now passed since the introduction of the deoxyglucose method, and numerous applications of it have been made. The results of this experience generally establish the validity and worth of the method, but there

FIG. 1-9. [^{14}C]DG autoradiograph of serial cornal sections of conscious rat brain and of calibrated [^{14}C]methyl methacrylate standards used to quantify ^{14}C concentration in tissues.

are some potential problems in special situations that require further theoretical and practical considerations.

The main potential sources of error are the rate constants and the lumped constant. The problem with them is that they are not determined in the same animals and at the same time when local cerebral glucose utilization is being measured. They are measured in separate groups of comparable animals and then used subsequently in other animals in which glucose utilization is being measured. The part played by these constants in the method is defined by their role in the operational equation of the method (Fig. 1-6).

Rate Constants

The rate constants k_1^*, k_2^*, and k_3^* for deoxyglucose have been fully determined for various cerebral tissues in the normal conscious albino rat (154) (Table 1-4), but they appear to be similar in other species. All the rate constants vary considerably from tissue to tissue, but the variation among gray structures and among white structures is considerably less than the differences between the two types of tissues (Table 1-4). The rate constants k_2^* and k_3^* appear in the equation only as their sum, and $(k_2^* + k_3^*)$ is equal to the rate constant for the turnover of the free [^{14}C]DG pool in the tissue. The half-life of the free [^{14}C]DG pool can then be calculated by dividing $(k_2^* + k_3^*)$ into the natural logarithm of 2 and has been found to average 2.4 min in gray matter and 4.5 min in white matter in the normal conscious rat (Table 1-4).

The rate constants not only vary from structure to structure but also can be expected to vary with the condition. For example, k_1^* and k_2^* are influenced by both blood flow and transport of [^{14}C]DG across the blood-brain barrier, and because of the competition for the transport carrier, the glucose concentrations in the plasma and tissue affect the transport of [^{14}C]DG and therefore also k_1^* and k_2^*. The constant k_3^* is related to phosphorylation of [^{14}C]DG and will certainly change when glucose utilization is altered. To minimize potential errors due to inaccuracies in the values of the rate constants used, it was decided to sacrifice time resolution for accuracy. If the [^{14}C]DG is given as an intravenous pulse and sufficient time is allowed for the plasma to be cleared of the tracer, then the influence of the rate constants and of the functions that they represent on the final result diminishes with increasing time until ultimately it becomes zero. This relationship is implicit in the structure of the operational equation (Fig. 1-6B); as C_p^* approaches zero, the terms containing the rate constants also approach zero with increasing time. The significance of this relationship is graphically illustrated in Fig. 1-10. From typical arterial plasma [^{14}C]DG and glucose concentration curves obtained in a normal conscious rat, the portion of the denominator of the operational equation underlined by the heavy bar was computed with a wide range of values for $(k_2^* + k_3^*)$ as a function of time. The values for $(k_2^* + k_3^*)$ are presented as their equivalent half-lives calculated as described above. The values of $(k_2^* + k_3^*)$ vary from infinite (i.e., $T_{1/2} = 0$ min) to 0.14/min (i.e., 14%/min and $T_{1/2} = 5$ min) and more than cover the range of values to be expected under physiological conditions. The portion of the equation underlined and computed represents the integral of the precursor pool specific activity in the tissue. The curves represent the time course of this function, one each for every value of $(k_2^* + k_3^*)$ examined. It can be seen that these curves are widely different at early times but converge with increasing time until at 45 min the differences over the entire range of $(k_2^* + k_3^*)$ equal only a small fraction of the value of the integral. These curves demonstrate that at short times enormous errors can occur if the values of the rate constants are not precisely known, but only negligible errors

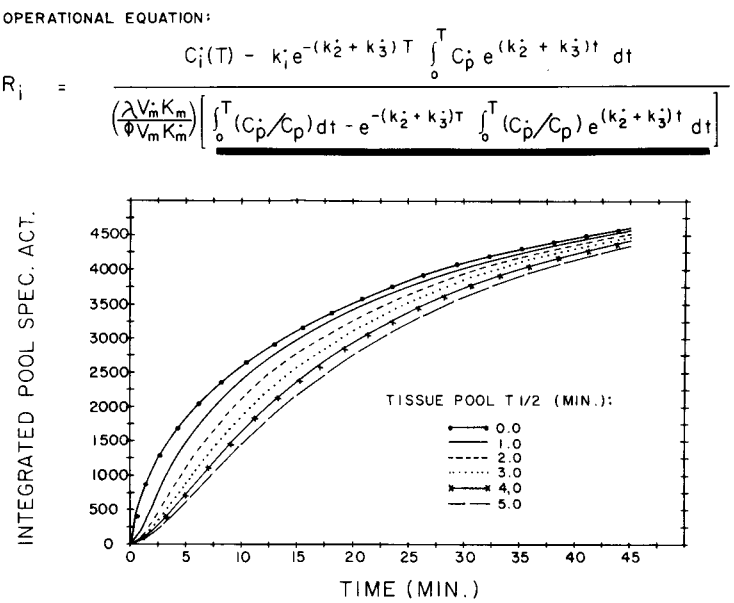

FIG. 1-10. Influence of time and rate constants ($k_2^* + k_3^*$) on integrated precursor pool specific activity in a normal conscious rat given an intravenous pulse of 50 μCi of [^{14}C]DG at zero time. The time courses of the arterial plasma [^{14}C]DG and glucose concentrations were measured following the pulse. The portion of the equation *underlined,* corresponding to integrated precursor pool specific activity, was computed as a function of time with different values of ($k_2^* + k_3^*$), as indicated by their equivalent half-lives, calculated according to $t_{1/2} = 0.693/(k_2^* + k_3^*)$. Courtesy of Sokoloff (151).

occur at 45 min, even over a wide range of rate constants of severalfold. In fact, it was precisely for this reason that [^{14}C]DG rather than [^{14}C]glucose was selected as the tracer for glucose metabolism. The relationships are similar for glucose. Because the products of [^{14}C]glucose metabolism are so rapidly lost from the tissues, it is necessary to limit the experimental period to short times when enormous errors can occur if the rate constants are not precisely known for each individual structure. [^{14}C]DG permits the prolongation of the experimental period to times when inaccuracies in rate constants have little effect on the final result.

It should be noted, however, that in pathological conditions, such as severe ischemia or hyperglycemia, the rate constants may fall far below the range examined in Fig. 1-10. There is evidence, for example, that this occurs with hyperglycemia and ischemia (42). Also in conditions of markedly depressed cerebral glucose utilization and/or slow clearance of the [^{14}C]DG from the plasma, the second term in the numerator, which contains the rate constants, may not be much smaller than $C_i^*(T)$, the first term in the numerator. Inaccuracies in the rate constants may then produce considerable errors in the numerator. In such abnormal conditions it is necessary and feasible to redetermine the rate constants for the particular condition under study (42) or else to prolong the experimental period to allow more time for the exponential terms to diminish further and correct for the loss of [^{14}C]DG-6-P that would then occur (49,105,153).

Lumped Constant

The lumped constant is composed of six separate constants. One of these, Φ, is a

measure of the steady-state hydrolysis of glucose-6-P to free glucose and phosphate. Because in normal brain tissue there is little such phosphohydrolase activity (44), Φ is normally approximately equal to unity. The other components are arranged in three ratios: λ, which is the ratio of distribution spaces in the tissue for deoxyglucose and glucose; V_m^*/V_m; and K_m/K_m^*. Although each individual constant may vary from structure to structure and condition to condition, it is likely that the ratios tend to remain the same under normal physiological conditions. For reasons described in detail previously (154), it is reasonable to believe that the lumped constant is the same throughout the brain and more or less characteristic of the species of animal under normal physiological conditions. Empirical experience thus far indicates that it is generally so, except in special pathophysiological states. The greatest experience has been accumulated in the albino rat. In this species the lumped constant for the brain as a whole has been determined under a variety of conditions (154). In the normal conscious rat local cerebral glucose utilization, determined by the [^{14}C]DG method with the single value of the lumped constant for the brain as a whole, correlates almost perfectly ($r = 0.96$) with local cerebral blood flow, measured by the [^{14}C]iodoantipyrine method, an entirely independent method (150). It is generally recognized that local blood flow is adjusted to local metabolic rate, but if the single value of the lumped constant did not apply to the individual structures studied, then errors in local glucose utilization would occur that might be expected to obscure the correlation. Also, the lumped constant has been directly determined in the albino rat in the normal conscious state, under barbiturate anesthesia, and during the inhalation of 5% CO_2; no significant differences were observed (Table 1-5). The lumped constant does vary with the species of animal. It has now also been determined in the rhesus monkey (61), cat (M. Miyaoka, J. Magnes, C. Kennedy, M. Shinohara, and L. Sokoloff, *unpublished data*), beagle puppy (20), sheep (1), and human (M. Reivich, *unpublished data*), and each species has a different value (Table 1-5). The values for local rates of glucose utilization determined with these lumped constants in these species are very close to what might be expected from measurement of energy metabolism in the brain as a whole by other methods (Table 1-6).

Although there is as yet no experimental evidence of more than negligible changes in the lumped constant under physiological conditions, it certainly does change in pathophysiological states. In severe hypoglycemia there is a progressive and appreciable increase in the lumped constant with falling plasma glucose concentration (159), and in severe hyperglycemia there is a small decrease (125). Indeed, theoretically the lumped constant could be expected to change whenever there is an alteration in the balance between glucose supply to the tissue and the tissue's rate of glucose utilization. It is only when the rate of glucose utilization becomes limited by the supply, however, that a major change in the lumped constant occurs. Also, tissue damage may disrupt the normal cellular compartmentation, and there is no assurance that λ, the ratio of the distribution spaces for [^{14}C]DG and glucose, is the same in damaged tissue as in normal tissue. In pathological states there may be release of lysosomal acid hydrolases that may hydrolyze glucose-6-P and thus alter the value of Φ. It is necessary, therefore, to determine the lumped constant in each pathological or pathophysiological state.

Glucose-6-Phosphatase

Glucose-6-phosphatase (glucose-6-Pase) activity is known to be very low in brain (44), and almost all the textbooks of biochemistry attest to this fact. Although low, some activity is present, but it appears to have no influence on the deoxyglucose

TABLE 1-6. *Representative values for local cerebral glucose utilization in the normal conscious albino rat and monkey (μmol/100 g/min)*

Structure	Albino rat (10)[a]	Monkey (7)[b]
Gray matter		
Visual cortex	107 ± 6	59 ± 2
Auditory cortex	162 ± 5	79 ± 4
Parietal cortex	112 ± 5	47 ± 4
Sensory-motor cortex	120 ± 5	44 ± 3
Thalamus: lateral nucleus	116 ± 5	54 ± 2
Thalamus: ventral nucleus	109 ± 5	43 ± 2
Medial geniculate body	131 ± 5	65 ± 3
Lateral geniculate body	96 ± 5	39 ± 1
Hypothalamus	54 ± 2	25 ± 1
Mamillary body	121 ± 5	57 ± 3
Hippocampus	79 ± 3	39 ± 2
Amygdala	52 ± 2	25 ± 2
Caudate-putamen	110 ± 4	52 ± 3
Nucleus accumbens	82 ± 3	36 ± 2
Globus pallidus	58 ± 2	26 ± 2
Substantia nigra	58 ± 3	29 ± 2
Vestibular nucleus	128 ± 5	66 ± 3
Cochlear nucleus	113 ± 7	51 ± 3
Superior olivary nucleus	133 ± 7	63 ± 4
Inferior colliculus	197 ± 10	103 ± 6
Superior colliculus	95 ± 5	55 ± 4
Pontine gray matter	62 ± 3	28 ± 1
Cerebellar cortex	57 ± 2	31 ± 2
Cerebellar nuclei	100 ± 4	45 ± 2
White matter		
Corpus callosum	40 ± 2	11 ± 1
Internal capsule	33 ± 2	13 ± 1
Cerebellar white matter	37 ± 2	12 ± 1
Weighted average for whole brain	68 ± 3	36 ± 1

The values are the means ± SEM from measurements made in the number of animals indicated in parentheses.
[a]From Sokoloff et al. (154).
[b]From Kennedy et al. (61).

method if the experimental period is limited to the prescribed duration, 45 min. Beyond this time its effects begin to appear, increasing in magnitude with increasing time. Significant glucose-6-Pase would affect the results by hydrolyzing the [^{14}C]DG-6-P and causing loss of product, and its effect would be accumulative with increasing time. If its activity were significant, it would cause the calculated rates of glucose utilization to be too low and to become progressively lower with increasing time. None of this happens in the first 45 min. In groups of rats studied over 20-, 30-, and 45-min periods, the calculated rates of glucose utilization remained constant (153). Also, by determining the average glucose utilization of all the structures in the brain weighted for their relative sizes, it is possible to obtain the weighted average glucose utilization of the brain as a whole and to compare this with the values obtained by the Kety-Schmidt method, the recognized standard method for measuring blood flow and energy metabolism of the brain as a whole by the Fick Principle (69). The deoxyglucose method provides values that are almost exactly those obtained with the

Kety-Schmidt method (Table 1-6). There is therefore no detectable influence of glucose-6-Pase during the first 45 min after the pulse of deoxyglucose because the values for glucose utilization that are obtained are not too low, nor do they decrease with time over that interval. After 45 min, however, effects of glucose-6-Pase begin to appear and become progressively greater with increasing time (153). The time course of the effects is compatible with the intracellular distributions of the [^{14}C]DG-6-P and the phosphatase. The [^{14}C]DG-6-P is formed in the cytosol, but the phosphatase is on the inner surface of the cisterns of the endoplasmic reticulum. The [^{14}C]DG-6-P must first be formed in the cytosol and then transported across the endoplasmic reticular membrane by a specific carrier before the phosphatase can act to hydrolyze it. The kinetics of this process, namely, a lag with zero phosphatase activity followed by progressively increasing activity, are exactly those to be expected from the separate compartmentalization of substrate and enzyme and a rate-limiting transport of the substrate across the membrane to the enzyme. This compartmentalization therefore allows a period of grace before the phosphatase can act on the DG-6-P, and it is a prolonged period of grace because, as Karnovsky and his associates (M. Karnovsky, *personal communication*) have found, the carrier for glucose-6-phosphate and DG-6-P is essentially absent in rat brain. The substrate then has access to the enzyme only by slow diffusion through the membrane.

If one extends the experimental period beyond 45 min, then correction must be made for the effects of phosphatase. It is a common misconception that phosphatase activity would invalidate the deoxyglucose method. It would not. In the original version, the model and the operational equation did not take phosphatase activity into account because the evidence described above indicated that there was no reason to do so, as long as the experimental period was limited to 45 min, which was the maximum period contemplated. It is a simple matter, however, to modify slightly the model and the derived operational equation to include a k_4^*, a rate constant for the phosphatase activity (49,105,153). It has been shown in humans with PET and [^{18}F]fluorodeoxyglucose that with inclusion of the dephosphorylation reaction the stability of the estimate of glucose utilization is achieved for periods of 3 hr or longer to within the statistical accuracy of the measurements ($\pm$4%) (49,105).

The evidence above, and other evidence as well, clearly indicates that phosphatase activity is of no significance to the deoxyglucose method if it is carried out within the prescribed 45 min. There have been three reports alleging that phosphatase activity is a major source of error in the deoxyglucose method. Two of these are glaring examples of misinterpretation or mishandling of their own experimental data or of obvious artifacts. In the first of these, Hawkins and Miller (41) applied the [^{14}C]DG technique to a series of rats but killed them at various times up to 45 min after the intravenous pulse of [^{14}C]DG and measured the [^{14}C]DG-6-P concentrations in the brains as a function of time by direct chemical analysis. They also measured the time courses of the arterial plasma [^{14}C]DG and glucose concentrations up to the time of killing, and with these data they used a transposed version of the operational equation (Fig. 1-6) of the method to calculate the theoretical time course of the brain [^{14}C]DG-6-P concentration (i.e., the numerator of the operational equation) predicted by the equation, which assumes no loss of [^{14}C]DG-6-P due to phosphatase activity or any other process. The computed theoretical curve that they published was two to three times higher than their measured concentrations, and they interpreted their results as proof that there was enormous loss of [^{14}C]DG-6-P during the exper-

imental period. Their computed theoretical curve was erroneous, however, because of a succession of errors, compounded one upon another, that led to their misinterpretation. To compute the [^{14}C]DG-6-P concentrations with the transposed equation it was necessary for them to assume values for the rate of glucose utilization and the lumped constant. They assumed a reasonable value, 0.7 to 0.8 μmol/g/min for the glucose utilization. For the lumped constant, however, they used a value of 1.1 to 1.25, which was two to three times greater than 0.48, the value experimentally measured in rats and reported (154). The use of the erroneous lumped constant was the direct result of an earlier error. They calculated the lumped constant at different times by dividing into the measured [^{14}C]DG-6-P concentration the product of the rate of glucose utilization and the integrated plasma specific activity corrected for the lag of the tissue behind the plasma. This calculation is based on another transposition of the operational equation of the method and is in principle valid. Again they assumed the reasonable value of 0.7 to 0.8 μmol/g/min for glucose utilization. The calculated plasma specific activity was wrong, however, because they did not measure the [^{14}C]DG concentration in the plasma during the first minute after the intravenous pulse of [^{14}C]DG. Instead, they extrapolated the arterial curve to zero time semilogarithmically from the measured values at 1 min and 2 min after the pulse. By doing so, they cut off the peak under the arterial curve that occurs within the first minute after the pulse and thereby lost a significant portion of the arterial specific activity curve during the first 5 min. In calculating the lumped constant, they therefore divided by too small a value for the integrated plasma specific activity during the first 5 min, but with increasing time the lost portion under the plasma specific activity curve became less significant and had less effect. This led to their erroneous conclusion that the lumped constant decreases with time; the decrease is due to diminishing influence of the error introduced by their failure to include the early peak in the arterial curve. The lumped constant that they used in their calculation of the theoretical tissue [^{14}C]DG-6-P curve was the most erroneous one of all, the one obtained at 5 min and equal to 1.1 to 1.25. When the theoretical curve for brain [^{14}C]DG-6-P concentrations is calculated from their data with the correct lumped constant, 0.48, the one that was directly measured (Table 1-5) and equal to the one they also found at 45 min, then the curve fits their measured values remarkably well, proving, contrary to their published conclusion, that there is no detectable loss of [^{14}C]DG-6-P from brain due to phosphatase activity or any other cause during the first 45 min after the pulse of [^{14}C]DG.

In the second report Sacks et al. (120) infused [^{14}C]glucose-6-P intravenously and measured cerebral arteriovenous differences of [^{14}C]glucose-6-P and [^{14}C]glucose during the infusion. They reported positive arteriovenous differences for the [^{14}C]glucose-6-P and negative arteriovenous differences for the [^{14}C]glucose, which they interpreted as evidence that the brain was taking up the [^{14}C]glucose-6-P, hydrolyzing it, and releasing [^{14}C]glucose as a result of phosphatase activity. It is generally recognized that hexose phosphates cannot cross the blood-brain barrier, and this has been confirmed by recent experiments (T. Nelson, G. Lucignani, and L. Sokoloff, *unpublished data*). When glucose-6-P labeled with ^{32}P is continuously infused for up to 10 min, no ^{32}P is found in brain above the levels present in the blood in the brain. Measurements of the brain uptake index by the Oldendorf technique (A. McCall, *personal communication*) or by the single pass extraction technique of Crone (T. Nelson, G. Lucignani, and L. Sokoloff, *unpublished data*) show that the transport of glucose-6-P across the blood-brain barrier is like that

of sucrose, which is essentially zero. There must have been some artifact in the experiments of Sacks et al. (120), because it would be an incredible feat for phosphatase in brain to hydrolyze a substance circulating in the blood that cannot cross the blood-brain barrier and have access to the enzyme.

The third report is by Huang and Veech (48), who injected in rats a mixture of [2-^{3}H]glucose and [U-^{14}C]glucose as a pulse into a carotid artery, removed the brains at various times up to 5 min later, and assayed the tissue glucose content for the ^{3}H/^{14}C ratio in it. The principle is as follows: any [2-^{3}H]glucose that reaches the fructose-6-P step in glycolysis loses the ^{3}H label, but [^{14}C]fructose-6-P does not lose the ^{14}C label. By the back reaction some fructose-6-P is converted to glucose-6-P, and if there is phosphatase activity the glucose moiety enters the glucose pool without losing the ^{14}C label, but without the ^{3}H label. The ^{3}H/^{14}C ratio in the glucose pool should then fall in case of phosphatase activity, and this is what they claim to have observed. There are problems, however, with their experiments that raise serious questions about their conclusions. The technique is technically difficult and fraught with numerous sources of artifacts. A key problem is the separation of glucose from all the other possible labeled products of glucose in the brain tissue to ensure that the ^{3}H and ^{14}C measurements are truly in glucose and nothing else; other labeled products, if present, could lead to the same results without the need to invoke phosphatase activity. In fact, when the procedure of Huang and Veech (48) is applied to rats with careful attention to ensure purity of the glucose fraction, there is no change in the ^{3}H/^{14}C ratio of the glucose in brain with time from the initial ratio present in the injection solution (T. Nelson, G. Lucignani, and L. Sokoloff, *unpublished data*). The result of Huang and Veech was the consequence of contamination of the fraction that they designated as glucose with labeled products of glucose metabolism.

In short, there is positive evidence of no influence of glucose-6-Pase in the deoxyglucose method if the experimental period is confined to 45 min. There is small but progressively increasing effect beyond that time, but it can easily be corrected for if necessary. Of the three reports alleging significant phosphatase activity at all times during the deoxyglucose procedure, all are demonstrably invalid.

Computerized Color-Coded Image Processing

The autoradiographs produced by the [^{14}C]DG method provide pictorial representations of only the relative concentrations of the isotope in the various tissues. Because of the use of a pulse followed by a long period before killing, the isotope is contained mainly in DG-6-P, which reflects the rate of glucose metabolism. The autoradiographs are therefore pictorial representations also of the relative but not the actual rates of glucose utilization in all the structures of the nervous system. Resolution of differences in relative rates, however, is limited by the ability of the human eye to recognize differences in shades of gray. Manual densitometric analysis permits the computation of actual rates of glucose utilization with a fair degree of resolution, but it generates enormous tables of data that fail to convey the tremendous heterogeneity of local cerebral metabolic rates, even within anatomic structures, or the full information contained within the autoradiographs. Goochee et al. (36) have developed a computerized image-processing system to analyze and transform the autoradiographs into color-coded maps of the exact distribution of the actual rates of glucose utilization throughout the central nervous system (see Plate I and Chapter 5). The autoradiographs are scanned automatically by a computer-controlled scanning

microdensitometer (Chapter 5). The optical density of each spot in the autoradiograph, from 25 to 100 μm as selected, is stored in a computer, converted to ^{14}C concentration on the basis of the optical densities of the calibrated ^{14}C-plastic standards, and then converted to local rates of glucose utilization by solution of the operational equation of the method. Colors are assigned to narrow ranges of the rates of glucose utilization, and the autoradiographs are then displayed in a color television monitor in color along with a calibrated color scale for identifying the rate of glucose utilization in each spot of the autoradiograph from its color. These color maps add a third dimension, the rate of glucose utilization on a color scale, to the spatial dimensions already present on the autoradiographs.

Rates of Local Cerebral Glucose Utilization

Local rates of cerebral glucose utilization determined by the 2-[^{14}C]DG method in normal conscious adult animals are presented in Table 1-6. The rates of local cerebral glucose utilization in the normal conscious rat vary widely throughout the brain. The values in white matter structures tend to group together and are always considerably below those of gray matter structures. The average value in gray matter is approximately three times that of white matter, but the individual values vary from approximately 50 to 200 μmol glucose/100 g/min. The highest values are in the structures involved in auditory functions, with the inferior colliculus clearly the most metabolically active structure in the brain.

The rates of local cerebral glucose utilization in the conscious monkey exhibit similar heterogeneity, but they are generally one-third to one-half the values in corresponding structures of the rat brain (Table 1-6). The differences in rates in the rat and monkey brain are consistent with the different cellular packing densities in the brains of these two species.

By use of the computerized image-processing system (36), it is possible to obtain average rates of glucose utilization in the brain as a whole, approximately weighted for the relative sizes of the component structures. Such values can then be compared with the values obtained with the Kety-Schmidt technique (69). The values so obtained with the deoxyglucose technique are remarkably close to those obtained with the Kety-Schmidt technique (Table 1-6).

General anesthesia produced by thiopental reduces the rates of glucose utilization in all structures of the rat brain (Table 1-7) (154). The effects are not uniform, however. The greatest reductions occur in the gray matter structures, particularly those of the primary sensory pathways. The effects in white matter, though definitely present, are relatively small compared to those of gray matter. These results are in agreement with those of previous studies in which anesthesia has been found to decrease the cerebral metabolic rate of the brain as a whole (64,76,147).

Relation Between Local Functional Activity and Energy Metabolism

The results of a variety of applications of the deoxyglucose method demonstrate a clear relationship between local cerebral functional activity and glucose consumption. The most striking demonstrations of the close coupling between function and energy metabolism are seen with experimentally induced local alterations in functional activity that are restricted to a few specific areas in the brain. The effects on local glucose consumption are then so pronounced that they are not only observed in the quantitative results but can be visualized directly on the autoradiographs which are really pictorial representations of the relative rates of glucose utilization in the various structural components of the brain.

TABLE 1-7. *Effects of thiopental anesthesia on local cerebral glucose utilization in the rat*[a]

Structure	Local cerebral glucose utilization (μmol/100 g/min)		
	Control (6)[b]	Anesthetized (8)[b]	% Effect
Gray matter			
Visual cortex	111 ± 5	64 ± 3	− 42
Auditory cortex	157 ± 5	81 ± 3	− 48
Parietal cortex	107 ± 3	65 ± 2	− 39
Sensory-motor cortex	118 ± 3	67 ± 2	− 43
Lateral geniculate body	92 ± 2	53 ± 3	− 42
Medial geniculate body	126 ± 6	63 ± 3	− 50
Thalamus: lateral nucleus	108 ± 3	58 ± 2	− 46
Thalamus: ventral nucleus	98 ± 3	55 ± 1	− 44
Hypothalamus	63 ± 3	43 ± 2	− 32
Caudate-putamen	111 ± 4	72 ± 3	− 35
Hippocampus: Ammon's horn	79 ± 1	56 ± 1	− 29
Amygdala	56 ± 4	41 ± 2	− 27
Cochlear nucleus	124 ± 7	79 ± 5	− 36
Lateral lemniscus	114 ± 7	75 ± 4	− 34
Inferior colliculus	198 ± 7	131 ± 8	− 34
Superior olivary nucleus	141 ± 5	104 ± 7	− 26
Superior colliculus	99 ± 3	59 ± 3	− 40
Vestibular nucleus	133 ± 4	81 ± 4	− 39
Pontine gray matter	69 ± 3	46 ± 3	− 33
Cerebellar cortex	66 ± 2	44 ± 2	− 33
Cerebellar nucleus	106 ± 4	75 ± 4	− 29
White matter			
Corpus callosum	42 ± 2	30 ± 2	− 29
Genu of corpus callosum	35 ± 5	30 ± 2	− 14
Internal capsule	35 ± 2	29 ± 2	− 17
Cerebellar white matter	38 ± 2	29 ± 2	− 24

[a]Determined at 30 min following pulse of [^{14}C]DG.
[b]The values are the means ± SEM obtained in the number of animals indicated in parentheses. All the differences are statistically significant at the $p < 0.05$ level.
From Sokoloff et al. (154).

Effects of Increased Functional Activity

Effects of sciatic nerve stimulation.

Electrical stimulation of one sciatic nerve in the rat under barbiturate anesthesia causes pronounced increases in glucose consumption (i.e., increased optical density in the autoradiographs) in the ipsilateral dorsal horn of the lumbar spinal cord (57).

Effects of experimental focal seizures.

The local injection of penicillin into the hand-face area of the motor cortex of the rhesus monkey has been shown to induce electrical discharges in the adjacent cortex and to result in recurrent focal seizures involving the face, arm, and hand on the contralateral side (12,47). Such seizure activity causes selective increases in glucose consumption in areas of motor cortex adjacent to the penicillin locus and in small discrete regions of the putamen, globus pallidus, caudate nucleus, thalamus, and substantia nigra of the same side (Fig. 1-11) (57). Similar studies in the rat have led to comparable results and provided evidence on the basis of an evoked metabolic response of a "mirror" focus in the motor cortex contralateral to the penicillin-induced epileptogenic focus (14).

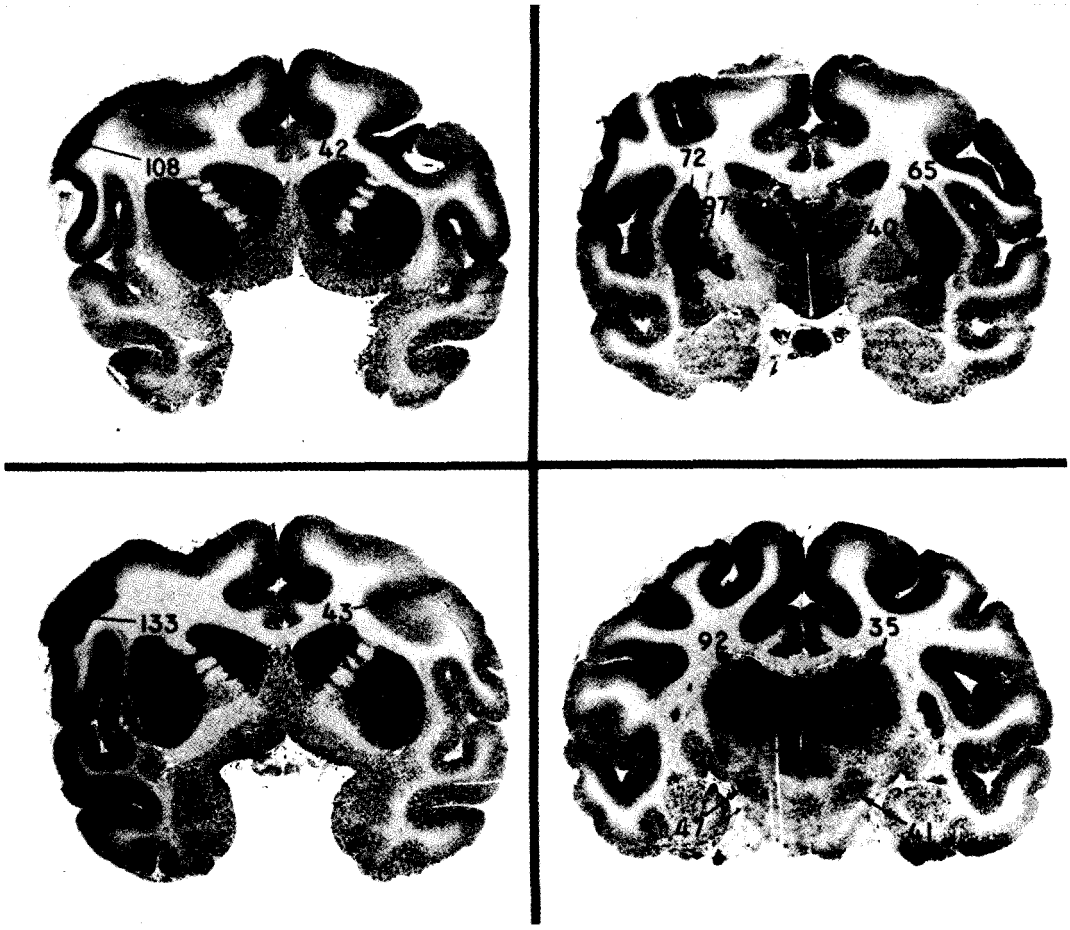

FIG. 1-11. Effects of focal seizures produced by local application of penicillin to motor cortex on local cerebral glucose utilization in the rhesus monkey. The penicillin was applied to the hand and face area of the left motor cortex. The left side of the brain is on the *left* in each of the autoradiographs in the figure. The numbers are the rates of local cerebral glucose utilization in μmol/100 g tissue/min. Note the following: *Upper left,* motor cortex in region of penicillin application and corresponding region of contralateral motor cortex. *Lower left,* ipsilateral and contralateral motor cortical regions remote from area of penicillin applications. *Upper right,* ipsilateral and contralateral putamen and globus pallidus. *Lower right,* ipsilateral and contralateral thalamic nuclei and substantia nigra. From Sokoloff (148).

Effects of Decreased Functional Activity

Decrements in functional activity result in reduced rates of glucose utilization. These effects are particularly striking in the auditory and visual systems of the rat and the visual system of the monkey.

Effects of auditory occlusion.

In the albino rat some of the highest rates of local cerebral glucose utilization are found in components of the auditory system, i.e., auditory cortex, medial geniculate nucleus, inferior colliculus, lateral lemniscus, superior olive, and cochlear nucleus (Table 1-6). Bilateral auditory deprivation by occlusion of both external auditory canals with wax markedly depresses the metabolic activity in all of these areas (148). The reductions are symmetrical bilaterally and range from 35 to 60%. Unilateral au-

ditory deprivation also depresses the glucose consumption of these structures but to a lesser degree, and some of the structures are asymmetrically affected. For example, the metabolic activity of the ipsilateral cochlear nucleus equals 75% of the activity of the contralateral nucleus. The lateral lemniscus, superior olive, and medial geniculate ganglion are slightly lower on the contralateral side, while the contralateral inferior colliculus is markedly lower in metabolic activity than the ipsilateral structure. These results demonstrate that there is some degree of lateralization and crossing of auditory pathways in the rat.

Visual occlusion in the rat.

In the rat the visual system is 80 to 85% crossed at the optic chiasma (75,90), and unilateral enucleation removes most of the visual input to the central visual structures of the contralateral side. In the conscious rat studied 2 to 24 hr after unilateral enucleation, there are marked decrements in glucose utilization in the contralateral superior colliculus, lateral geniculate ganglion, and visual cortex as compared to the ipsilateral side (57).

Visual occlusion in the monkey.

In animals with binocular visual systems, such as the rhesus monkey, there is only approximately 50% crossing of the visual pathways, and the structures of the visual system on each side of the brain receive equal inputs from both retinae. Although each retina projects more or less equally to both hemispheres, their projections remain segregated and terminate in six well-defined laminae in the lateral geniculate ganglia, three each for the ipsilateral and contralateral eyes (50,51,111,165). This segregation is preserved in the optic radiations that project the monocular representations of the two eyes for any segment of the visual field to adjacent regions of layer IV of the striate cortex (50,51). The cells responding to the input of each monocular terminal zone are distributed transversely through the thickness of the striate cortex, resulting in a mosaic of columns, 0.3 to 0.5 mm in width, alternately representing the monocular inputs of the two eyes. The nature and distribution of these ocular dominance columns have previously been characterized by electrophysiological techniques (50), Nauta degeneration methods (51), and autoradiographic visualization of axonal and transneuronal transport of [^{3}H]proline- and [^{3}H]fucose-labeled protein and/or glycoprotein (111,165). Bilateral or unilateral visual deprivation, either by enucleation or by the insertion of opaque plastic discs, produces consistent changes in the pattern of distribution of the rates of glucose consumption, all clearly visible in the autoradiographs, that coincide closely with the changes in functional activity expected from known physiological and anatomical properties of the binocular visual system (58).

In animals with intact binocular vision, no bilateral asymmetry is seen in the autoradiographs of the structures of the visual system (Figs. 1-12A and 1-13A). The lateral geniculate and oculomotor nuclei appear to be of fairly uniform density and essentially the same on both sides (Fig. 1-12A). The visual cortex is also the same on both sides (Fig. 1-13A), but throughout all of area 17 there is heterogeneous density distributed in a characteristic laminar pattern. These observations indicate that in animals with binocular visual input the rates of glucose consumption in the visual pathways are essentially equal on both sides of the brain and relatively uniform in the oculomotor and lateral geniculate nuclei, but markedly different in the various layers of the striate cortex.

Autoradiographs from animals with both eyes occluded exhibit generally decreased labeling of all components of the visual system, but the bilateral symmetry is fully retained (Figs. 1-12B and 1-13B), and the density within each lateral geniculate body is for the most part fairly uniform (Fig. 1-12B). In the striate cortex, however, the marked differences in the densities of the

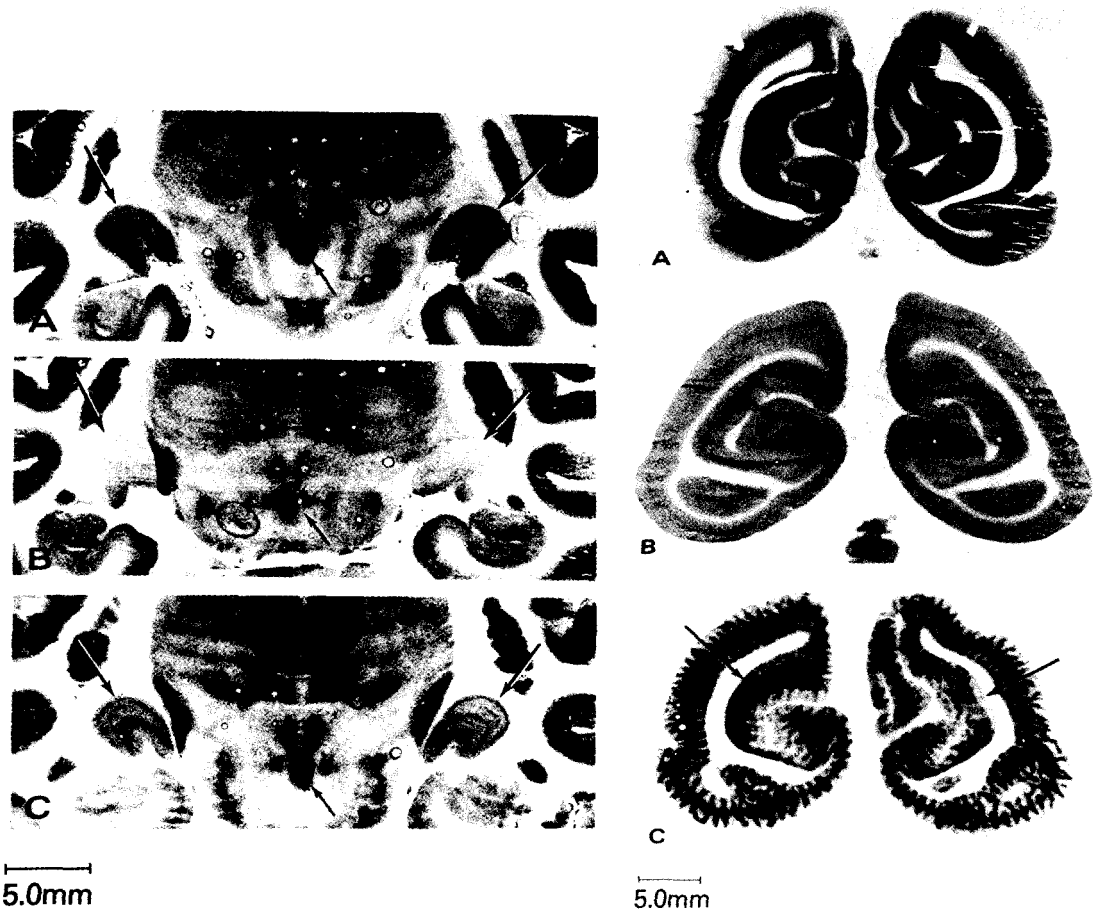

FIG. 1-12. (*Left.*) [^{14}C]DG autoradiography of coronal brain sections of monkey at the level of the lateral geniculate bodies. *Large arrows* point to the lateral geniculate bodies; *small arrows* point to oculomotor nuclear complex. **A:** Animal with intact binocular vision. Note the bilateral symmetry and relative homogeneity of the lateral geniculate bodies and oculomotor nuclei. **B:** Animal with bilateral visual occlusion. Note the reduced relative densities, the relative homogeneity, and the bilateral symmetry of the lateral geniculate bodies and oculomotor nuclei. **C:** Animal with right eye occluded. The left side of the brain is on the *left* side of the photograph. Note the laminae and the inverse order of the dark and light bands in the two lateral geniculate bodies. Note also the lesser density of the oculomotor nuclear complex on the side contralateral to the occluded eye. Courtesy of Kennedy et al. (58).

FIG. 1-13. (*Right.*) [^{14}C]DG autoradiographs of coronal brain sections from rhesus monkeys at the level of the striate cortex. **A:** Animal with normal binocular vision. Note the laminar distribution of the density; the dark band corresponds to layer IV. **B:** Animal with bilateral visual deprivation. Note the almost uniform and reduced relative density, especially the virtual disappearance of the dark band corresponding to layer IV. **C:** Animal with right eye occluded. The half-brain on the *left* side of the photograph represents the left hemisphere contralateral to the occluded eye. Note the alternate dark and light striations, each approximately 0.3 to 0.4 mm in width, that represent the ocular dominance columns. These columns are most apparent in the dark band corresponding to layer IV, but extend through the entire thickness of the cortex. The *arrows* point to regions of bilateral asymmetry where the ocular dominance columns are absent. These are presumably areas with normally only monocular input. The one on the *left,* contralateral to occluded eye, has a continuous dark lamina corresponding to layer IV which is completely absent on the side ipsilateral to the occluded eye. These regions are believed to be the loci of the cortical representations of the blind spots. Courtesy of Kennedy et al. (58).

various layers seen in the animals with intact bilateral vision (Fig. 1-13A) are virtually absent, so that, except for a faint delineation of a band within layer IV, the concentration of the label is essentially homogeneous throughout the striate cortex (Fig. 1-13B).

Autoradiographs from monkeys with only monocular input because of unilateral visual occlusion exhibit markedly different patterns from those described above. Both lateral geniculate bodies exhibit exactly inverse patterns of alternating dark and light bands corresponding to the known laminae representing the regions receiving the different inputs from the retinae of the intact and occluded eyes (Fig. 1-12C). Bilateral asymmetry is also seen in the oculomotor nuclear complex; a lower density is apparent in the nuclear complex contralateral to the occluded eye (Fig. 1-12C). In the striate cortex the pattern of distribution of the [^{14}C]DG-6-P appears to be a composite of the patterns seen in the animals with intact and bilaterally occluded visual input. The pattern found in the former regularly alternates with that of the latter in columns oriented perpendicularly to the cortical surface (Fig. 1-13C). The dimensions, arrangement, and distribution of these columns are identical to those of the ocular dominance columns described by Hubel and Wiesel (50,51,165). These columns reflect the interdigitation of the representations of the two retinae in the visual cortex. Each element in the visual fields is represented by a pair of contiguous bands in the visual cortex, one for each of the two retinae or their portions that correspond to the given point in the visual fields. With symmetrical visual input bilaterally, the columns representing the two eyes are equally active, and therefore not visualized in the autoradiographs (Fig. 1-13A). When one eye is blocked, however, only those columns representing the blocked eye become metabolically less active, and the autoradiographs then display the alternate bands of normal and depressed activities corresponding to the regions of visual cortical representation of the two eyes (Fig. 1-13C).

There can be seen in the autoradiographs from the animals with unilateral visual deprivation a pair of regions in the folded calcarine cortex that exhibit bilateral asymmetry (Fig. 1-13C). The ocular dominance columns are absent on both sides, but on the side contralateral to the occluded eye this region has the appearance of visual cortex from an animal with normal bilateral vision, and on the ipsilateral side this region looks like cortex from an animal with both eyes occluded (Fig. 1-13). These regions are the loci of the cortical representation of the blind spots of the visual fields and normally have only monocular input (58,59). The area of the optic disc in the nasal half of each retina cannot transmit to this region of the contralateral striate cortex, which therefore receives its sole input from an area in the temporal half of the ipsilateral retina. Occlusion of one eye deprives this region of the ipsilateral striate cortex of all input while the corresponding region of the contralateral striate cortex retains uninterrupted input from the intact eye. The metabolic reflection of this ipsilateral monocular input is seen in the autoradiograph in Fig. 1-13C.

The results of these studies with the [^{14}C]DG method in the binocular visual system of the monkey represent the most dramatic demonstration of the close relationship between physiological changes in functional activity and the rate of energy metabolism in specific components of the central nervous system.

Applications of the Deoxyglucose Method

The results of studies like those described above on the effects of experimentally induced focal alterations of functional activity on local glucose utilization have demonstrated a close coupling between local functional activity and energy metabolism

in the central nervous system. The effects are often so pronounced that they can be visualized directly on the autoradiographs, which provide pictorial representations of the relative rates of glucose utilization throughout the brain. This technique of autoradiographic visualization of evoked metabolic responses offers a powerful tool to map functional neural pathways simultaneously in all anatomical components of the central nervous system, and extensive use has been made of it for this purpose (108). The results have clearly demonstrated the effectiveness of metabolic responses, either positive or negative, in identifying regions of the central nervous system involved in specific functions.

The method has been used most extensively in qualitative studies in which regions of altered functional activity are identified by the change in their visual appearance relative to other regions in the autoradiographs. Such qualitative studies are effective only when the effects are lateralized to one side or when only a few discrete regions are affected; other regions serve as the controls. Quantitative comparisons cannot, however, be made for equivalent regions between two or more animals. To make quantitative comparisons between animals, the fully quantitative method must be used, which takes into account the various factors, particularly the plasma glucose level, that influence the magnitude of labeling of the tissues. The method must be used quantitatively when the experimental procedure produces systemic effects and alters metabolism in many regions of the brain.

A comprehensive review of the many qualitative and quantitative applications of the method is beyond the scope of this report. Only some of the many neurophysiological, neuroanatomical, and pharmacological applications of the method in which our laboratory has been directly or indirectly involved will be briefly noted, merely to illustrate the broad extent of its potential usefulness.

Neurophysiological and Neuroanatomical Applications

Many of the physiological applications of the [^{14}C]DG method were in studies designed to test the method and to examine the relationship between local cerebral functional and metabolic activities. These applications have been described above. The most dramatic results have been obtained in the visual systems of the monkey and the rat. The method has, for example, been used to define the nature, conformation, and distribution of the ocular dominance columns in the striate cortex of the monkey (Fig. 1-13C) (58). It has been used by Hubel et al. (53) to do the same for the orientation columns in the striate cortex of the monkey. A by-product of the studies of the ocular dominance columns was the identification of the loci of the visual cortical representation of the blind spots of the visual fields (Fig. 1-13C) (58). Studies are in progress to map the pathways of higher visual functions beyond the striate cortex; the results thus far demonstrate extensive areas of involvement of the inferior temporal cortex in visual processing (81). Des Rosiers et al. (18) have used the method to demonstrate functional plasticity in the striate cortex of the infant monkey. The ocular dominance columns are already present on the first day of life, but if one eye is kept patched for 3 months, the columns representing the open eye broaden and completely take over the adjacent regions of cortex containing the columns for the eye that had been patched. Inasmuch as there is no longer any cortical representation for the patched eye, the animal becomes functionally blind in one eye. This phenomenon is almost certainly the basis for the cortical blindness or amblyopia that often occurs in children with uncorrected strabismus.

There have also been extensive studies of the visual system of the rat. This species has little if any binocular vision and therefore lacks the ocular dominance columns.

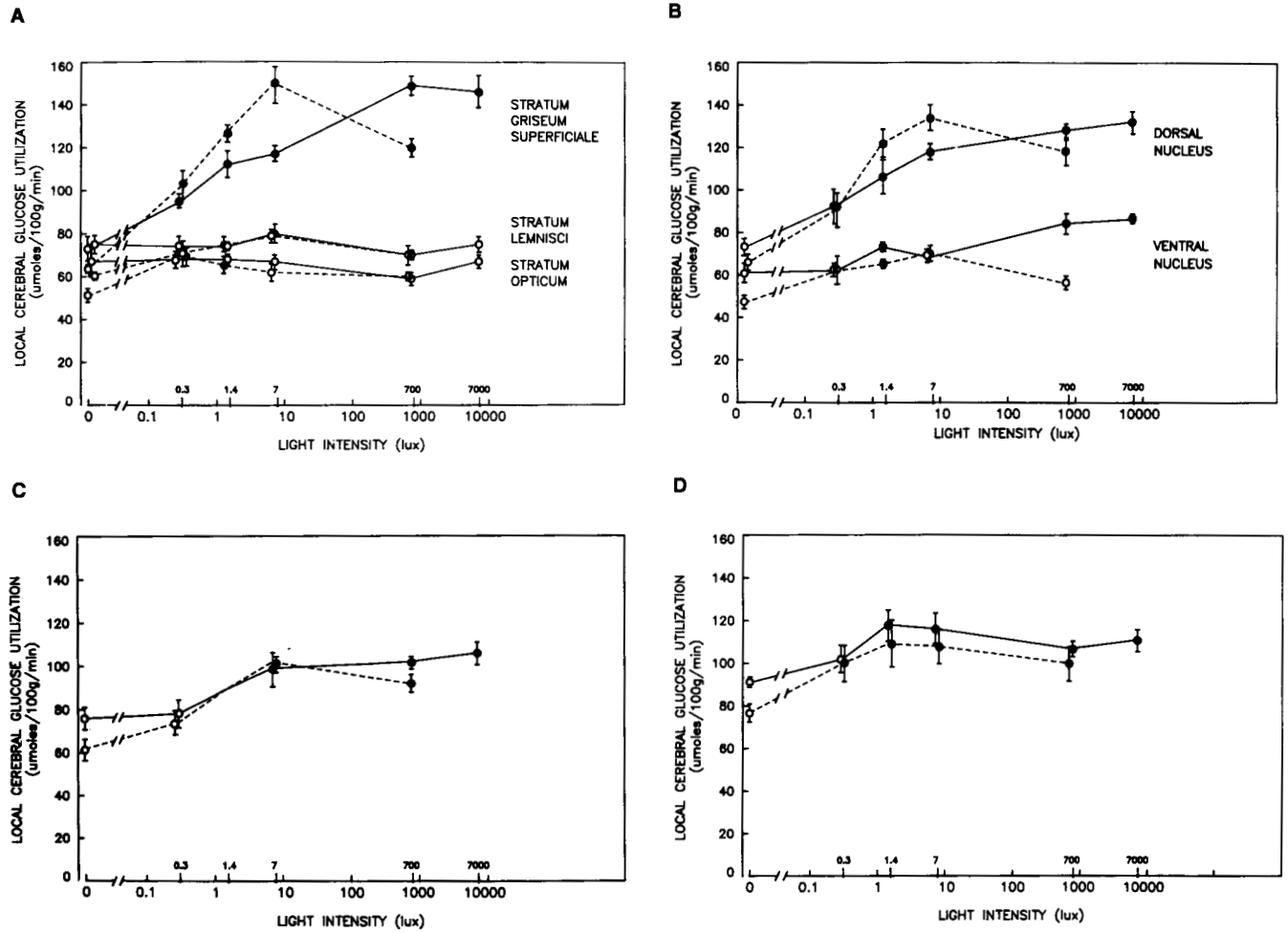

FIG. 1-14. Effects of intensity of retinal illumination with randomly spaced light flashes on local cerebral glucose utilization in components of the visual system of the albino *(dash line)* and Norway brown *(solid line)* rat. Note that the local glucose utilization is proportional to the logarithm of the intensity of illumination at the lower levels of intensity in the primary projection areas of the retina. **A**: Superior colliculus; **B:** lateral geniculate nucleus; **C:** posterolateral nucleus of the thalamus; **D:** visual cortex. Courtesy of Miyaoka et al. (89).

Batipps et al. (6) have compared the rates of local cerebral glucose utilization in albino and Norway brown rats during exposure to ambient light. The rates in the two strains were essentially the same throughout the brain except in the components of the primary visual system. The metabolic rates in the superior colliculus, lateral geniculate, and visual cortex of the albino rat were significantly lower than those in the pigmented rat. Miyaoka et al. (89) have studied the influence of the intensity of retinal stimulation with randomly spaced light flashes on the metabolic rates in the visual systems of the two strains. In dark adapted animals there is relatively little difference between the two strains. With increasing intensity of light, the rates of glucose utilization first increase in the primary projection areas of the retina, i.e., superficial layer of the superior colliculus and lateral geniculate body, and the slopes of the increase are steeper in the albino rat (Fig. 1-14). At 7 lux, however, the metabolic rates peak in the albino rat and then decrease with increasing light intensity. In contrast, the metabolic rates in the pigmented rat rise until they reach a plateau at about 700 lux, approximately the ambient light intensity in the laboratory. At this level the metabolic rates in the visual structures of the albino rat are considerably below those of the pigmented rat. These results are consistent with the greater intensity of light reaching the visual cells of the retina in the albino rats because of lack of pigment and the subsequent damage to the rods at higher light intensities. It is of considerable interest that the rates of glucose utilization in these visual structures obey the Weber-Fechner Law, i.e., the metabolic rate is directly proportional to the logarithm of the intensity of stimulation (89). Inasmuch as this law was first developed from behavioral manifestations, these results imply that there is a quantitative relationship between behavioral and metabolic responses.

Although less extensive, there have also been applications of the method to other sensory systems. In studies of the olfactory system Sharp et al. (132) have found that olfactory stimulation with specific odors activates glucose utilization in localized regions of the olfactory bulb. In addition to the experiments in the auditory system described above, there have been studies of tonotopic representation in the auditory system. Webster et al. (163) have obtained clear evidence of selective regions of metabolic activation in the cochlear nucleus, superior olivary complex, nuclei of the lateral lemnisci, and inferior colliculus in cats in response to different frequencies of auditory stimulation. Similar results have been obtained by Silverman et al. (134) in the rat and guinea pig. Studies of the sensory cortex have demonstrated metabolic activation of the "whisker barrels" by stimulation of the vibrissae in the rat (21,40). Each vibrissa is represented in a discrete region of the sensory cortex; their precise location and extent have been elegantly mapped by Hand et al. (40) and Hand (39) by means of the [^{14}C]DG method (Plate I).

Thus far, there has been relatively little application of the method to the physiology of motor functions. Kennedy et al. (60) have studied monkeys that were conditioned to perform a task with one hand in response to visual cues; in the monkeys that were performing they observed metabolic activation throughout the appropriate areas of the motor as well as sensory systems from the cortex to the spinal cord.

An interesting physiological application of the [^{14}C]DG method has been to the study of circadian rhythms in the central nervous system. Schwartz and his co-workers (127,128) found that the suprachiasmatic nucleus in the rat exhibits circadian rhythmicity in metabolic activity, high during the day and low during the night (Fig. 1-15). None of the other structures in the brain that they examined showed rhythmic activity. The normally low activity present

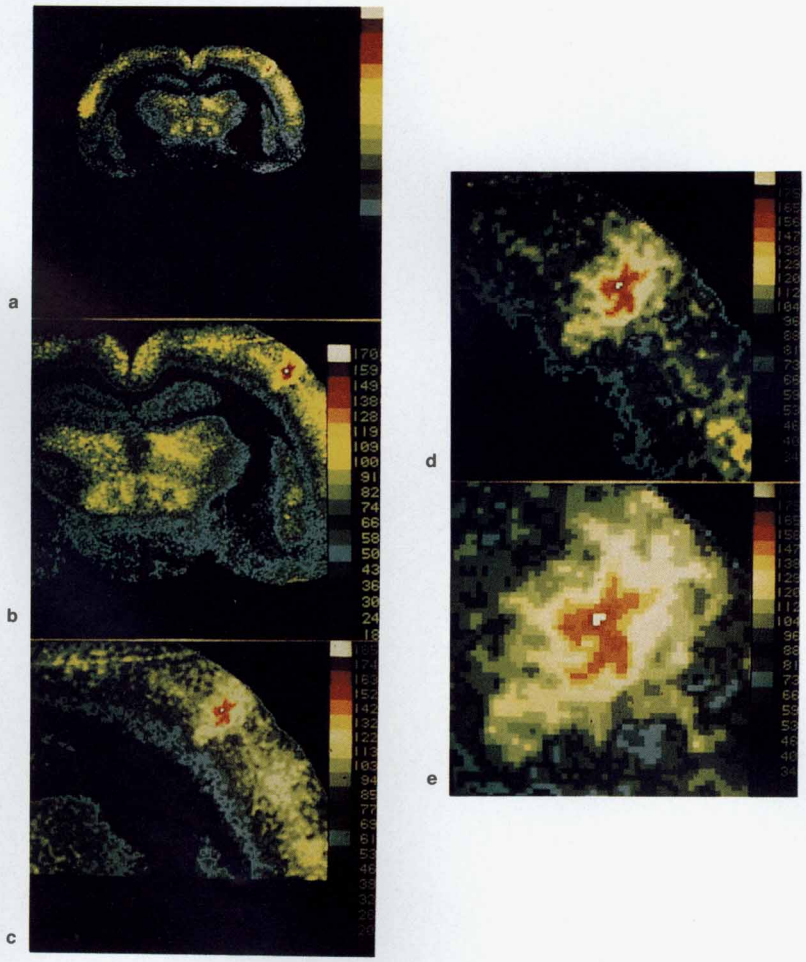

PLATE 1-I. [^{14}C]DG autoradiographs of rat brain showing sensory cortex response to stroking of a single whisker after intravenous injection of [^{14}C]DG. Each whisker of the rat has a discrete sensory representation known as the "whisker barrel." Autoradiographs show discrete metabolic activation in a single whisker barrel as a stimulated response to stroking. Autoradiographs **a–e** are successive enlargements. Color scale is in units of μmol/100 g/min. Courtesy of Hand (39).

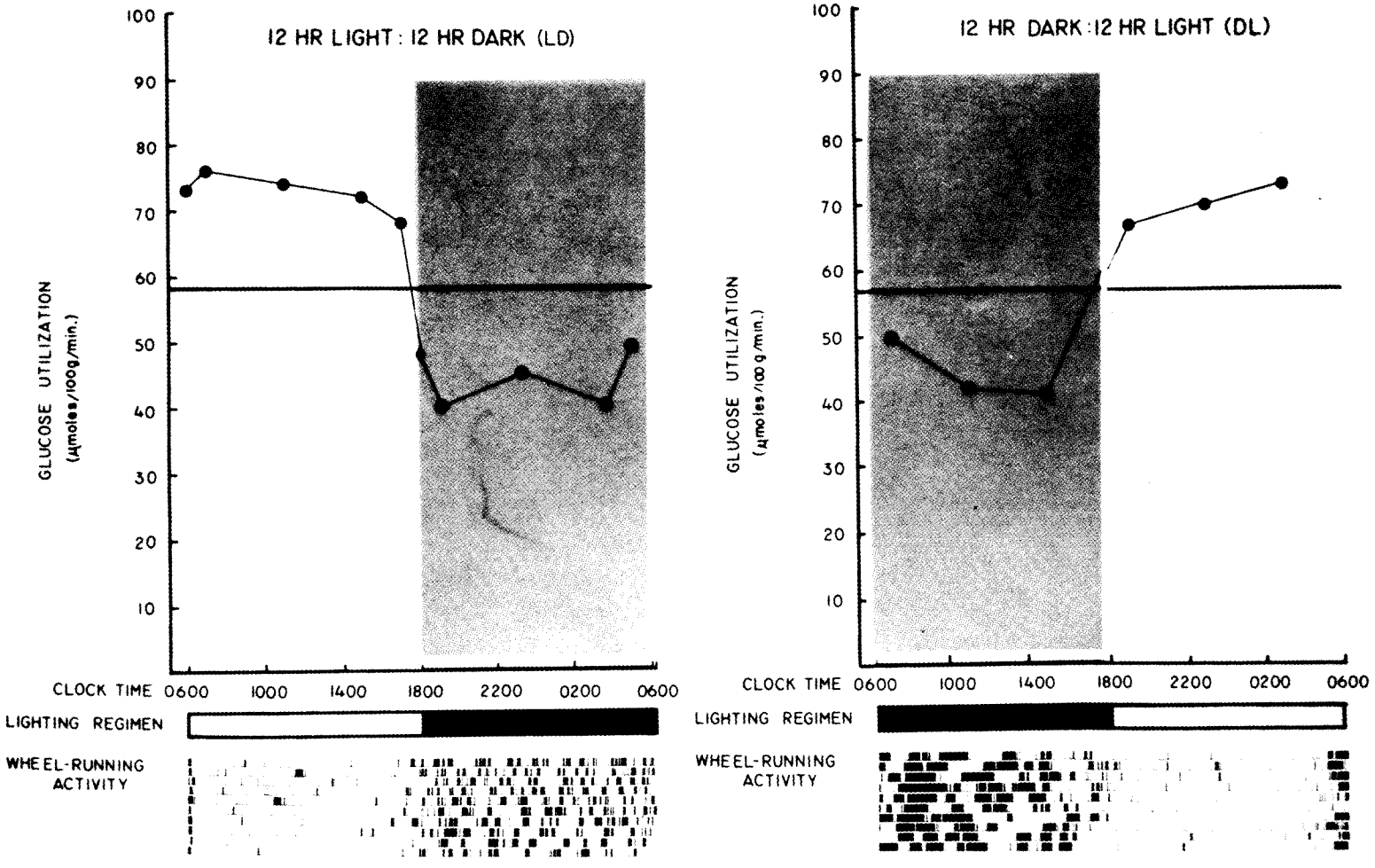

FIG. 1-15. Circadian rhythm in glucose utilization in suprachiasmatic nucleus in the rat. *Left panel,* animals entrained to 12 hr of light during day and 12 hr of darkness during night. *Right panel,* animals entrained to opposite light-dark regimen. Courtesy of Schwartz et al. (127).

in the nucleus in the dark could be markedly increased by light, but darkness did not reduce the glucose utilization during the day. The rhythm is entrained to light; reversal of the light-dark cycle leads not only to reversal of the rhythm in running activity but also in the cycle of metabolic activity in the suprachiasmatic nucleus. These studies lend support to a role of the suprachiasmatic nucleus in the organization of circadian rhythms in the central nervous system.

Studies of circadian rhythms with the deoxyglucose method have been extended to natural sleep in monkeys. The results have demonstrated that during slow wave, nonrapid eye movement (REM) sleep, glucose utilization is diffusely depressed 25 to 30% throughout the central nervous system (59). No structure in the brain showed an increased rate of glucose utilization, not even structures proposed as hypnogenic centers which allegedly are activated and depress functional activity in the other parts of the nervous system. The generalized uniformity of the metabolic depression suggests a chemical rather than a neurophysiological mechanism as the basis of slow-wave sleep. Studies in REM sleep have not yet been successfully carried out because of the short duration of REM episodes relative to the time resolution of the method.

Much of our knowledge of neurophysiology has been derived from studies of the electrical activity of the nervous system. Indeed, from the heavy emphasis that has been placed on electrophysiology one might gather that the brain is really an electric organ rather than a chemical one that functions mainly by the release of chemical transmitters at synapses. Nevertheless, electrical activity is unquestionably fundamental to the process of conduction, and it is appropriate to inquire how the local metabolic activities revealed by the [^{14}C]DG method are related to the electrical activity of the nervous system. This question has been examined by Yarowsky and his co-workers (169) in the superior cervical ganglion of the rat. The advantage of this structure is that its preganglionic input and postganglionic output can be isolated and electrically stimulated and/or monitored *in vivo*. The results indicate a clear relationship between electrical input to the ganglion and its metabolic activity. Glucose utilization in the superior cervical ganglion is enhanced by electrical stimulation of the afferent nerves. The metabolic activation is frequency dependent in the physiological range of 5 to 15 Hz, increasing in magnitude with increasing frequency of the stimulation (Fig. 1-16). Similar effects of electrical stimulation on the oxygen and glucose consumption of the excised ganglion studied *in vitro* have been observed (30,46,74). Recent studies have also shown that antidromic stimulation of the postganglionic efferent pathways from the ganglion has similar effects; stimulation of the external carotid nerve antidromically activates glucose utilization in the region of distri-

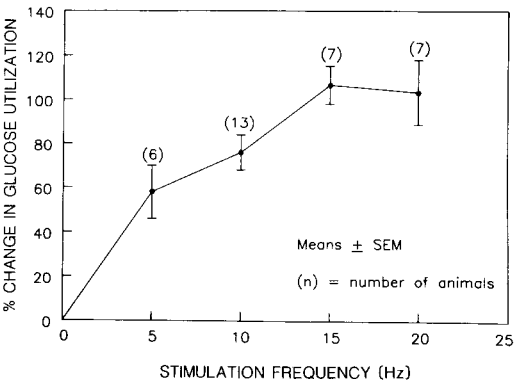

FIG. 1-16. Relationship between frequency of electrical stimulation of cervical sympathetic trunk and the percent increase in the rate of glucose utilization in the superior cervical ganglion above that of the control ganglion on the other side. The values represent the means ± SEM of the individual percent effects. Courtesy of Yarowsky et al. (169).

bution of the cell bodies of this efferent pathway, indicating that not only the preganglionic axonal terminals are metabolically activated, but the postganglionic cell bodies as well (168). As already demonstrated in the neurohypophysis (82), the effects of electrical stimulation on energy metabolism in the superior cervical ganglion are also probably due to the ionic currents associated with the spike activity and the consequent activation of the Na^+,K^+-ATPase activity to restore the ionic gradients. Electrical stimulation of the afferents to sympathetic ganglia has been shown to increase extracellular K^+ concentration (30,32). Each spike is normally associated with a sharp transient rise in extracellular K^+ concentration, which then rapidly falls and transiently undershoots before returning to the normal level (32); ouabain slows the decline in K^+ concentration after the spike and eliminates the undershoot. Continuous stimulation at a frequency of 6 Hz produces a sustained increase in cellular K^+ concentration (32). It is likely that the increased extracellular K^+ concentration and, almost certainly, increased intracellular Na^+ concentration activate the Na^+,K^+-ATPase, which in turn leads to the increased glucose utilization.

Shinohara et al. (133) studied the effects of local applications of KCl on the dura overlying the parietal cortex of conscious rats or directly on the pial surface of the parietal cortex of anesthetized rats in order to determine if K^+ stimulates cerebral energy metabolism *in vivo* as it is well known to do *in vitro*. The results demonstrate a marked increase in cerebral cortical glucose utilization in response to the application of KCl; NaCl has no such effect (Fig. 1-17). Such application of KCl, however, also produces the phenomenon of spreading cortical depression. This condition is characterized by a spread of transient intense neuronal activity followed by membrane depolarization, electrical depression, and a negative shift in the cortical DC potential in all directions from the site of initiation at a rate of 2 to 5 mm/min. The depressed cortex also exhibits a number of chemical changes, including an increase in extracellular K^+, lost presumably from the cells. At the same time that the cortical glucose utilization is increased, most subcortical structures that are functionally connected to the depressed cortex exhibit decreased rates of glucose utilization. During recovery from the spreading cortical depression, the glucose utilization in the cortex is still increased, but it is distributed in columns oriented perpendicularly through the cortex. This columnar arrangement may reflect the columnar functional and morphological arrangement of the cerebral cortex. It is likely that the increased glucose utilization in the cortex during spreading cortical depression is the consequence of the increased extracellular K^+ and activation of the Na^+,K^+-ATPase.

Many of the behavioral consequences of aging are directly attributable to decrements in functions of the central nervous system (10). Normal human aging has been found to be associated with a decrease in average glucose utilization of the brain as a whole (146). Smith et al. (141) have employed the quantitative [^{14}C]DG method to study normal aging in Sprague-Dawley rats between 5 to 6 and 36 months of age. Their results show widespread but not homogeneous reductions of local cerebral glucose utilization with age. The sensory systems, particularly auditory and visual, are particularly severely affected. The basal ganglia are metabolically depressed, and preliminary experiments indicate that they lose responsivity to dopamine agonists, such as apomorphine, with age (C. Smith and J. McCulloch, *unpublished observations*). A striking effect was the loss of metabolically active neuropil in the cerebral cortex; layer IV is markedly decreased in metabolic activity and extent. Some of these changes

may be related to specific functional disabilities that develop in old age.

Neuroendocrinological Applications

The deoxyglucose method has thus far been applied only sparingly to neuroendocrinology. Several studies have, however, been carried out or are in progress.

Hypothalamoneurohypophysial system.

Physiological stimulation of the neurohypophysial system by salt loading, which enhances vasopressin secretion, has been found to be associated with increased glucose utilization in the posterior pituitary (Fig. 1-18) (130). Surprisingly, there were no detectable effects in the supraoptic and paraventricular nuclei, the loci of the cell

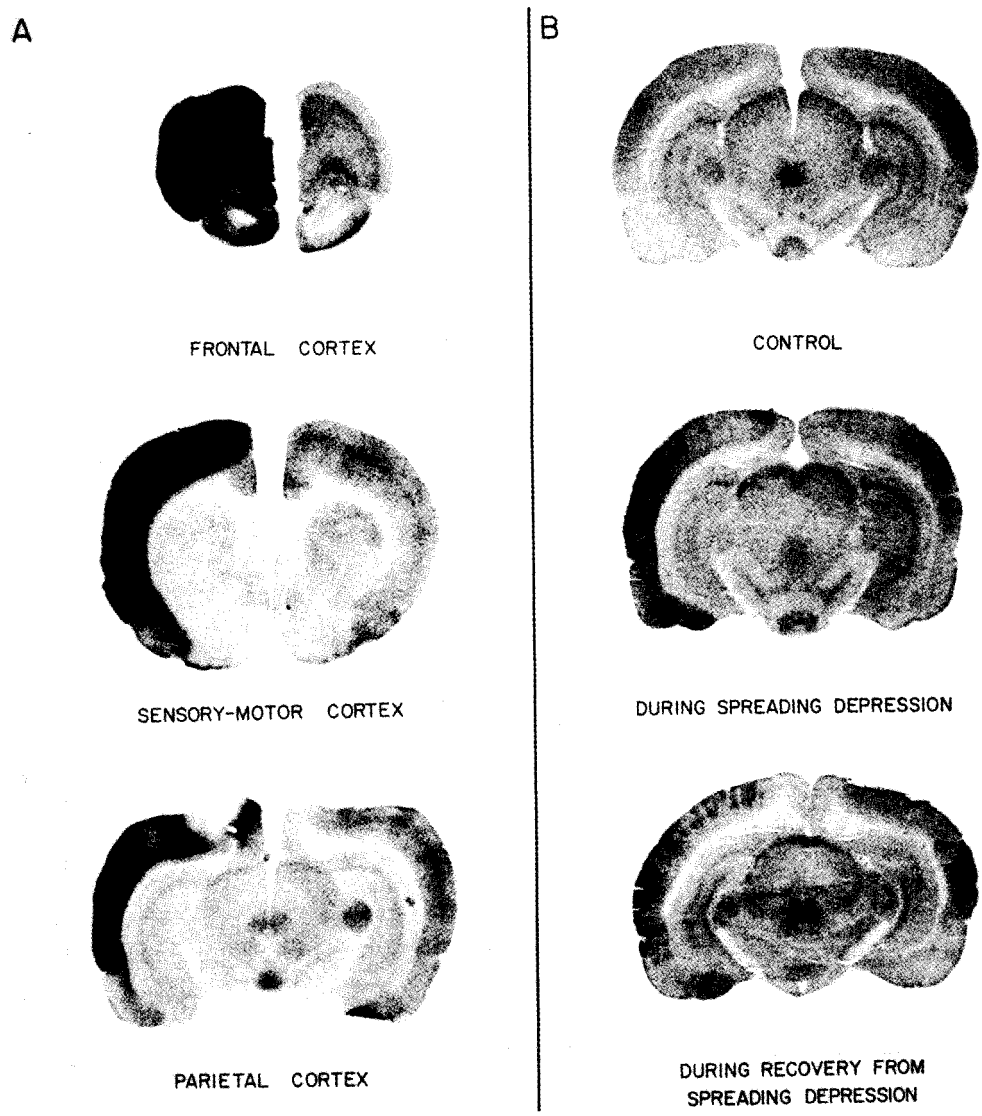

bodies that project to the posterior pituitary. Obviously the entire pathway had been activated by the osmotic stimulation. Approximately 42% of the posterior pituitary consists of axonal terminals of the hypothalamohypophysial tract (96), and the discrepancy between the effects on the cell bodies and in the regions of termination of their projections may reflect the greater sensitivity of axonal terminals or synaptic elements than that of perikarya to metabolic activation. That the supraoptic and paraventricular nuclei can be metabolically activated is evident from the effects of the α-adrenergic blocking agent phenoxybenzamine (Fig. 1-18D), or any other condition that produces hypotension (124). In hypotension, however, these nuclei are activated by reflex activity, and it may well be that it is the afferent axonal terminals in these nuclei rather than the cell bodies that exhibit the increased utilization of glucose.

Kadekaro et al. (55) have applied the deoxyglucose method to studies of the Brattleboro rat, a variant of the Long-Evans strain with a recessive genetic defect in vasopressin synthesis. This rat exhibits the characteristic signs of diabetes insipidus, an abnormally high water intake and a high output of hypoosmolar urine. Despite the deficiency in vasopressin synthesis, glucose utilization was found to be markedly increased in the posterior pituitary and also in the subfornical organ, a structure that has been found to mediate drinking behavior in response to high plasma levels of angiotensin II, and angiotensin II is elevated in the Brattleboro rat. As in the normal rat stimulated by salt loading, the supraoptic and paraventricular nuclei were not metabolically more active in the Brattleboro rat. The reason for the high metabolic rate in the posterior pituitary of the Brattleboro rat is still obscure, but it may be related to histological changes that also are present in the gland.

Altered thyroid function.

Hyperthyroidism is known not to alter the average energy metabolism in the mature brain as a whole (155). Studies with the deoxyglucose method (D. Dow-Edwards and C. B. Smith, *unpublished observations*) reveal that there are also no changes in glucose utilization in any anatomical components of the mature brain of the rat. The thyroid hormones are, however, fundamentally involved in the structural and

FIG 1-17. [^{14}C]DG autoradiographs of sections of rat brains during spreading cortical depression and during recovery. The autoradiographs are pictorial representations of the relative rates of glucose utilization in various parts of the brain; the greater the density, the greater the rate of glucose utilization. The left sides of the brain are represented by the left hemispheres in the autoradiographs. In all the experiments illustrated, the control hemisphere was treated the same as the experimental side except that equivalent concentrations of NaCl rather than KCl were used. The NaCl did not lead to any detectable differences from hemispheres over which the skull was left intact and no NaCl was applied. **A:** Autoradiographs of sections of brain at different levels of cerebral cortex from a conscious rat during spreading cortical depression induced on the left side by application of 5 M KCl to the intact dura overlying the left parietal cortex. The spreading depression was sustained by repeated applications of the KCl at 15- to 20-min intervals throughout the experimental period. **B:** Autoradiographs from sections of brain at the level of the parietal cortex from three animals under barbiturate anesthesia. The *top* section is from a normal anesthetized animal; the *middle* section is from an animal during unilateral spreading cortical depression induced and sustained by repeated applications of 80 mM KCl in artificial cerebrospinal fluid directly on the surface of the left parietooccipital cortex. At the *bottom* is a comparable section from an animal studied immediately after the return of cortical DC potential to normal after a single wave of spreading depression induced by a single application of 80 mM KCl to the parietooccipital cortex of the left side. Courtesy of Shinohara et al. (133).

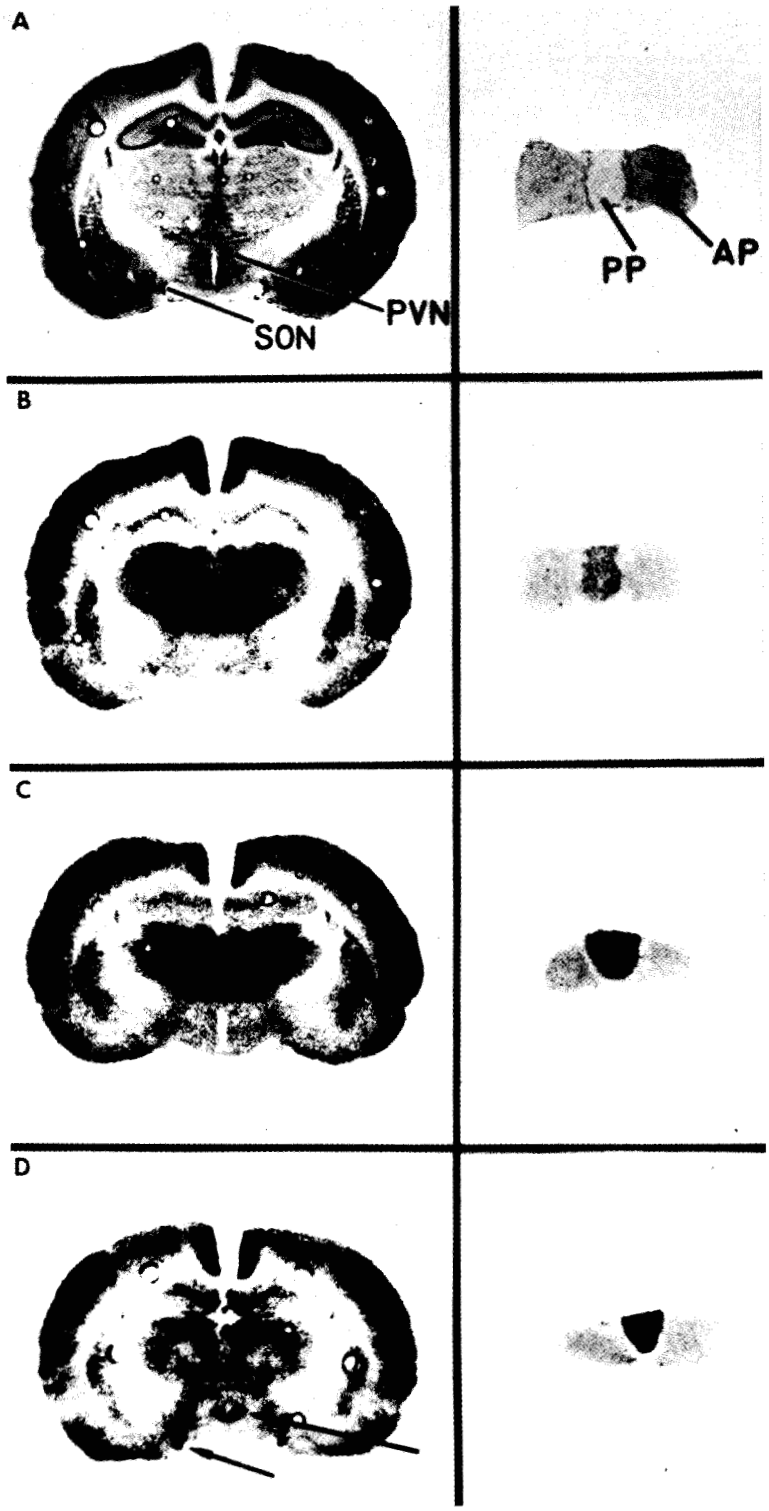
A
SON
PVN
PP
AP
B
C
D

functional maturation of the brain (23). Dow-Edwards et al. (19) have applied the deoxyglucose method to rats radiothyroidectomized at birth but studied at approximately 5 months of age, when the brain of normal rats has achieved maturity. Glucose utilization was significantly reduced in all regions of the brain examined. Particularly affected were the cerebral cortical regions and the sensory systems, particularly the auditory system. These metabolic changes are consistent with the histological pattern of impaired brain development in cretinism.

Sex hormones and sexual behavior.

The deoxyglucose method has been used to demonstrate selective metabolic activation of a number of structures in the female rat brain by vaginocervical stimulation that also elicited lordotic behavior (2). The structures so activated were the medial preoptic nucleus, mesencephalic reticular formation, red nucleus of the stria terminalis, dorsal raphe nucleus, and the globus pallidus. Some but not all of these areas had been previously shown by electrical recording, lesioning, and stimulating techniques to participate in the behavioral and physiological responses to coitus. These results provide additional information about the concurrent processing of sensory stimulation in the brain and also indicate that the medial preoptic area is a receptive area for copulatory stimulation.

The female gonadal hormones estrogen and progesterone influence sexual behavior and have potent influences on the central nervous system, particularly the hypothalamus. Porrino et al. (109) have used the deoxyglucose method in an attempt to identify regions of the brain affected by these hormones. In ovariectomized rats estradiol treatment stimulated glucose utilization in anterior, ventromedial, lateral, and posterior areas of the hypothalamus. Progesterone alone had very little effect in these areas. When progesterone was administered to animals that had been implanted previously with estradiol, glucose utilization was reduced in the lateral preoptic area, medial preoptic area, and anterior hypothalamus below the levels of the ovariectomized controls. These data suggest an anatomical separation of the effects of gonadal steroids in the hypothalamus; estradiol may facilitate neural activity in the mid and posterior areas of the hypothalamus whereas estrogen in combination with progesterone suppresses activity in the anterior preoptic area. These two patterns in the anterior and posterior hypothalamus may reflect differential involvement in feminine sexual behavior.

Neuropharmacological Applications

The ability of the deoxyglucose method to map the entire brain for localized regions of altered functional activity on the basis of changes in energy metabolism offers a potent tool to identify the neural sites of action of agents with neuropharmacological and psychopharmacological actions. It

FIG. 1-18. [^{14}C]DG autoradiographs (B, C, D) and stained histological sections (A) of coronal brain sections *(left)* and pituitary sections *(right).* **A:** Photographs illustrate the positions of the supraoptic (SON) and paraventricular (PVN) nuclei in the brain section after cresyl violet (Nissl) staining. The positions of the posterior pituitary (PP) and anterior pituitary (AP) are illustrated on the right side in (A) after toluidine blue staining. **B:** Autoradiographs characteristic of control rats, which were allowed to drink water freely. **C:** Autoradiographs of brain and pituitary typical of dehydrated rats, which were given 2% NaCl to drink for 5 days. Note the intense labeling in the posterior pituitary, without comparable change in the SON or PVN. **D:** Autoradiographs characteristic of normal rats given an intravenous injection of an α-adrenergic blocker, phenoxybenzamine (20 mg/kg), approximately 45 to 60 min before injection of [^{14}C]DG. Note the dramatic increase in labeling of the SON, PVN, and PP. Courtesy of Schwartz et al. (129).

does not, however, discriminate between the direct and indirect effects of the drug. An entire pathway may be activated even though the direct action of the drug may be exerted only at the origin of the pathway. This is of advantage for relating behavioral effects to central actions, but it is a disadvantage if the goal is to identify the primary site of action of the drug. To discriminate between direct and indirect actions of a drug the [^{14}C]DG method must be combined with selectively placed lesions in the central nervous system that interrupt afferent pathways to the structure in question. If the metabolic effect of the drug then remains, it is due to direct action; if lost, the effect is likely to be indirect and mediated via the interrupted pathway. Nevertheless, the method has proved to be useful in a number of pharmacological studies (83).

Effects of γ-butyrolactone.

γ-Hydroxybutyrate and γ-butyrolactone, which is hydrolyzed to γ-hydroxybutyrate in plasma, produce trance-like behavioral states associated with marked suppression of electroencephalographic activity (118). These effects are reversible, and these drugs have been used clinically as anesthetic adjuvants. There is evidence that these agents lower neuronal activity in the nigrostriatal pathway and may act by inhibition of dopaminergic synapses (117). Studies in rats with the [^{14}C]DG technique have demonstrated that γ-butyrolactone produces profound dose-dependent reductions of glucose utilization throughout the brain (167). At the highest doses studied, 600 mg/kg of body weight, glucose utilization was reduced by approximately 75% in gray matter and 33% in white matter, but there was no obvious further specificity with respect to the local cerebral structures affected. The reversibility of the effects and the magnitude and diffuseness of the depression of cerebral metabolic rate suggest that this drug might be considered as a chemical substitute for hypothermia in conditions in which profound reversible reduction of cerebral metabolism is desired.

Pharmacological studies of dopaminergic systems.

The most extensive applications of the deoxyglucose method to pharmacology have been in studies of dopaminergic systems. Ascending dopaminergic pathways appear to have a potent influence on glucose utilization in the forebrain of rats. Electrolytic lesions placed unilaterally in the lateral hypothalamus or pars compacta of the substantia nigra caused marked ipsilateral reductions of glucose metabolism in numerous forebrain structures rostral to the lesion, particularly the frontal cerebral cortex, caudate-putamen, and parts of the thalamus (126,129). Similar lesions in the locus ceruleus had no such effects.

Enhancement of dopaminergic synaptic activity by administration of the agonist of dopamine, apomorphine (11), or of amphetamine (164), which stimulates release of dopamine at the synapse, produces marked increases in glucose consumption in some of the components of the extrapyramidal system known or suspected to contain dopamine-receptive cells. With both drugs, the greatest increases noted were in the zona reticulata of the substantia nigra and the subthalamic nucleus. Surprisingly, none of the components of the dopaminergic mesolimbic system appeared to be affected.

The studies with amphetamine (164) were carried out with the fully quantitative [^{14}C]DG method. The results in Table 1-8 illustrate the comprehensiveness with which this method surveys the entire brain for sites of altered activity due to actions of the drug. It also allows for quantitative comparison of the relative potencies of related drugs. For example, in Table 1-8, the comparative effects of *d*-amphetamine and the less potent dopaminergic agent *l*-amphetamine are compared; the quantitative results clearly reveal that the effects of *l*-

TABLE 1-8. *Effects of* d-*amphetamine and* l-*amphetamine on local cerebral glucose utilization in the conscious rat (μmol/100 g/min)*[a]

Structure	Control	*d*-Amphetamine (5 mg/kg)	*l*-Amphetamine (5 mg/kg)
Gray matter			
Visual cortex	102 ± 8	135 ± 11[b]	105 ± 8
Auditory cortex	160 ± 11	162 ± 6	141 ± 6
Parietal cortex	109 ± 9	125 ± 10	116 ± 4
Sensory-motor cortex	118 ± 8	139 ± 9	111 ± 4
Olfactory cortex	100 ± 6	93 ± 5	94 ± 3
Frontal cortex	109 ± 10	130 ± 8	105 ± 4
Prefrontal cortex	146 ± 10	166 ± 7	154 ± 4
Thalamus			
Lateral nucleus	97 ± 5	114 ± 8	117 ± 6
Ventral nucleus	85 ± 7	108 ± 6[b]	96 ± 4
Habenula	118 ± 10	71 ± 5[c]	82 ± 2[c]
Dorsomedial nucleus	92 ± 6	111 ± 8	106 ± 6
Medial geniculate	116 ± 5	119 ± 4	116 ± 4
Lateral geniculate	79 ± 5	88 ± 5	84 ± 4
Hypothalamus	54 ± 5	56 ± 3	52 ± 3
Suprachiasmatic nucleus	94 ± 4	75 ± 4[c]	67 ± 1[c]
Mamillary body	117 ± 8	134 ± 5	142 ± 5[b]
Lateral olfactory nucleus[d]	92 ± 6	95 ± 5	99 ± 6
A_{13}	71 ± 4	91 ± 4[c]	81 ± 4
Hippocampus			
Ammon's horn	79 ± 5	73 ± 2	81 ± 6
Dentate gyrus	60 ± 4	55 ± 3	67 ± 7
Amygdala	46 ± 3	46 ± 3	44 ± 2
Septal nucleus	56 ± 3	55 ± 2	54 ± 3
Caudate nucleus	109 ± 5	132 ± 8[b]	127 ± 3[b]
Nucleus accumbens	76 ± 5	80 ± 3	78 ± 3
Globous pallidus	53 ± 3	64 ± 2[b]	65 ± 3[b]
Subthalamic nucleus	89 ± 6	149 ± 10[c]	107 ± 2
Substantia nigra			
Zona reticulata	58 ± 2	105 ± 4[c]	72 ± 4
Zona compacta	65 ± 4	88 ± 6[c]	72 ± 3
Red nucleus	76 ± 5	94 ± 5[b]	86 ± 2
Vestibular nucleus	121 ± 11	137 ± 5	130 ± 4
Cochlear nucleus	139 ± 6	126 ± 1	141 ± 5
Superior olivary nucleus	144 ± 4	143 ± 4	147 ± 6
Lateral lemniscus	107 ± 3	96 ± 5	98 ± 3
Inferior colliculus	193 ± 10	169 ± 5	150 ± 8[c]
Dorsal tegmental nucleus	109 ± 5	112 ± 7	122 ± 6
Superior colliculus	80 ± 5	89 ± 3	91 ± 3
Pontine gray	58 ± 4	65 ± 3	60 ± 1
Cerebellar flocculus	124 ± 10	146 ± 15	153 ± 10
Cerebellar hemispheres	55 ± 3	68 ± 6	64 ± 2
Cerebellar nuclei	102 ± 4	105 ± 8	110 ± 3
White matter			
Corpus callosum	23 ± 3	24 ± 2	23 ± 1
Genu of corpus callosum	29 ± 2	30 ± 2	26 ± 2
Internal capsule	21 ± 1	24 ± 2	19 ± 2
Cerebellar white	28 ± 1	31 ± 2	31 ± 2

[a]All values are the means ± SEM for five animals.
[b]Significant difference from the control at the $p < 0.05$ level.
[c]Significant difference from the control at the $p < 0.01$ level.
[d]It was not possible to correlate precisely this area on autoradiographs with a specific structure in the rat brain. It is, however, most likely the lateral olfactory nucleus.
From Wechsler et al. (164).

amphetamine on local cerebral glucose utilization are more limited in distribution and of lesser magnitude than those of *d*-amphetamine. Indeed, in similar quantitative studies with apomorphine, McCulloch et al. (84,86) have been able to generate complete dose-response curves for the effects of the drug on the rates of glucose utilization in various components of dopaminergic systems. They have also demonstrated metabolically the development of supersensitivity to apomorphine in rats maintained chronically on the dopamine antagonist haloperidol (J. McCulloch, H. E. Savaki, A. Pert, W. Bunney, and L. Sokoloff, *unpublished observations*). In the course of these studies with apomorphine, McCulloch et al. (85) obtained evidence of a retinal dopaminergic system that projects specifically to the superficial layer of the superior colliculus in the rat. Apomorphine administration activated metabolism in the superficial layer of the superior colliculus, as well as in other structures, but the effect in the superficial layer was prevented by prior enucleation. Miyaoka (*unpublished observations*) subsequently observed that intraocular administration of minute amounts of apomorphine caused increased glucose utilization only in the superficial layer of the superior colliculus of the contralateral side.

Effects of α- and β-adrenergic blocking agents.

Savaki et al. (122) have studied the effects of the α-adrenergic blocking agent phentolamine and the β-adrenergic blocking agent propranolol. Both drugs produce widespread dose-dependent depressions of glucose utilization throughout the brain but exhibit particularly striking and opposite effects in the complete auditory pathway from the cochlear nucleus to the auditory cortex. Propranolol markedly depresses and phentolamine markedly enhances glucose utilization in this pathway. The functional significance of these effects is unknown but they seem to correlate with corresponding effects on the electrophysiological responsiveness of this sensory system. Propranolol depresses and phentolamine enhances the amplitude of all components of evoked auditory responses (31).

The effects of phentolamine on glucose utilization of the auditory system do not appear to reflect specific effects of α-adrenergic blockade. Other α-adrenergic blocking agents, e.g., phenoxybenzamine and yohimbine, fail to stimulate glucose utilization in the auditory system (123). All the α-adrenergic blocking agents produce generally widespread dose-dependent decreases in glucose utilization in the rat brain (123), except for increases in some brainstem and hypothalamic nuclei that are involved in the regulation of arterial blood pressure and are also activated by arterial hypotension (124). Inasmuch as all the α-adrenergic blocking agents produce arterial hypotension, it is difficult to disentangle the central direct effects and the consequences of systemic effects of the α-adrenergic blocking agents on the basis of the results obtained with the deoxyglucose method (83).

Microscopic Resolution

The resolution of the present [^{14}C]DG method is at best approximately 100 to 200 μm (138; Chapter 5). The use of [^{3}H]DG does not greatly improve the resolution when the standard autoradiographic procedure is used. The limiting factor is the diffusion and migration of the water-soluble labeled compound in the tissue during the freezing of the brain and the cutting of the brain sections (138). Des Rosiers and Descarries (17) attempted to extend the resolution of the method to the light and electron microscopic levels by the use of [^{3}H]DG and dipping emulsion techniques applied to brain that was fixed, dehydrated, and embedded by perfusion *in situ*. They

could localize grain counts over individual cells or portions of them, but loss of label and therefore also of quantitative reliability undoubtedly occurred. An alternative promising approach to microscopic resolution is the use of freeze-substitution techniques (101,131,138).

Potential Usefulness of [^{14}C]DG Method

The deoxyglucose method provides the means to determine quantitatively the rates of glucose utilization simultaneously in all structural and functional components of the central nervous system and to display them pictorially superimposed on the anatomical structures in which they occur. Because of the close relationship between local functional activity and energy metabolism, the method makes it possible to identify all structures with increased or decreased functional activity in various physiological, pharmacological, and pathophysiological states. The images provided by the method do resemble histological sections of nervous tissue, and the method is therefore sometimes misconstrued to be a neuroanatomical method and contrasted with physiological methods, such as electrophysiological recording. This classification obscures the most significant and unique feature of the method. The images are not of structure but of a dynamic biochemical process, glucose utilization, which is as much a physiological as an electrical activity. In most situations changes in functional activity result in changes in energy metabolism, and the images can be used to visualize and identify the sites of altered activity. The images are, therefore, analogous to infrared maps; they record quantitatively the rates of a kinetic process and display them pictorially exactly where they exist. The fact that they depict the anatomical structures is fortuitous; it indicates that the rates of glucose utilization are distributed according to structure, and specific functions in the nervous system are associated with specific anatomical structures. The deoxyglucose method represents, therefore, in a real sense, a new type of encephalography, metabolic encephalography. At the very least, it should serve as a valuable supplement to more conventional types, such as electroencephalography. Because, however, it provides a new means to examine another aspect of function simultaneously in all parts of the brain, it is hoped that it will open new roads to the understanding of how the brain works in health and disease.

DEVELOPMENT OF AUTORADIOGRAPHIC METHOD FOR MEASUREMENT OF LOCAL CEREBRAL PROTEIN SYNTHESIS

The basic biochemical principles for the measurement of metabolic rates *in vivo,* which were so effectively applied in the deoxyglucose technique, also apply to other metabolic processes. A metabolic activity of broad interest is protein synthesis. This biochemical activity is not likely to reflect directly functional activity, at least not acutely, but it may well be involved in slower, more gradual processes in the nervous system, such as growth and development, plasticity, regeneration and repair, response to drugs and hormones, and possibly learning and memory. Protein synthesis may also be altered in pathological states, such as brain tumors, mental retardation due to metabolic errors, aging and senility, Alzheimer's disease, Huntington's disease, endocrine diseases, etc. (Chapter 11).

A method for the measurement of local rates of protein synthesis in the nervous system is under development (140) (Chapters 7 and 10). Like the deoxyglucose method, it is designed to achieve localization by quantitative autoradiography, but it is also being adapted to PET (107). Also like the deoxyglucose method, it is based on the same biochemical principles as

those described above, but their application to the measurement of local cerebral protein synthesis may be far more complex because of still undefined properties and kinetics of the equilibration of the precursor amino acid pool in the tissue with the circulating amino acid pool in the plasma.

Theory

The two essential variables that must be determined in any quantitative radioactive assay of the rate of a reaction are the amount of product formed and the integrated precursor specific activity over a measured interval of time. Because autoradiographic or emission tomographic techniques measure the concentration only of the radioisotope and not that of the radioactive product itself, it is essential that the method be so designed that the label in the tissue remains confined only to a specific product of the reaction or, at least, in well-defined chemical species that can be quantified separately. This problem is mitigated by the use of carboxyl labeled L-leucine, an essential amino acid that is prevalent in most proteins and that, if not incorporated into protein, follows a single simple pathway of metabolic degradation (Fig. 10-19). In the pathway of degradation, the amino acid is first transaminated and then rapidly decarboxylated; the label is then lost as radioactive CO_2, which because of dilution by the large pool of unlabeled CO_2 constantly generated by carbohydrate metabolism, the relatively slow rate of CO_2 fixation, and the rapid removal of CO_2 from brain tissue by the blood flow, is removed from the tissues. The label is then retained only in the product of the reaction, labeled protein, and in the residual unincorporated amino acid. The concentration of free labeled amino acid remaining in the tissue can be calculated from the history of the plasma concentration and the kinetic constants for the equilibration of the tissue free amino acid pools with the plasma. The concentration of free labeled amino acid in the tissue at the time of killing can be minimized by its intravenous administration as a pulse at zero time followed by the allowance of a sufficiently long time for its clearance from the plasma and tissue. One hour after the pulse the fraction of total radioactivity in the tissue that is in the free amino acid pool is small (less than 10%) in the adult rat. In adult monkey and apparently in humans (107), however, it is large (30–50%) because of the relatively slow rates of protein synthesis and of clearance of the free amino acid pools. The error in subtracting a poorly defined free amino acid pool concentration from a total concentration that is not a great deal larger may, of course, be large. With autoradiography this error can be eliminated by histological fixation, which washes out all water-soluble radioactivity, including the free [^{14}C]leucine pool and any of its initial metabolite α-[^{14}C]ketoisocaproate that might be present, while leaving the labeled protein product intact. This simple procedural solution of a complex theoretical problem cannot, however, be used in humans with PET.

An even more difficult problem is the determination of the integrated precursor pool specific activity in the tissue from measurements in the plasma. To accomplish this, it is necessary to know the kinetics of the equilibration of the precursor pool in the cells with that of the plasma. What makes this problem particularly perplexing is that there is evidence that amino acids in the cells are compartmentalized with only a fraction of the total intracellular amino acid content representative of the pool that serves as precursor for protein synthesis. Therefore, although it is relatively simple to measure the rate constants for the equilibration of the total amino acid pool with that of the plasma, there is little assurance that this pool reflects the kinetic behavior of the fraction of it that is the precursor for protein synthesis. A further com-

plication is the possibility of significant dilution of the intracellular precursor amino acid pool by unlabeled amino acid derived from the slow but continuous turnover of the protein components of the cell. The magnitude of this potential dilution is even more difficult to evaluate. Nevertheless, studies are currently in progress in our laboratory that are designed to resolve these problems. If successful, they will not only determine the rate constants for the turnover of the true precursor pool but also the degree of admixture of unlabeled amino acids derived from protein breakdown with the labeled amino acids in the precursor pool.

Applications of [^{14}C]Leucine Method

Although the method is not yet fully developed, experiments with our first and most primitive model already indicate the potential usefulness of a technique that measures local cerebral protein synthesis. This simple model is essentially the same as that for the deoxyglucose method; it assumes a single tissue pool of free amino acid, all of which equilibrates uniformly with the plasma and serves as the precursor pool for protein synthesis with no dilution by unlabeled amino acids derived from protein degradation (140). Although the quantitative values obtained with this version of the method are probably of limited accuracy and may be underestimates of the true rates of L-leucine incorporation into protein, the results demonstrate that the rates of protein synthesis do change in specific regions of the brain in response to altered function. For example, in the rat sectioning of one hypoglossal nerve is followed by increased protein synthesis in the ipsilateral hypoglossal nucleus after a lag of close to 2 to 4 days (139). The increase reaches a maximum between 20 and 30% above the contralateral hypoglossal nucleus, and protein synthesis does not return to normal until after regeneration and restoration of functional activity in the hypoglossal nerve are complete.

The method has also been used to study plasticity in the binocular visual system of the newborn rhesus monkey (63). The outputs from the retinae of the two eyes are crossed approximately 50%, and the optic tracts terminate in the lateral geniculate nuclei in six discrete laminae: 1, 4, and 6, the sites of termination of the pathways from the contralateral retina, and 2, 3, and 5, the laminae supplied by the ipsilateral eye. The cells in these laminae project via the geniculocalcarine tracts to the ipsilateral striate cortex in such a way that the two retinal outputs for each point in the visual field converge to two adjacent cortical columns, one for each eye, for the same spot in the visual field. These are the ocular dominance columns, first described by Hubel and Wiesel (50), and demonstrated autoradiographically by the [^{14}C]DG method (Fig. 1-13C) (58).

The visual system of the newborn monkey exhibits plasticity. Chronic occlusion of one eye in a newborn monkey leads to widening of the ocular dominance columns for the functioning eye at the expense of the columns for the deprived eye until eventually the columns disappear, and the entire striate cortex is taken over to subserve the function of the undeprived eye (18,52). Presumably the axonal terminals of the geniculocalcarine pathway for the functioning eye grow into and take over the synaptic connections in the adjacent columns normally reserved for the deprived eye. If so, changes in protein synthesis required for axonal growth and sprouting could be involved, and the protein synthesis used for this process occurs in the cell bodies of origin of the pathway, i.e., in the lateral geniculate nuclei. Illustrated in Fig. 1-19 are the results of application of the local protein synthesis technique to this question. The laminae in the geniculate bodies are clearly visible and relatively uniform in the autoradiographs of the 25-day-old normal

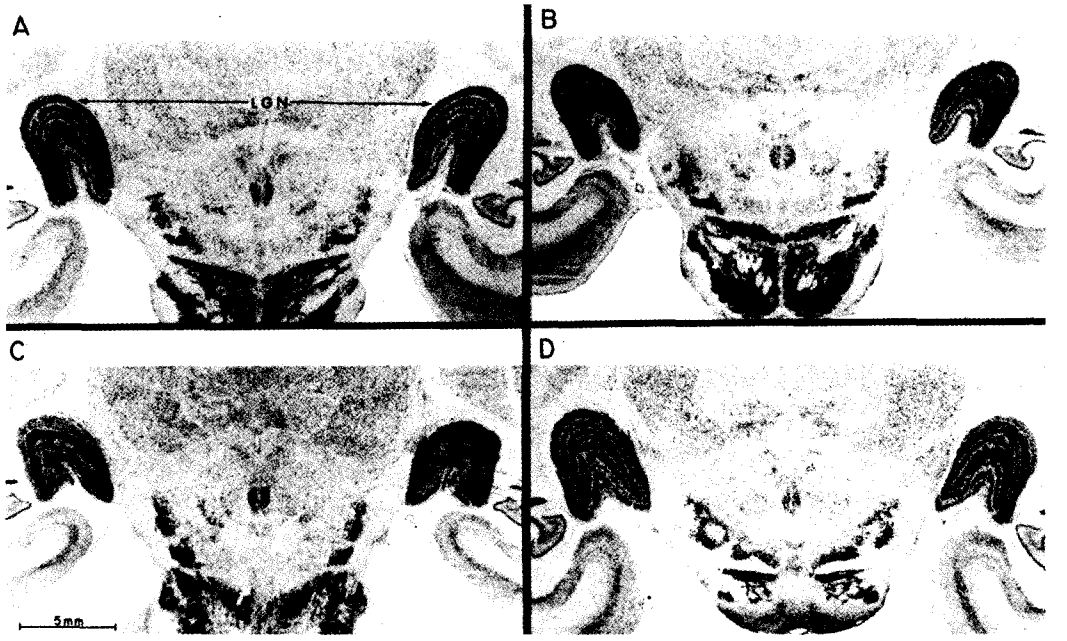

FIG. 1-19. Autoradiographs of coronal sections of monkey lateral geniculate nuclei (LGN) obtained with the [^{14}C]leucine method for the measurement of local cerebral protein synthesis. The left side of the brain is on the *left* side of the autoradiographs. **A:** Twenty-five-day-old monkey with intact binocular vision. **B:** Twenty-five-day-old monkey with acute occlusion (3 hr) of the left eye. **C:** Twenty-five-day-old monkey with chronic occlusion of right eye initiated on second day of life. **D:** Twenty-five-day-old monkey with chronic occlusion of left eye initiated on second day of life. Note the decreased labeling and therefore decreased rate of protein synthesis in laminae 1, 4, and 6 of the lateral geniculate nucleus contralateral to the deprived eye and in laminae 2, 3, and 5 of the nucleus ipsilateral to the deprived eye. Courtesy of Kennedy et al. (63).

monkey. Acute monocular deprivation for 3 hr does not alter the rates of protein synthesis in any of the laminae, including those for the deprived eye. Chronic monocular deprivation from 2 to 25 days of age results in marked reduction in protein synthesis in the laminae served by the deprived eye. Apparently chronic reduction in functional activity, in contrast to the acute state, results in a lowering of protein synthesis in the affected pathway. These results suggest that the loss of ocular dominance columns in the striate cortex for the chronically deprived eye is the result of depressed protein synthesis and deficient axonal growth in the geniculocalcarine pathways for the deprived eye.

It is hoped that measurement of local rates of protein synthesis in the nervous system may be useful to study normal and abnormal neural processes that may not be accessible to other autoradiographic and tomographic procedures—processes such as growth, maturation, plasticity, and actions of hormones. The full potential of this approach must, however, await the development of a fully accurate and reliable method.

ACKNOWLEDGMENT

The author expresses his appreciation to J. D. Brown for his skilled photographic reproduction and to Brenda Sandler for her

excellent editorial and bibliographic assistance.

REFERENCES

1. Abrams, R., Ito, M., Frisinger, J. E., Patlak, C. S., Pettigrew, K. D., and Kennedy, C. (1984): Local cerebral glucose utilization in fetal and neonatal sheep. *Am. J. Physiol.*, 246:R608–R618.
2. Allen, T. O., Adler, N. T., Greenberg, J. H., and Reivich, M. (1981): Vaginocervical stimulation selectively increases metabolic activity in the rat brain. *Science*, 211:1070–1072.
3. Allweis, C., Landau, T., Abeles, M., and Magnes, J. (1966): The oxidation of uniformly labelled albumen-bound palmitic acid to CO_2 by the perfused cat brain. *J. Neurochem.*, 13:795–804.
4. Bachelard, H. S. (1971): Specificity and kinetic properties of monosaccharide uptake into guinea pig cerebral cortex *in vitro*. *J. Neurochem.*, 18:213–222.
5. Baños, G., Daniel, P. M., Moorhouse, S. R., and Pratt, O. E. (1973): The influx of amino acids into the brain of the rat *in vivo*: The essential compared with some non-essential amino acids. *Proc. R. Soc. Lond. (Biol.)*, 183:59–70.
6. Batipps, M., Miyaoka, M., Shinohara, M., Sokoloff, L., and Kennedy, C. (1981): Comparative rates of local cerebral glucose utilization in the visual system of conscious albino and pigmented rat. *Neurology*, 31:58–62.
7. Beattie, D. S., and Basford, R. E. (1965): Brain mitochondria. III. Fatty acid oxidation by bovine brain mitochondria. *J. Neurochem.*, 12:103–111.
8. Betz, E. (1972): Cerebral blood flow: Its measurement and regulation. *Physiol. Rev.*, 52:595–630.
9. Bidder, T. G. (1968): Hexose translocation across the blood-brain interface: Configurational aspects. *J. Neurochem.*, 15:867–874.
10. Birren, J. E., Butler, R. N., Greenhouse, S. W., Sokoloff, L., and Yarrow, M. R., eds. (1963): *Human Aging. A Biological and Behavioral Study.* Public Health Service Publication No. 985, U.S. Government Printing Office, Washington, D.C.
11. Brown, L. L., and Wolfson, L. I. (1978): Apomorphine increases glucose utilization in the substantia nigra, subthalamic nucleus and corpus striatum of rat. *Brain Res.*, 140:188–193.
12. Caveness, W. F. (1969): Ontogeny of focal seizures. In: *Basic Mechanisms of the Epilepsies*, edited by H. H. Jasper, A. A. Ward, and A. Pope, pp. 517–534. Little, Brown and Co., Boston.
13. Chaplin, E. R., Goldberg, A. L., and Diamond, I. (1976): Leucine oxidation in brain slices and nerve endings. *J. Neurochem.*, 26:701–707.
14. Collins, R. C., Kennedy, C., Sokoloff, L., and Plum, F. (1976): Metabolic anatomy of focal motor seizures. *Arch. Neurol.*, 33:536–542.
15. Cremer, J. E., and Heath, D. F. (1974): The estimation of rates of utilization of glucose and ketone bodies in the brain of suckling rat using compartmental analysis of isotopic data. *Biochem. J.*, 142:527–544.
16. Davson, H. (1967): *Physiology of the Cerebrospinal Fluid.* Churchill, London.
17. Des Rosiers, M. H., and Descarries, L. (1978): Adaptation de la méthode au désoxyglucose à l'échelle cellulaire: Préparation histologique du système nerveux central en vue de la radio-autographie à haute résolution. *C. R. Acad. Sci. Paris, Series D*, 287:153–156.
18. Des Rosiers, M. H. Sakurado, O., Jehle, J., Shinohara, M., Kennedy, C., and Sokoloff, L. (1978): Functional plasticity in the immature striate cortex of the monkey shown by the [^{14}C]deoxyglucose method. *Science*, 200:447–449.
19. Dow-Edwards, D. L., Crane, A., Kennedy, C., and Sokoloff, L. (1982): Alterations of brain glucose metabolism in cretinism. *Soc. Neurosci. Abstr.*, 8:872.
20. Duffy, T. E., Cavazzuti, M., Cruz, N. F., and Sokoloff, L. (1982): Local cerebral glucose metabolism in newborn dogs: Effects of hypoxia and halothane anesthesia. *Ann. Neurol.*, 11:233–246.
21. Durham, D., and Woolsey, T. A. (1977): Barrels and columnar cortical organization: Evidence from 2-deoxyglucose (2-DG) experiments. *Brain Res.*, 137:169–174.
22. Dymsza, H. A., Czajka, D. M., and Miller, S. A. (1964): Influence of artificial diet on weight gain and body composition of the neonatal rat. *J. Nutr.*, 84:100–106.
23. Eayrs, J. T. (1964): Endocrine influence on cerebral development. *Arch. Biol. Liege*, 75:529–565.
24. Eckman, W. W., Phair, R. D., Fenstermacher, J. D., Patlak, C. S., Kennedy, C., and Sokoloff, L. (1975): Permeability limitation in estimation of local brain blood flow with [^{14}C]antipyrine. *Am. J. Physiol.*, 229:215–221.
25. Eklöf, B., Lassen, N. A., Nilsson, L., Norberg, K., Siesjö, B. K., and Torlöf, P. (1974): Regional cerebral blood flow in the rat measured by the tissue sampling technique: A critical evaluation using four indicators, C^{14}-antipyrine, C^{14}-ethanol, H^3-water, and xenon^{133}. *Acta Physiol. Scand.*, 91:1–10.
26. Felig, P., Wahren, J., and Ahlborg, G. (1973): Uptake of individual amino acids by the human brain. *Proc. Soc. Exp. Biol. Med.*, 142:230–231.
27. Finnerty, F. A., Jr., Witkin, L., and Fazekas, J. F. (1954): Cerebral hemodynamics during cerebral ischemia induced by acute hypotension. *J. Clin. Invest.*, 33:1227–1232.
28. Frackowiak, R. S. J., Lenzi, G.-L., Jones, T., and Heather, J. D. (1980): Quantitative measurement of regional cerebral blood flow and oxygen metabolism in man using ^{15}O and positron emission tomography. *J. Comput. Assist. Tomogr.*, 4:727–736.
29. Freygang, W. H., Jr., and Sokoloff, L. (1958): Quantitative measurement of regional circulation in the central nervous system by the use of radioactive inert gas. *Adv. Biol. Med. Physics*, 6:263–279.
30. Friedli, C. (1978): Kinetics of changes in pO_2 and extracellular potassium activity in stimulated rat sympathetic ganglia. In: *Advances in Experimental Medicine and Biology: Oxygen Transport to Tissue III*, edited by I. A. Silver, M. Erecinska, and H. I. Bicher, pp. 747–754. Plenum Press, New York.
31. Furlow, T. W., Hallenbeck, J. M., and Goodman, J. C. (1980): Adrenergic blocking agents modify the auditory-evoked response in the rat. *Brain Res.*, 189:269–273.
32. Galvan, M., Ten Bruggencate, G., and Senekowitsch, R. (1979): The effects of neuronal stimulation and ouabain upon extracellular K^+ and Ca^{2+} levels in rat isolated sympathetic ganglia. *Brain Res.*, 160:544–548.
33. Geiger, A. (1958): Correlation of brain metabolism and function by the use of a brain perfusion method *in situ*. *Physiol. Rev.*, 38:1–20.
34. Gjedde, A., Caronna, J. J., Hindfelt, B., and Plum, F. (1975): Whole-brain blood flow and oxygen metabolism in the rat during nitrous oxide anesthesia. *Am. J. Physiol.*, 229:113–118.
35. Gjedde, A., and Crone, C. (1975): Induction process in blood-brain transfer of ketone bodies during starvation. *Am. J. Physiol.*, 229:1165–1169.
36. Goochee, C., Rasband, W., and Sokoloff, L. (1980): Computerized densitometry and color coding of [^{14}C]deoxyglucose autoradiographs. *Ann. Neurol.*, 7:359–370.

37. Gotoh, F., Meyer, J. S., and Tomita, M. (1966): Hydrogen method for determining cerebral blood flow in man. *Arch. Neurol.*, 15:549–559.
38. Göttstein, U., Held, K., Müller, W., and Berghoff, W. (1972): Utilization of ketone bodies by the human brain. In: *Research on the Cerebral Circulation: Fifth International Salzburg Conference,* edited by J. S. Meyer, M. Reivich, H. Lechner, and O. Eichhorn, pp. 137–145. Charles C Thomas, Springfield, IL.
39. Hand, P. J. (1981): The 2-deoxyglucose method. In: *Neuroanatomical Tract Tracing Methods,* edited by L. Heimer and M. J. Robards, pp. 511–538. Plenum Press, New York.
40. Hand, P. J., Greenberg, J. H., Miselis, R. R., Weller, W. L., and Reivich, M. (1978): A normal altered cortical column: A quantitative and qualitative (^{14}C)-2 deoxyglucose (2 DG) mapping study. *Soc. Neurosci. Abstr.*, 4:533.
41. Hawkins, R. A., and Miller, D. L. (1978): Loss of radioactive 2-deoxy-D-glucose-6-phosphate from brains of conscious rats: Implications for quantitative autoradiographic determination of regional glucose utilization. *Neuroscience,* 3:251–258.
42. Hawkins, R., Phelps, M., Huang, S. C., and Kuhl, D. (1981): Effect of ischemia upon quantification of local cerebral metabolic rates for glucose with 2-(F-18)fluorodeoxyglucose (FDG). *J. Cereb. Blood Flow Metab.*, 1(*Suppl.* 1):S9–S10.
43. Hawkins, R. A., Williamson, D. H., and Krebs, H. A. (1971): Ketone-body utilization by adult and suckling rat brain *in vivo. Biochem, J.*, 122:13–18.
44. Hers, H. G. (1957): *Le Métabolisme du Fructose,* p. 102. Editions Arscia, Bruxelles.
45. Himwich, H. E., and Nahum, L. H. (1929): The respiratory quotient of testicle. *Am. J. Physiol.*, 88:680–685.
46. Horowicz, P., and Larrabee, M. G. (1958): Glucose consumption and lactate production in a mammalian sympathetic ganglion at rest and in activity. *J. Neurochem.*, 2:102–118.
47. Hosokawa, S., Iguchi, T., Caveness, W. F., Kato, M., O'Neill, R. R., Wakisaka, S., and Malamut, B. L. (1980): Effects of manipulation of the sensorimotor system on focal motor seizures in the monkey. *Ann. Neurol.*, 7:222–229.
48. Huang, M.-T., and Veech, R. L. (1982): The quantitative determination of the *in vivo* dephosphorylation of glucose 6-phosphate in rat brain. *J. Biol. Chem.*, 257:11358–11363.
49. Huang, S. C., Phelps, M. E., Hoffman, E. J., Sideris, K., Selin, C. J., and Kuhl, D. C. (1980): Noninvasive determination of local cerebral metabolic rate of glucose in man. *Am. J. Physiol.*, 128:E69–E82.
50. Hubel, D. H., and Wiesel, T. N. (1968): Receptive fields and functional architecture of monkey striate cortex. *J. Physiol.*, 195:215–243.
51. Hubel, D. H., and Wiesel, T. N. (1972): Laminar and columnar distribution of geniculo-cortical fibers in the macaque monkey. *J. Comp. Neurol.*, 146:421–450.
52. Hubel, D. H., Wiesel, T. N., and LeVay, S. (1977): Plasticity of ocular dominance columns in monkey striate cortex. *Phil. Trans. R. Soc. Lond. (Biol.),* 278:377–409.
53. Hubel, D. H., Wiesel, T. N., and Stryker, M. P. (1978): Anatomical demonstration of orientation columns in macaque monkey. *J. Comp. Neurol.*, 177:361–380.
54. Itoh, T., and Quastel, J. H. (1970): Acetoacetate metabolism in infant and adult rat brain *in vitro. Biochem. J.*, 116:641–655.
55. Kadekaro, M., Gross, P. M., Sokoloff, L., Holcomb, H. H., and Saavedra, J. M. (1983): Elevated glucose utilization in subfornical organ and pituitary neural lobe of the Brattleboro rat. *Brain Res.*, 275:189–193.
56. Katzman, R. (1976): Blood-brain-CSF barriers. In: *Basic Neurochemistry,* 2nd ed., edited by G. J. Siegel, R. W. Albers, R. Katzman, and B. W. Agranoff, pp. 414–428. Little, Brown, Boston.
57. Kennedy, C., Des Rosiers, M., Reivich, M., Sharp, F., Jehle, J. W., and Sokoloff, L. (1975): Mapping of functional neural pathways by autoradiographic survey of local metabolic rate with [^{14}C]deoxyglucose. *Science,* 187:850–853.
58. Kennedy, C., Des Rosiers, M. H., Sakurada, O., Shinohara, M., Reivich, M., Jehle, J. W., and Sokoloff, L. (1976): Metabolic mapping of the primary visual system of the monkey by means of the autoradiographic [^{14}C]deoxyglucose technique. *Proc. Natl. Acad. Sci. USA,* 73:4230–4234.
59. Kennedy, C., Gillin, J. C., Mendelson, W., Suda, S., Miyaoka, M., Ito, M., Nakamura, R. K., Storch, F. I., Pettigrew, K., Mishkin, M., and Sokoloff, L. (1982): Local cerebral glucose utilization in non-rapid eye movement sleep. *Nature,* 297:325–327.
60. Kennedy, C., Miyaoka, M., Suda, S., Macko, K., Jarvis, C., Mishkin, M., and Sokoloff, L. (1980): Local metabolic responses in brain accompanying motor activity. *Trans. Am. Neurol. Assoc.*, 105:13–17.
61. Kennedy, C., Sakurada, O., Shinohara, M., Jehle, J., and Sokoloff, L. (1978): Local cerebral glucose utilization in the normal conscious macaque monkey. *Ann. Neurol.*, 4:293–301.
62. Kennedy, C., and Sokoloff, L. (1957): An adaptation of the nitrous oxide method to the study of the cerebral circulation in children: Normal values for cerebral blood flow and cerebral metabolic rate in childhood. *J. Clin. Invest.*, 36:1130–1137.
63. Kennedy, C., Suda, S., Smith, C. B., Miyaoka, M., Ito, M., and Sokoloff, L. (1981): Changes in protein synthesis underlying functional plasticity in immature monkey visual system. *Proc. Natl. Acad. Sci. USA,* 78:3950–3953.
64. Kety, S. S. (1950): Circulation and metabolism of the human brain in health and disease. *Am. J. Med.*, 8:205–217.
65. Kety, S. S. (1951): The theory and applications of the exchange of inert gas at the lungs and tissues. *Pharmacol. Rev.*, 3:1–41.
66. Kety, S. S. (1957): The general metabolism of the brain *in vivo.* In: *The Metabolism of the Nervous System,* edited by D. Richter, pp. 221–237. Pergamon Press, London.
67. Kety, S. S. (1960): The cerebral circulation. In: *Handbook of Physiology: Neurophysiology, Vol. III,* edited by J. Field, H. W. Magoun, and V. E. Hall, pp. 1751–1760. American Physiological Society, Washington, D.C.
68. Kety, S. S., Polis, B. D., Nadler, C. S., and Schmidt, C. F. (1948): The blood flow and oxygen consumption of the human brain in diabetic acidosis and coma. *J. Clin. Invest.*, 27:500–510.
69. Kety, S. S., and Schmidt, C. F. (1948): The nitrous oxide method for the quantitative determination of cerebral blood flow in man: Theory, procedure, and normal values. *J. Clin. Invest.*, 27:476–483.
70. Kety, S. S., Woodford, R. B., Harmel, M. H., Freyhan, F. A., Appel, K. E., and Schmidt, C. F. (1948): Cerebral blood flow and metabolism in schizophrenia. The effects of barbiturate semi-narcosis, insulin coma, and electroshock. *Am. J. Psychiatry,* 104:765–770.
71. Krebs, H. A., Williamson, D. H., Bates, M. W., Page, M. A., and Hawkins, R. A. (1971): The role of ketone bodies in caloric homeostasis. *Adv. Enzyme Regul.* 9:387–409.
72. Lajtha, A., and Ford, D. H., eds. (1968): *Brain Barrier Systems.* Elsevier, Amsterdam.

73. Landau, W. H., Freygang, W. H., Rowland, L. P., Sokoloff, L., and Kety, S. S. (1955): The local circulation of the living brain: Values in the unanesthetized and anesthetized cat. *Trans. Am. Neurol. Assoc.*, 80:125–129.
74. Larrabee, M. G. (1958): Oxygen consumption of excised sympathetic ganglia at rest and in activity. *J. Neurochem.*, 2:81–101.
75. Lashley, K. S. (1934): The mechanism of vision. VII. The projection of the retina upon the primary optic centers of the rat. *J. Comp. Neurol.*, 59:341–373.
76. Lassen, N. A. (1959): Cerebral blood flow and oxygen consumption in man. *Physiol. Rev.*, 39:183–238.
77. Lassen, N. A., and Ingvar, D. H. (1972): Radioisotopic assessment of regional cerebral blood flow. *Prog. Nucl. Med.*, 1:376–409.
78. Lassen, N. A., and Munck, O. (1955): The cerebral blood flow in man determined by the use of radioactive krypton. *Acta Physiol. Scand.*, 33:30–49.
79. Lewis, B. M., Sokoloff, L., Wechsler, R. L., Wentz, W. B., and Kety, S. S. (1960): A method for the continuous measurement of cerebral blood flow in man by means of radioactive krypton (Kr^{79}). *J. Clin. Invest.*, 39:707–716.
80. Little, J. R., Hori, S., and Spitzer, J. J. (1969): Oxidation of radioactive palmitate and glucose infused into the cortical subarachnoid space. *Am. J. Physiol.*, 217:919–922.
81. Macko, K. A., Jarvis, C. D., Kennedy, C., Miyaoka, M., Shinohara, M., Sokoloff, L., and Mishkin, M. (1982): Mapping the primate visual system with [2-^{14}C]deoxyglucose. *Science*, 218:394–396.
82. Mata, M., Fink, D. J., Gainer, H., Smith, C. B., Davidsen, L., Savaki, H., Schwartz, W. J., and Sokoloff, L. (1980): Activity-dependent energy metabolism in rat posterior pituitary primarily reflects sodium pump activity. *J. Neurochem.*, 34:213–215.
83. McCulloch, J. (1982): Mapping functional alterations in the CNS with [^{14}C]deoxyglucose. In: *Handbook of Psychopharmacology, Vol. 15*, edited by L. Iversen, S. Iversen, and S. Snyder, pp. 331–410. Plenum Publishing Corp., New York.
84. McCulloch, J., Savaki, H. E., McCulloch, M. C., and Sokoloff, L. (1979): Specific distribution of metabolic alterations in cerebral cortex following apomorphine administration. *Nature*, 282:303–305.
85. McCulloch, J., Savaki, H. E., McCulloch, M. C., and Sokoloff, L. (1980): Retina-dependent activation by apomorphine of metabolic activity in the superficial layer of the superior colliculus. *Science*, 207:313–315.
86. McCulloch, J., Savaki, H. E., and Sokoloff, L. (1980): Influence of dopaminergic systems on the lateral habenula nucleus of the rat. *Brain Res.*, 194:117–124.
87. McKhann, G. M., Albers, R. W., Sokoloff, L., Mickelson, O., and Tower, D. B. (1960): The quantitative significance of the gamma-aminobutyric acid pathway in cerebral oxidative metabolism. In: *Inhibition in the Nervous System and γ-Aminobutyric Acid*, edited by E. Roberts, pp. 169–181. Pergamon Press, Oxford.
88. Meyer, J. S., Ryu, T., Toyoda, M., Shinohara, Y., Wiederholt, I., and Guiraud, B. (1969): Evidence for a Pasteur effect regulating cerebral oxygen and carbohydrate metabolism in man. *Neurology (Minneap.)*, 19:954–962.
89. Miyaoka, M., Shinohara, M., Batipps, M., Pettigrew, K. D., Kennedy, C., and Sokoloff, L. (1979): The relationship between the intensity of the stimulus and the metabolic response in the visual system of the rat. *Acta Neurol. Scand.*, 60(*Suppl.* 72):16–17.
90. Montero, V. M., and Guillery, R. W. (1968): Degeneration in the dorsal lateral geniculate nucleus of the rat following interruption of the retinal or cortical connections. *J. Comp. Neurol.*, 134:211–242.
91. Moore, T. J., Lione, A. P., Sugden, M. C., and Regen, D. M. (1976): β-Hydroxybutyrate transport in rat brain: Developmental and dietary modulations. *Am. J. Physiol.*, 230:619–630.
92. Nelson, T., Kaufman, E. E., and Sokoloff, L. (1984): 2-Deoxyglucose incorporation into rat brain glycogen during measurement of local cerebral glucose utilization by the 2-deoxyglucose method. *J. Neurochem.*, 43:949–956.
93. Nemoto, E. M., Hoff, J. T., and Severinghaus, J. W. (1974): Lactate uptake and metabolism by brain during hyperlactatemia and hypoglycemia. *Stroke*, 5:48–53.
94. Nemoto, E. M., and Severinghaus, J. W. (1974): Stereospecific permeability of rat blood-brain barrier to lactic acid. *Stroke*, 5:81–84.
95. Nilsson, B., And Siesjö, B. K. (1976): A method for determining blood flow and oxygen consumption in the rat brain. *Acta Physiol. Scand.*, 96:72–82.
96. Nordmann, J. J. (1977): Ultrastructural morphometry of the rat neurohypophysis. *J. Anat.*, 123:213–218.
97. Odessey, R., and Goldberg, A. L. (1972): Oxidation of leucine by rat skeletal muscle. *Am. J. Physiol.*, 223:1376–1383.
98. Oldendorf, W. H. (1971): Brain uptake of radiolabeled amino acids, amines, and hexoses after arterial injection. *Am. J. Physiol.*, 221:1629–1638.
99. Oldendorf, W. H. (1973): Carrier-mediated blood-brain barrier transport of short-chain monocarboxylic organic acids. *Am. J. Physiol.*, 224:1450–1453.
100. Oldendorf, W. H., and Szabo, J. (1976): Amino acid assignment to one of three blood-brain barrier amino acid carriers. *Am. J. Physiol.*, 230:94–98.
101. Ornberg, R. L., Neale, E. A., Smith, C. B., Yarowsky, P., and Bowers, L. M. (1979): Radioautographic localization of glucose utilization by neurons in culture. *J. Cell Biol. Abstr.*, 83:CN142A.
102. Owen, O. E., Morgan, A. P., Kemp, H. G., Sullivan, J. M., Herrera, M. G., and Cahill, G. F. (1967): Brain metabolism during fasting. *J. Clin. Invest.*, 46:1589–1595.
103. Persson, B., Settergren, G., and Dahlquist, G. (1972): Cerebral arterio-venous difference of acetoacetate and D-β-hydroxybutyrate in children. *Acta Paediatr. Scand.*, 61:273–278.
104. Phelps, M. E., Hoffman, E. J., Mullani, N. A., and Ter Pogossian, M. M. (1975): The application of annihilation coincidence detection to transaxial reconstruction tomography. *J. Nucl. Med.*, 16:210–224.
105. Phelps, M. E., Huang, S. C., Hoffman, E. J., Selin, C., Sokoloff, L., and Kuhl, D. E. (1979): Tomographic measurement of local cerebral glucose metabolic rate in humans with (F-18)2-fluoro-2-deoxy-*d*-glucose: Validation of method. *Ann. Neurol.*, 6:371–388.
106. Phelps, M. E., Mazziotta, J. C., and Huang, S. C. (1982): Study of cerebral function with positron computed tomography. *J. Cereb. Blood Flow Metab.*, 2:113–162.
107. Phelps, M. E., Barrio, J. R., Huang, S.-C., Keen, R. E., Chugani, H., and Mazziotta, J. C. (1985): Measurement of cerebral protein synthesis in man with positron computerized tomography: Model, assumptions, and preliminary results. In: *The Metabolism of the Human Brain Studied with Positron Emission Tomography*, edited by T. Greitz, D. H. Ingvar, and L. Widén, pp. 215–232. Raven Press, New York.
108. Plum, F., Gjedde, A., and Samson, F. E. (1976): Neuroanatomical functional mapping by the radioactive 2-deoxy-D-glucose method. *Neurosci. Res. Prog. Bull.*, 14:457–518.
109. Porrino, L., Namba, H., Crane, A., Jehle, J., and Sokoloff, L. (1982): Modulation of local cerebral glucose me-

tabolism by estrogen and progesterone in the hypothalamus of ovariectomized female rats. *Soc. Neurosci. Abstr.*, 8:69.
110. Pull, I., and McIlwain, H. (1971): 3-Hydroxybutyrate dehydrogenase of rat brain on dietary change and during maturation. *J. Neurochem.*, 18:1163–1165.
111. Rakic, P. (1976): Prenatal genesis of connections subserving ocular dominance in the rhesus monkey. *Nature*, 261:467–471.
112. Rapoport, S. (1976): *Blood-Brain Barrier in Physiology and Medicine.* Raven Press, New York.
113. Raskin, N. H., and Sokoloff, L. (1970): Alcohol dehydrogenase activity in rat brain and liver. *J. Neurochem.*, 17:1677–1687.
114. Reivich, M., Jehle, J., Sokoloff, L., and Kety, S. S. (1969): Measurement of regional cerebral blood flow with antipyrine-^{14}C in awake cats. *J. Appl. Physiol.*, 27:296–300.
115. Reivich, M., Kuhl, D., Wolf, A., Greenberg, J., Phelps, M., Ido, T., Cassella, V., Fowler, J., Hoffman, E., Alavi, A., Som, P., and Sokoloff, L. (1979): The [^{18}F]fluorodeoxyglucose method for the measurement of local cerebral glucose utilization in man. *Circ. Res.*, 44:127–137.
116. Rossen, R., Kabat, H., and Anderson, J. P. (1943): Acute arrest of cerebral circulation in man. *Arch. Neurol. Psychiatry*, 50:510–528.
117. Roth, R. H. (1976): Striatal dopamine and gamma-hydroxybutyrate. *Pharmacol. Ther.*, 2:71–88.
118. Roth, R. H., and Giarman, N. J. (1966): γ-Butyrolactone and γ-hydroxybutyric acid. I. Distribution and metabolism. *Biochem. Pharmacol.*, 15:1333–1348.
119. Sacks, W. (1969): Cerebral metabolism *in vivo.* In: *Handbook of Neurochemistry, Vol. I*, edited by A. Lajtha, pp. 301–324. Plenum Press, New York.
120. Sacks, W., Sacks, S., and Fleischer, A. (1983): A comparison of the cerebral uptake and metabolism of labeled glucose and deoxyglucose *in vivo* in rats. *Neurochem. Res.*, 8:661–685.
121. Sakurada, O., Kennedy, C., Jehle, J., Brown, J. D., Carbin, G. L., and Sokoloff, L. (1978): Measurement of local cerebral blood flow with [^{14}C]iodoantipyrine. *Am. J. Physiol.*, 234:H59–H66.
122. Savaki, H. E., Kadekaro, M., Jehle, J., and Sokoloff, L. (1978): α- And β-adrenoreceptor blockers have opposite effects on energy metabolism of the central auditory system. *Nature*, 276:521–523.
123. Savaki, H. E., Kadekaro, M., McCulloch, J., and Sokoloff, L. (1982): Central noradrenergic systems in the rat: A metabolic mapping with three α-blocking agents. *Brain Res.*, 234:65–79.
124. Savaki, H. E., McCulloch, J., Kadekaro, M., and Sokoloff, L. (1982): Influence of α-receptor blocking agents upon metabolic activity in nuclei involved in central control of blood pressure. *Brain Res.*, 233:347–358.
125. Schuier, F., Orzi, F., Suda, S., Kennedy, C., and Sokoloff, L. (1981): The lumped constant for the [^{14}C]deoxyglucose method in hyperglycemic rats. *J. Cereb. Blood Flow Metab.*, 1:S63.
126. Schwartz, W. J. (1978): A role for the dopaminergic nigrostriatal bundle in the pathogenesis of altered brain glucose consumption after lateral hypothalamic lesions. Evidence using the ^{14}C-labeled deoxyglucose technique. *Brain Res.*, 158:129–147.
127. Schwartz, W. J., Davidsen, L. C., and Smith, C. B. (1980): *In vivo* metabolic activity of a putative circadian oscillator, the rat suprachiasmatic nucleus. *J. Comp. Neurol.*, 189:157–167.
128. Schwartz, W. J., and Gainer, H. (1977): Suprachiasmatic nucleus: Use of ^{14}C-labeled deoxyglucose uptake as a functional marker. *Science*, 197:1089–1091.
129. Schwartz, W. J., Sharp, F. R., Gunn, R. H., and Evarts, E. V. (1976): Lesions of ascending dopaminergic pathways decrease forebrain glucose uptake. *Nature*, 261:155–157.
130. Schwartz, W. J., Smith, C. B., Davidsen, L., Savaki, H., Sokoloff, L., Mata, M., Fink, D. J., and Gainer, H. (1979): Metabolic mapping of functional activity in the hypothalamo-neurohypophysical system of the rat. *Science*, 205:723–725.
131. Sejnowski, T. J., Reingold, S. C., Kelley, D. B., and Gelperin, A. (1980): Localization of [^{3}H]-2-deoxyglucose in single molluscan neurones. *Nature*, 287:449–451.
132. Sharp, F. R., Kauer, J. S., and Shepherd, G. M. (1975): Local sites of activity-related glucose metabolism in rat olfactory bulb during olfactory stimulation. *Brain Res.*, 98:596–600.
133. Shinohara, M., Dollinger, B., Brown, G., Rapoport, S., and Sokoloff, L. (1979): Cerebral glucose utilization: Local changes during and after recovery from spreading cortical depression. *Science*, 203:188–190.
134. Silverman, M. S., Hendrickson, A. E., and Clopton, B. M. (1977): Mapping of the tonotopic organization of the auditory system by uptake of radioactive metabolites. *Soc. Neurosci. Abstr.*, 3:11.
135. Sloviter, H. A., and Kamimoto, T. (1970): The isolated, perfused rat brain preparation metabolizes mannose but not maltose. *J. Neurochem.*, 17:1109–1111.
136. Sloviter, H. A., Shimkin, P., and Suhara, K. (1966): Glycerol as a substrate for brain metabolism. *Nature*, 210:1334–1336.
137. Sloviter, H. A., and Suhara, K. (1967): A brain-infusion method for demonstrating utilization of glycerol by rabbit brain *in vivo*. *J. Appl. Physiol.*, 23:792–797.
138. Smith, C. B. (1983): Localization of activity-associated changes in metabolism of the central nervous system with the deoxyglucose method: Prospects for cellular resolution. In: *Current Methods in Cellular Neurobiology*, edited by J. L. Barker and J. F. McKelvy, pp. 269–317. John Wiley & Sons, New York.
139. Smith, C. B., Crane, A. M., Kadekaro, M., Agranoff, B. W., and Sokoloff, L. (1984): Stimulation of protein synthesis and glucose utilization in the hypoglossal nucleus induced by axotomy. *J. Neurosci.*, 4:2489–2496.
140. Smith, C. B., Davidsen, L., Deibler, G., Patlak, C., Pettigrew, K., and Sokoloff, L. (1980): A method for the determination of local rates of protein synthesis in brain. *Trans. Am. Soc. Neurochem.*, 11:94.
141. Smith, C. B., Goochee, C., Rapoport, S. I., and Sokoloff, L. (1980): Effects of ageing on local rates of cerebral glucose utilization in the rat. *Brain*, 103:351–365.
142. Sokoloff, L. (1959): The action of drugs on the cerebral circulation. *Pharmacol. Rev.*, 11:1–85.
143. Sokoloff, L. (1960): Quantitative measurements of cerebral blood flow in man. In: *Methods in Medical Research, Vol. VIII*, edited by H. D. Bruner, pp. 253–261. Year Book Publishers, Chicago.
144. Sokoloff, L. (1960): The metabolism of the cerebral nervous system *in vivo*. In: *Handbook of Physiology: Neurophysiology, Vol. III*, edited by J. Field, H. W. Magoun, and V. E. Hall, pp. 1843–1864. American Physiological Society, Washington, D.C.
145. Sokoloff, L. (1961): Local cerebral circulation at rest and during altered cerebral activity induced by anesthesia or visual stimulation. In: *The Regional Chemistry, Physiology and Pharmacology of the Nervous System*, edited by S. S. Kety and J. Elkes, pp. 107–117. Pergamon Press, Oxford.
146. Sokoloff, L. (1966): Cerebral circulatory and metabolic changes associated with aging. *Res. Publ. Assoc. Res. Nerv. Ment. Dis.*, 41:237–254.

147. Sokoloff, L. (1976): Circulation and energy metabolism of the brain. In: *Basic Neurochemistry,* 2nd ed., edited by G. J. Siegel, R. W. Albers, R. Katzman, and B. W. Agranoff, pp. 388–413. Little, Brown, Boston.
148. Sokoloff, L. (1977): Relation between physiological function and energy metabolism in the central nervous system. *J. Neurochem.,* 29:13–26.
149. Sokoloff, L. (1978): Mapping cerebral functional activity with radioactive deoxyglucose. *Trends Neurosci.,* 1:75–79.
150. Sokoloff, L. (1978): Local cerebral energy metabolism: Its relationships to local functional activity and blood flow. In: *Ciba Foundation Symposium 56: Cerebral Vascular Smooth Muscle and Its Control,* edited by M. J. Purves and K. Elliott, pp. 171–197. Elsevier/Excerpta Medica/North-Holland, Amsterdam.
151. Sokoloff, L. (1979): The [^{14}C]deoxyglucose method: Four years later. *Acta Neurol. Scand.,* 60(*Suppl.* 70):640–649.
152. Sokoloff, L. (1981): Localization of functional activity in the central nervous system by measurement of glucose utilization with radioactive deoxyglucose. *J. Cereb. Blood Flow Metab.,* 1:7–36.
153. Sokoloff, L. (1982): The radioactive deoxyglucose method: Theory, procedure, and applications for the measurement of local glucose utilization in the central nervous system. In: *Advances in Neurochemistry, Vol. 4,* edited by B. W. Agranoff and M. H. Aprison, pp. 1–82. Plenum Publishing Corp., New York.
154. Sokoloff, L., Reivich, M., Kennedy, C., Des Rosiers, M. H., Patlak, C. S., Pettigrew, K. D., Sakurada, O., and Shinohara, M. (1977): The [^{14}C]deoxyglucose method for the measurement of local cerebral glucose utilization: Theory, procedure, and normal values in the conscious and anesthetized albino rat. *J. Neurochem.,* 28:897–916.
155. Sokoloff, L., Wechsler, R. L., Mangold, R., Balls, K., and Kety, S. S. (1953): Cerebral blood flow and oxygen consumption in hyperthyroidism before and after treatment. *J. Clin. Invest.,* 32:202–208.
156. Sols, A., and Crane, R. K. (1954): Substrate specificity of brain hexokinase. *J. Biol. Chem.,* 210:581–595.
157. Spitzer, J. J., and Weng, J. T. (1972): Removal and utilization of ketone bodies by the brain of newborn puppies. *J. Neurochem.,* 19:2169–2173.
158. Spitzer, J. J., and Wolf, E. H. (1971): Uptake and oxidation of FFA administered by ventriculocisternal perfusion in the dog. *Am. J. Physiol.,* 221:1426–1430.
159. Suda, S., Shinohara, M., Miyaoka, M., Kennedy, C., and Sokoloff, L. (1981): Local cerebral glucose utilization in hypoglycemia. *J. Cereb. Blood Flow Metab.,* 1:S62.
160. Swaiman, K. F., and Milstein, J. M. (1965): Oxidation of leucine, isoleucine, and related ketoacids in developing rabbit brain. *J. Neurochem.,* 12:981–986.
161. Tower, D. B. (1958): The effects of 2-deoxy-D-glucose on metabolism of slices of cerebral cortex incubated *in vitro. J. Neurochem.,* 3:185–205.
162. Volk, M. E., Millington, R. H., and Weinhouse, S. (1952): Oxidation of endogenous fatty acids of rat tissues *in vitro. J. Biol. Chem.,* 195:493–501.
163. Webster, W. R., Serviere, J., Batini, C., and LaPlante, S. (1978): Autoradiographic demonstration with 2-[^{14}C]deoxyglucose of frequency selectivity in the auditory system of cats under conditions of functional activity. *Neurosci. Lett.,* 10:43–48.
164. Wechsler, L. R., Savaki, H. E., and Sokoloff, L. (1979): Effects of *d*- and *l*-amphetamine on local cerebral glucose utilization in the conscious rat. *J. Neurochem.,* 32:15–22.
165. Wiesel, T. N., Hubel, D. H., and Lam, D. M. K. (1974): Autoradiographic demonstration of ocular dominance columns in the monkey striate cortex by means of transneuronal transport. *Brain Res.,* 79:273–279.
166. Williamson, D. H., Bates, M. W., Page, M. A., and Krebs, H. A. (1971): Activities of enzymes involved in acetoacetate utilization in adult mammalian tissues. *Biochem. J.,* 121:41–47.
167. Wolfson, L. I., Sakurada, O., and Sokoloff, L. (1977): Effects of γ-butyrolactone on local cerebral glucose utilization in the rat. *J. Neurochem.,* 29:777–783.
168. Yarowsky, P. J., Crane, A. M., and Sokoloff, L. (1980): Stimulation of neuronal glucose utilization by antidromic electrical stimulation in the superior cervical ganglion of the rat. *Soc. Neurosci. Abstr.,* 6:340.
169. Yarowsky, P., Kadekaro, M., and Sokoloff, L. (1983): Frequency-dependent activation of glucose utilization in the superior cervical ganglion by electrical stimulation of cervical sympathetic trunk. *Proc. Natl. Acad. Sci. USA,* 80:4179–4183.